PENSOFT

SENCKENBERG
world of biodiversity

Leibniz Association

Between sand, rocks and branches: an integrative taxonomic revision of Angolan *Hemidactylus* Goldfuss, 1820, with description of four new species

Javier Lobón-Rovira[1,2], Werner Conradie[3,4], David Buckley Iglesias[5,6], Raffael Ernst[7], Luis Veríssimo[8], Ninda Baptista[1,2,9], Pedro Vaz Pinto[1,8,9]

1 *CIBIO Centro de Investigação em Biodiversidade e Recurso Genéticos, Universidade do Porto, Rua Padre Armando Quintas, Campus de Vairão, 4485-661 Vairão, Portugal*

2 *Faculdade de Ciências da Universidade do Porto, Porto, Portugal*

3 *Port Elizabeth Museum (Bayworld), P.O. Box 13147, Humewood 6013, South Africa*

4 *Department of Nature Conservation Management, Natural Resource Science and Management Cluster, Faculty of Science, George Campus, Nelson Mandela University, George, South Africa*

5 *Departament de Biología (Genética), Facultad de Ciencias, Universidad Autónoma de Madrid (UAM), c/Darwin 2, 28049, Madrid, Spain*

6 *Centro de Investigación en Biodiversidad y Cambio Global CIBC-UAM, Facultad de Ciencias, Universidad Autónoma de Madrid, c/Darwin 2, 28049-Madrid, Spain*

7 *Museum of Zoology, Senckenberg Natural History Collections Dresden, Königsbrücker Landstr. 159, D-01109, Dresden, Germany*

8 *Fundação Kissama, Rua 60 Casa 560, Lar do Patriota, Luanda, Angola*

9 *TwinLab CIBIO/ISCED, Instituto Superior de Ciências da Educação da Huíla, Rua Sarmento Rodrigues s/n, Lubango, Angola*

http://zoobank.org/5496169A-0D7D-4C80-9B72-BF0AF03A6109

Corresponding author: Javier Lobón-Rovira (j.lobon.rovira@hotmail.com)

Academic editor Uwe Fritz | **Received** 22 February 2021 | **Accepted** 25 July 2021 | **Published** 9 August 2021

Citation: Lobón-Rovira J, Conradie W, Buckley Iglesias D, Ernst R, Veríssimo L, Baptista N, Pinto PV (2021) Between sand, rocks and branches: an integrative taxonomic revision of Angolan *Hemidactylus* Goldfuss, 1820, with description of four new species. Vertebrate Zoology 71: 465–501. https://doi.org/10.3897/vz.73.e64781

Abstract

The taxonomy of Angolan *Hemidactylus* has recently been revised. However, the lack of fresh material for some groups and regions, has led to the misidentification of some taxa and an underestimation of actual diversity in others. To shed light on the evolutionary history and systematics of Angolan *Hemidactylus*, we generated a new phylogenetic hypothesis for the group, and updated the taxonomy following an integrative approach. This resulted in the description of four new species (*H. pfindaensis* **sp. nov.**, *H. faustus* **sp. nov.**, *H. carivoensis* **sp. nov.** and *H. cinganji* **sp. nov.**), the reevaluation of two recently described species (*H. vernayi* and *H. paivae*) and the synonymization of a recently described species (*H. hannahsabinnae*). We estimate divergence times for these lineages, providing a preliminary interpretation of their speciation process. Moreover, we suggest and outline 13 Angolan Main Biogeographic Units (AMBUs) in the area, defining a new biogeographic context for future works on Angolan herpetofauna. We now recognize eleven *Hemidactylus* species in Angola, and we provide here a new morphological key for Angolan *Hemidactylus* to help with identifications and species assignments in this group.

Keywords

Angola, biogeography, Gekkota, *Hemidactylus*, systematics, taxonomy

Introduction

Angola, the seventh largest African country, is also remarkably biodiverse. Six biomes and 14 terrestrial ecoregions are recognized within its borders, and, in the continent, the country ranks first and second in terms of biomes and ecoregions, respectively (Burgess et al. 2004; Huntley 2019). The Angolan topography and climates are very heterogenous, which is reflected in a panoply of vegetation types present from the Atlantic coastline to montane environments and spanning from xeric deserts to moist evergreen rainforests. Not surprisingly, such diversity in habitats leads to intricate biogeographic patterns for local vertebrate taxa, including reptiles (Marques et al. 2018; Branch et al. 2019). Nevertheless, Angola has remained one of the least studied African countries throughout the second half of the 20th century due to political instability and a civil war, which ended in 2002 (Huntley and Ferrand 2019).

In the last two decades, Angolan herpetological knowledge has greatly improved, thanks to enhanced social stability and accessibility to previously unexplored regions, which helped to unearth this incredible local biodiversity (Marques et al. 2018; Huntley et al. 2019). These efforts have led to the description of new species (Haacke 2008; Conradie et al. 2012, 2020; Stanley et al. 2016; Marques et al. 2019a,b, 2020; Branch et al. 2019b, 2021; Ceríaco et al. 2020a,b,c; Hallerman et al. 2020), the rediscovery of several poorly known species, and documenting new range extensions and additions to the country's species list (Branch and Conradie 2013; Conradie and Bourquin 2013; Ceríaco et al. 2014; Ernst et al. 2014, 2015; Ceríaco et al. 2016; Branch 2018; Branch et al. 2019a; Vaz Pinto et al. 2019; Baptista et al. 2019, 2020; Ernst et al. 2020, 2021).

Integrative taxonomic approaches have become prominent to delimit species boundaries in natural groups (Padial et al. 2010). The merging of different character sets approaches and disciplines (such as phylogeography, comparative morphology, and ecology) to describe taxonomic units based on robust evidence has helped adopting rigorous and falsifiable taxonomic hypothesis and decisions (Schlick-Steiner et al. 2010; Vascocelos et al. 2011; Mirza et al. 2018; Ampai et al. 2020).

The increment in number of species described in Angola has been most noticeable within the Gekkonidae, in which there has been an increase from 32 to 40 recognized species in the last two years alone (see Marques et al. 2020; Ceríaco et al. 2020a, b; Branch et al. 2021). These recent discoveries emphasize the importance of Angola as a center of Gekkonidae diversification in west-central Africa. On the other hand, it should be noted that the number of species within the Angolan territory remains apparently underestimated and the proportion of cryptic species is unclear, due to the lack of recent material from still unexplored or hardly accessible areas, as well as from some historical type localities (Branch et al. 2019c).

Angolan *Hemidactylus* Goldfuss, 1820 has recently been investigated in detail by Ceríaco et al. (2020a, b), who addressed some previous nomenclatural inconsistencies and described several new species. However, the lack of new material for genetic studies from key regions, including historical type localities, coupled with some complex substructuring patterns observed, hampered a thorough systematic revision of the group. *Hemidactylus* in Angola is currently represented by eight species: *H. bayonii* Bocage, 1893, *H. benguellensis* Bocage, 1893, *H. longicephalus* Bocage, 1873, *H. mabouia* (Moreau de Jonnès, 1818), *H. nzingae* Ceríaco et al. 2020a, *H. paivae* Ceríaco et al. 2020a, *H. hannahsabinae* Ceríaco et al. 2020b and *H. vernayi* Ceríaco et al. 2020b. However, due to incomplete geographical coverage, and the lack of key genetic and morphological data for various taxa, species delimitations and distributions remain obscure and are in need of more detailed studies.

To explore the patterns and levels of diversity within *Hemidactylus* in Angola, we conducted a thorough and integrative analysis that involved (i) establishing a robust phylogenetic hypothesis based on one mitochondrial and one nuclear molecular marker for 346 individuals, representing all currently described species and potentially independent evolutionary lineages; (ii) a comparative morphological analysis of all lineages recovered in the phylogenetic study; and (iii) an assessment of potential distributions and niche breath for these lineages. This integrative systematic analysis forms the foundation for an updated taxonomy for the group, which includes the description of four new species, the updated description and diagnose of a recently described species, and some nomenclatural adjustments necessary to clarify the taxonomy of *Hemidactylus* in Angola. Finally, we also present here a morphological dichotomous key that we hope will help researchers for field identification.

Material and Methods

Sampling. Since 2011, *Hemidactylus* specimens and samples were collected across the western half of Angola, a vast region which includes a significant part of the biomes and biogeographic units present in the country (Fig. 1; Tables S2). Specimens collected as vouchers were euthanized with oral application of benzocaine gel or injection of tricaine methanesulfonate (MS222) (Conroy et al. 2009). After euthanasia, some specimens were fixed in 10% formalin and others in 96% ethanol, after which they were transferred to 70% ethanol for long-term storage in the Port Elizabeth Museum (PEM), South Africa; the Museum für Tierkunde, Senckenberg Natural History Collections Dresden (MTD); the Museum für Naturkunde (ZMB), Germany; the Museo Nacional de Ciencias Naturales (MNCN-CSIC), Spain; and Instituto Superior de Ciências da Educação da Huíla (ISCED) and Fundação Kissama (FKH), Angola. For molecular analyses, liver or muscle samples were collected and stored in 95–99% ethanol. For each sample collected, its location was recorded using precise coordinates, in the WGS84 coordinate system.

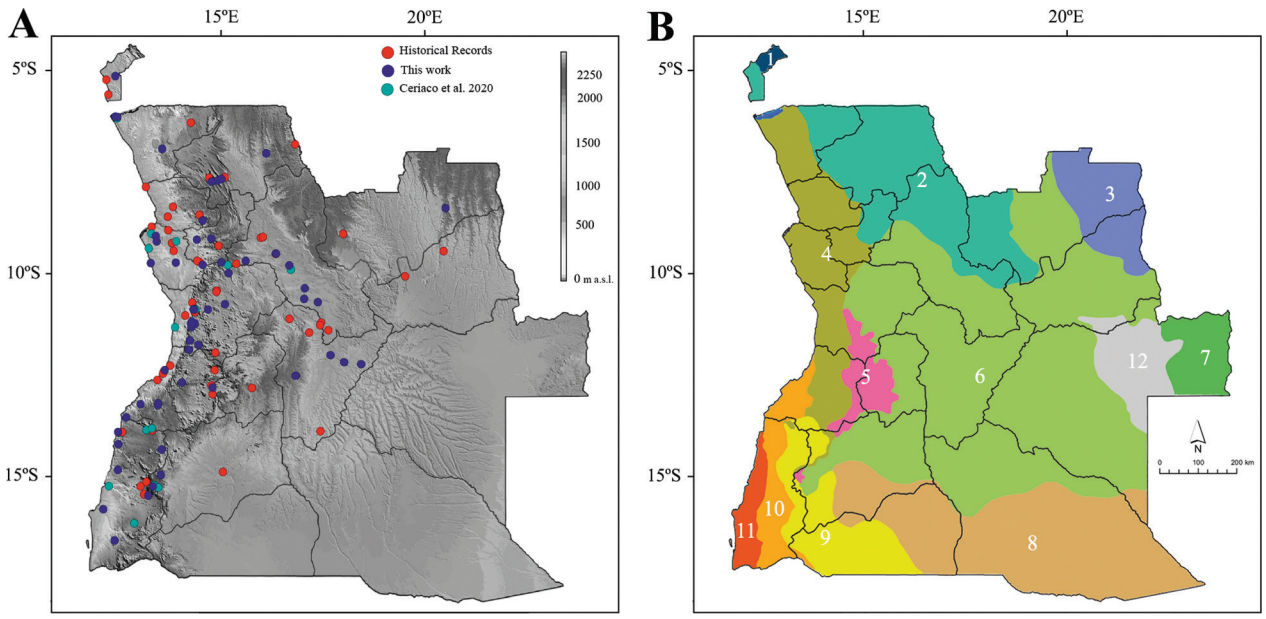

Figure 1. A – Topographic map with all *Hemidactylus* records of Angola (for detail about records see Table S2). **B** – Map of spatial distribution of Angolan Main Biogeographic Units (AMBUs). Numbers represent: 1 – Mayombe Forest, 2 – Northwestern Forest-Savanna Mosaic, 3 – Northeastern Forest-Savanna Mosaic, 4 – Scarp and Transitional Zone, 5 – Angolan Highlands, 6 – Angolan Miombo Woodlands, 7 – Zambezian Miombo Woodlands, 8 – Baikiaea Woodlands, 9 – Mopane Woodlands, 10 – Semi-arid Savannas, 11 – Namib Desert, 12 – Zambezian Flooded Grasslands and 13 – Mangroves (for AMBUs detail specification see Table S1).

Molecular data. We used phylogenetic analysis to explore and support the morphological findings. We generated 228 new *Hemidactylus* sequences from individuals across Angola. Mitochondrial gene ND2 (1041 bp) and partial fragments of the nuclear gene RAG1 (1035 bp) were generated for most individuals (Table S2). DNA was extracted using EasySpin Genomic DNA Tissue Kit, following the manufacturer's protocols. PCR amplifications were performed using the following primers (ND2: MetF1 and TRP R3 H5540, Macey et al. 2007; RAG1: RAG1skink F2 and RAG1skink R1200, Portik *et al*. 2010) and concentration (5 µl QIAGEN PCR MasterMix, 0.4 µl each Primer, each Primer, 3.2 µl H_2O and 2 µl DNA (DNA elution were adjust to extraction results). PCR reactions were adjusted as follows: for ND2, initial denaturing step at 95°C for 15 min, followed by 5 cycles of 95°C for 30 s, 64°C for 20 s, and 72°C for 60 s (decreasing –0.5°C/cycle), followed by 35 cycles of 95°C for 30 s, 64°C for 20 s, and 72°C for 60 s, with a final extension at 60°C for 10 min; for RAG1, initial denaturing step at 95°C for 15 min, followed by 40 cycles of 95°C for 30 s, 50°C for 30 s, and 72°C for 60 s, with a final extension at 60°C for 10 min. For phylogenetic comparisons we combined the newly generated sequences with 219 previously published *Hemidactylus* sequences, deposited in GenBank, of West and Central African *Hemidactylus* species as well as representatives from the other major clades of the genus (Carranza and Arnold 2006; Bauer et al. 2010; Ceríaco et al. 2020a), using *Cyrtodactylus*, the sister genus of *Hemidactylus* + *Dravidogecko* (Gamble et al. 2012; Chaitanya et al. 2019; Ceríaco et al. 2020), as the outgroup. Sequences were cleaned and visual inspected using BIOEDIT v7.2 (Hall 1999), posteriorly being aligned using MUSCLE in AliView v1.26 (Larsson 2014). For nuclear loci (RAG1), heterozygous individuals were identified based on the presence of two peaks of approximately equal height at a single nucleotide site and DNAsp v6.12 software was used with default settings, and not considering recombination, to resolve phased haplotypes (Rozas et al. 2017). Phased nuclear sequences were used for the network analyses and the unphased sequences for the phylogenetic analyses. Finally, sequences were concatenated using MESQUITE v3.6 (Madisson and Madisson 2019). All sequences have been deposited in GenBank (Table S2).

Phylogenetic analysis and network analysis. Bayesian Inference (BI) and Maximum Likelihood (ML) analyses were performed using sequence data of 346 specimens in three subsets: ND2, RAG1, and combined ND2+RAG1. The partitioning schemes were determined using PartitionFinder2 (Lanfear et al. 2016) and the best substitution model of sequence evolution were selected using ModelFinder (Kalyaanamoorthy et al. 2017) in IQ-Tree v1.6.12, with the Bayesian Information Criterion (BIC). The best partition scheme were three partitions (by codon position) for each gene, ND2 and RAG1. The bets-fit substitution models were GTR + I + G (ND2 codon positon 1), GTR + G (ND2 codon positions 1 and 2), TN+F+G4 (RAG1 1st, 2nd and 3rd codon position). We partitioned the combined dataset by gene and codon position (six partitions), as suggested in PartitionFinder. Phylogenies were constructed based on concatenate data. Bayesian inference analyses were conducted with MrBayes v3.2.7 (Ronquist et al. 2012) on CIPRESS (Miller et al. 2010) with six partitions of concatenated dataset, while ML was performed in IQ-Tree v1.6.12 (Trifinopoulos et al. 2016), with six partitions of the concatenated dataset. The final

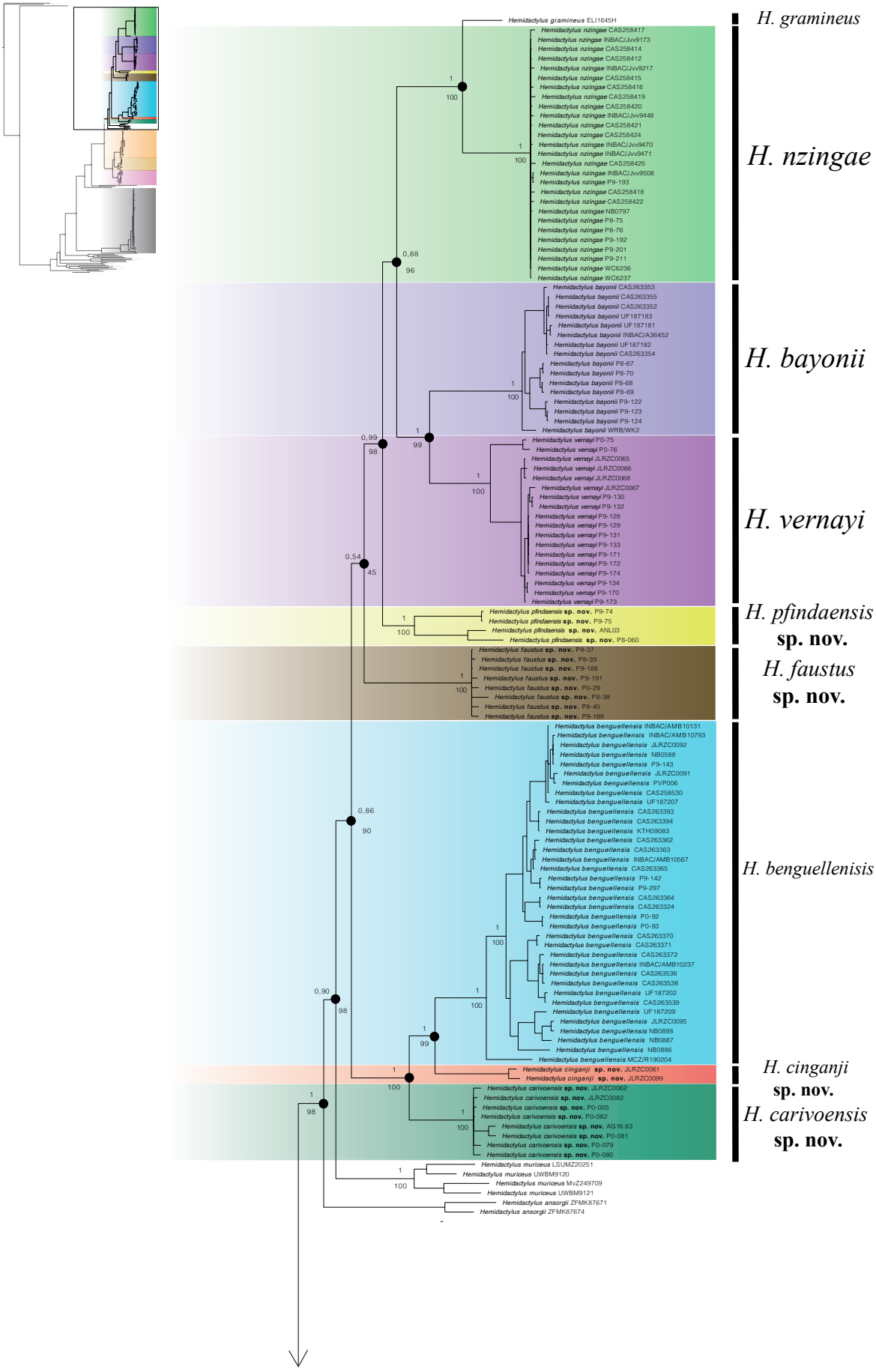

Figure 2A. Bayesian Inference (BI) phylogenetic tree based on ND2+RAG1 concatenated data, with Maximum Likelihood (ML) support overlaid. Numbers above the key nodes indicates BI posterior probability (≥ 0.90 were considered supported), while below the key nodes indicate ML bootstrap values (≥ 75% were considered supported). Major clades are marked with a thick vertical line.

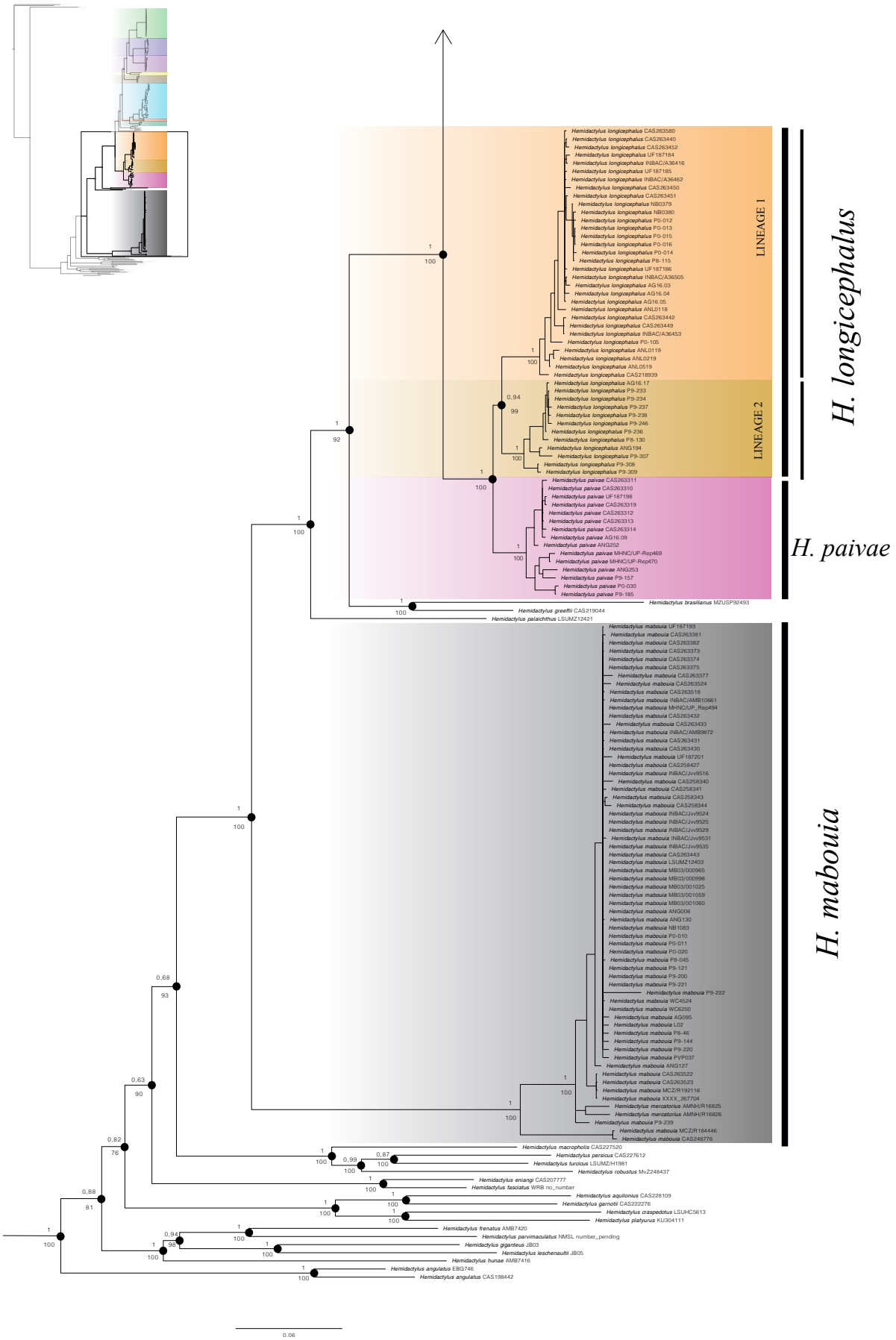

Figure 2B [Continuation]. Bayesian Inference (BI) phylogenetic tree based on ND2+RAG1 concatenated data, with Maximum Likelihood (ML) support overlaid. Numbers above the key nodes indicates BI posterior probability (≥ 0.90 were considered supported), while below the key nodes indicate ML bootstrap values (≥ 75% were considered supported). Major clades are marked with a thick vertical line.

BI analysis was run for 10×10^6 generations of the Metropolis-Coupled Markov (MC3) Monte Carlo, sampled every 1000 generations. Convergence was determined based on the standard deviation of split frequencies (<0.01) and 25% of the obtained trees were discarded as burn-in, to generate a 50% majority rule consensus tree in MrBayes. We explored the substitution model space with the option lset nst=mixed rates=invgamma. Posterior probabilities (PP) were used to assess nodal support, and PP ≥ 0.95 were considered strongly supported. Bootstrap analyses (BS) with 1000 pseudoreplicates in the ML analysis were used to evaluate relative branch support in the ML analysis. Bootstrap values of 70% or were considered as supported (Huelsenbeck and Hillis 1993). Uncorrected pairwise sequence divergences (p-distance) were calculated for ND2 sequences in MEGA v10.1.7 (Table 1). Median-joining haplotype networks were constructed for the phased nuclear alleles (RAG1) using Networks v4.6.1.1 (Bandelt et al. 1999), applying default settings and with parsimony cut-off of 95%.

Species trees and divergence times calibration. We estimated a time-calibrated species tree Startbeast using BEAST v2.6.3. We used a pruned dataset (selected target species) to reduce missing data and avoid unrealistic estimation. Best-fit substitution models were obtain using bmodel-test package implemented in BEAST2 (Bouckaert and Drummond 2017). A relaxed uncorrelated log-normal clock prior was selected for the two genes (Carranza and Arnold 2012). We used Birth-Death Process model with random starting trees as the tree prior. Due to the absence of fossils or ancestral information available for any of the nodes, we used secondary calibration points derived from Carranza and Arnold (2012), using calibration points for the crown divergence of the Arabian clade of *Hemidactylus* (Šmíd et al. 2019), which was in our dataset represented by *H. robustus*, *H. persicus*, and *H. turcicus* (mean=13.9 mya, sigma=3). This point was selected because of the topological congruence of this clade in previous studies. We constructed the calibration prior using a log-normal distribution and adjusted the mean and sigma parameters so that the distribution matches the 95% credible intervals from the primary study. Uninformative priors (gamma distribution, with parameters α=0.1 and β=10) were set for the parameters of the molecular clock, which were then estimated during the analysis.

Morphology. For this study, we examined newly collected material from different expeditions, and deposited at different museums listed before (see Table S2). High quality photographs of specimens of different *Hemidactylus* species were also analyzed. We examined 132 specimens of Angolan *Hemidactylus* and compared these to published material by Ceríaco et al. (2020a, b, 2021). For this comparison, measurement and meristic details were collected following Ceríaco et al. (2020). The morphometric characters assessed were: snout-vent length (SVL), trunk length (TRL), body width (BW; maximum width of body), crus length (CL; from base of heel to knee), tail length (TL), tail width (TW), head length (HL), head width (HW), head height (HH), forearm length (FL), orbital diameter (OD), nares to eye distance (NE), snout to eye distance (SE), eye to ear distance (EE), internarial distance (IN), interorbital distance (IO). All measurements were taken in millimeters (mm) with a digital caliper (accuracy of 0.1 mm). The meristic data (pholidosis and lepidosis) collected were: number of supralabials, number of infralabials, dorsal tubercles row at midbody (DTR), number of ventral scale across the belly, precloacal and femoral pores, subdigital lamellae from the base of the digits to the claw and including the claw sheath (Lam F/T for fingers and toes), morphology and arrangement of body and tail tuberculation, subcaudal scale morphology, number of postcloacal spurs on each side of tail base and size relative to dorsal tubercles. Meristic data were collected with the help of a Leica LD2500 or Nikon SMZ1270 dissecting microscope. For those taxa for which minor phylogenetic differences were observed but meristic characters exhibit unclear results, we performed further morphometric analysis between those taxa with ANOVA, using SVL and posteriorly 12 ratio-values (understood as measurements transformed by SVL). Principal Component Analysis (PCA) was used to study the overall morphometric variation, based on lognormal transformed values. Statistical analyses were performed in R v3.6.2.

Habitat assessment. The currently available published information on Angola's biogeographical characteristics is limited and often authors have relied on the work of Burgess et al. (2004), as a tool for conservation planning and to assist interpreting biogeographic patterns in Angola. However, Burgess et al. (2004) defined a total of 119 terrestrial ecoregions for Africa, of which 14 are represented in Angola, which consists of a rather rough approach when applied to a country-level scale like Angola (Huntley 2019). Instead, we here propose an alternative approach, in part supported by a novel preliminary outline of Angola's Main Biogeographic Units (AMBUs), reflecting ongoing research and assessments of Angola's ecologic and biogeographic characterization (Verissimo et al. in prep.). This allows to better reflect the specificities of the country's broad biogeographic contexts within the *Hemidactylus* findings and revisions presented in this work. Therefore, we outline 13 AMBUs within the Angolan territory (Fig. 1B; Table S1). Based on these broad units, the identified records for each species were plotted to assist in the examination of species spatial segregation. Moreover, during fieldwork individual habitat preferences for each specimen were recorded, to further substantiate ecologic and geographic inferences.

Species assessment. The species delimitation followed in this work is based on an integrative approximation (Vieites et al. 2008; Schlick-Steiner et al. 2010), considering separate species when a linage is well supported based on phylogenetic, morphological, and biogeographic/ecological differences.

Table 1. Average uncorrected pairwise distances (ND2) between selected Angolan *Hemidactylus* taxa, closely related species and outgroups. Bold numbers represent mean divergence within species. * represents lower than 10% p–distance between species.

Species	1	2	3	4	5	6	7	8	9	10	11	12	13	14	15	16	17	18
1. *Cyrtodactylus angularis*	–																	
2. *Cyrtodactylus ayeyarwadyensis*	27.44	–																
3. *Dravidogecko janakiae*	29.43	29.53	–															
4. *H. ansorgii*	31.73	30.01	31.48	**5.03**														
5. *H. bayonii*	32.99	30.83	30.85	17.55	**2.47**													
6. *H. benguellensis*	32.50	30.61	30.38	17.27	16.71	**3.84**												
7. *H. gramineus*	33.06	32.24	32.66	16.84	16.26	16.06	–											
8. *H. longicephalus*	31.41	30.41	31.55	17.87	18.61	16.34	16.81	**4.59**										
9. *H. mabouia*	34.27	31.84	31.59	26.89	27.24	27.22	30.62	27.19	2.06									
10. *H. mercatorius*	34.40	31.96	32.63	26.90	28.11	28.35	30.34	28.67	5.90	**5.05**								
11. *H. muriceus*	31.69	28.78	31.57	17.58	17.28	16.23	16.47	16.73	27.66	27.78	**8.54**							
12. *H. nzingae*	30.75	29.60	31.39	17.46	15.75	17.63	8.42*	17.67	28.24	28.56	16.30	**0.23**						
13. *H. paivae*	31.91	29.27	31.50	17.31	18.35	16.33	16.11	9.66*	27.31	27.68	16.49	18.02	**3.01**					
14. *H. vernayi*	33.99	30.94	30.37	17.92	14.18	15.30	14.76	18.13	27.18	28.29	16.47	15.77	17.65	**1.52**				
15. *H. cinganji* **sp. nov.**	31.80	29.61	29.75	17.87	16.21	11.64	14.55	16.47	27.18	27.82	15.97	15.88	15.86	15.89	**1.57**			
16. *H. pfindaensis* **sp. nov.**	32.87	30.56	30.84	16.42	15.17	14.74	14.51	16.96	27.80	27.79	15.53	14.91	16.58	14.36	14.72	**7.70**		
17. *H. carivoensis* **sp. nov.**	32.79	29.71	30.62	16.85	15.78	12.48	15.81	17.24	26.86	27.40	14.93	16.42	17.22	15.83	12.51	15.06	**0.84**	
18. *H. faustus* **sp. nov.**	30.85	28.64	32.47	19.28	18.29	16.68	18.15	17.67	28.88	29.20	17.32	17.85	18.14	18.47	16.68	16.57	17.01	**0.36**

Results

Phylogenetic relationships and network analyses. Both the Bayesian Inference and Maximum Likelihood analyses are largely concordant, yielding a well-supported topology, as they did with the single mtDNA (not shown). Phylogenetic analyses confirm the Western and Central African *Hemidactylus* relationship proposed by Ceríaco et al. (2020a) (PP: 1, BS: 98). However, the Angolan *Hemidactylus* clade (excluding *H. mabouia*) is here resolved into eleven genetically well-supported clades (Fig. 2), encompassed within six groups that show consistently large genetic ND2 p-distance between them (12.77–17.82%, Table 1).

Firstly, a large clade sister to the others includes all the members of the *H. mabouia*-complex, which differs >26 % (ND2 p-distance) from all remaining Angolan congeners. The latter can be subdivided in six main Angolan groups (in color in Fig. 2). The first major group represents the *H. longicephalus*-complex (PP: 1, BS: 100), which is sister to the other congeners. This clade further splits into two smaller subclades (*H. longicephalus* LINEAGE 1 and LINEAGE 2, with 8.99% ND2 p-distance between them (PP: 0.94, BS: 99)) in western Angola, and a third subclade representing *H. paivae*, mostly present on the Angolan plateau (PP: 1, BS: 99.9). The latter subclade differs by 10.22% ND2 p-distance from *H. longicephalus* LINAGE 1 and 8.82% ND2 p-distance from *H. longicephalus* LINAGE 2.

Another main group corresponds to the *H. benguellensis*-group, sister to the *H. bayonii*-group and related species (PP: 0.86, BS: 90). This *H. benguellensis*-group includes three subclades, all of them well differentiated (≥11.64% minimum ND2 p-distance between subclades, see Table 1; PP: 1, BS: 100 for all nodes): a new clade, based on topotypic material from near the original type locality of Cahata (Bocage 1893), a new species from the coastal southwestern region of Benguela, and a third variable species representing material recently assigned to *H. benguellensis* by Ceríaco et al. (2020a). The *benguellensis*-clade constitutes a monophyletic group in relation to remaining Angolan species.

Four additional main groups could be differentiated in the phylogenetic tree (Fig. 2). First, a group which includes the smaller-sized *Hemidactylus*, the *H. bayonii*-group, divided in two clades from the coastal plain, one present in dry forests and thickets of northwestern Angola and corresponding to *H. bayonii* sensu stricto, and a newly documented clade from the semi-arid coastal regions of Namibe Province, that represents the recently described sister species *H. vernayi* (PP: 1, BS: 99). This *bayonii*-group clade is closely related to a fourth main clade present on the Angolan plateau and associated with miombo woodlands (*H. nzingae*) (PP: 0.88, BS: 96). Recently, *H. gramineus,* a sister species to *H. nzingae* was described from the Democratic Republic of Congo (Ceríaco et al. 2021), which so far was not recorded from Angola (PP: 1, BS: 100). In addition, and as sister to the previous two groups, a fifth main group is represented by a moist forest clade found in Cabinda and Uíge provinces (PP: 0.99, BS: 98). Uncorrelated p-distance for ND2 between all clades were above 14% with exception of *H. gramineus*, which differs 8.42% from *H. nzingae* (see Table 1).

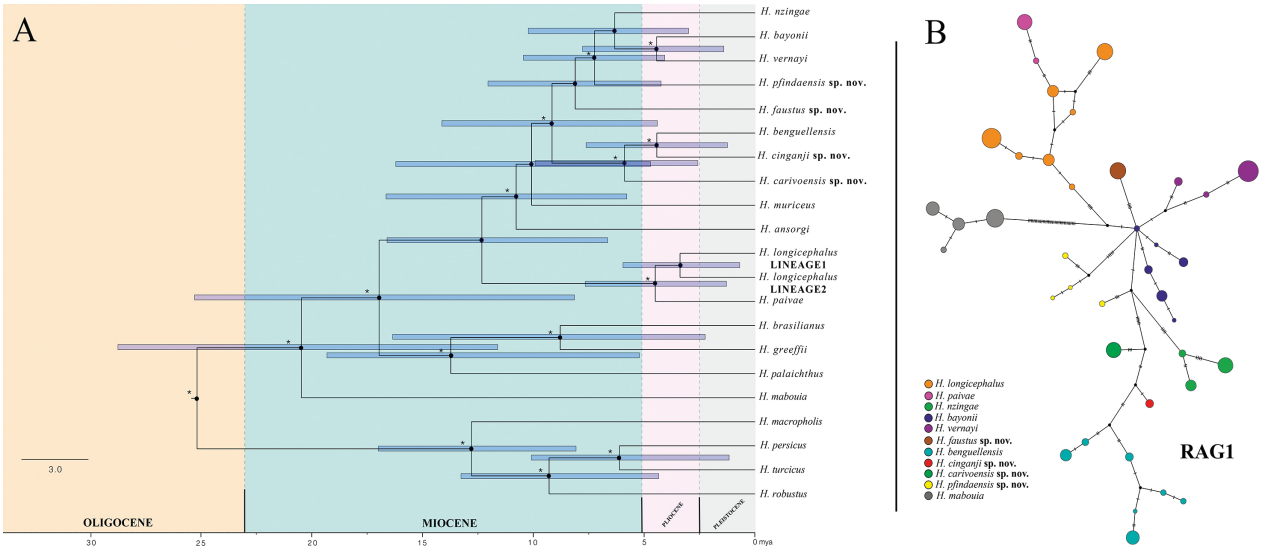

Figure 3. A – Species tree and Bayesian chronogram of divergences among Angolan *Hemidactylus*. Branches with posterior probability > 0.9 are denoted by asterisks (*) at relevant nodes. Blue bars depict 95% HPD intervals on estimated divergence date (95% HPD: High Probability Density). **B** – Median-joining nuclear allele network showing the relationships between Angolan *Hemidactylus* species, inferred from RAG1 nuclear gene. In all network, circle frequency of alleles and small lines represent mutational steps.

Finally, an independent clade was recovered from Pungo Andongo, without well-supported phylogenetic relationships (PP: 0.54, BS: 45; Fig. 2–3), making it difficult to disentangle its evolutionary position in relation to the other Angolan congeners. However, this group represents a genetically well-differentiated clade, displaying somewhat closest ND2 p-distance to the *H. benguellensis*-group compared to *H. bayonii*-group (16.7% and 18.3%, respectively).

The median-joining network for the RAG1 nuclear marker (Fig. 3B) recovered a total of 39 alleles, which grouped largely consistent with the 11 *Hemidactylus* species considered. No allele sharing was detected between species. The relative relationship among alleles is agreement with the phylogenetic results, suggesting *H. mabouia* as the most divergent species, with *H. benguellensis* and the *H. longicephalus* grouping at opposite ends of the network and the remaining species displayed in intermediate positions. The highest number of alleles (n=7) was observed within *H. benguellensis* and *H. longicephalus*, likely reflecting an expected higher diversity for the two most common and widespread Angolan species. In contrast, only one allele was recovered for the newly described species, possibly highlighting restricted range distributions in these species. The highest intraspecific divergence was found within one of the new species described here, with nine point mutations separating the material from Cabinda from the material found in Uíge Province.

The topology recovered in the time calibrated species tree is congruent with the phylogenetic tree from the ML and BI concatenated analyses. The Time to the Most Recent Common Ancestor (TMRCA) fort the Angolan *Hemidactylus* is dated to ~11 mya (95% HPD: 6.2–15.9 mya). Most of the TMRCAs for the lineages studied fell also within the Miocene, with the exception for *H. bayonii* and *H. vernayi* (~4.43 mya, 95% HPD: 1.6–8.5 mya), *H. benguellensis* and one of the lineages described here as a new species (~4.42 mya, 95% HPD: 1.7–8.1 mya), and *H. longicephalus* and *H. paivae* (~4.5, 95% HPD: 1.8–8.5 mya), which were all of Pliocene age (Fig. 3A). The analysis carried out provides our study with a general temporal framework for the evolution of *Hemidactylus* in Angola. However, and given the lack of a suitable fossil calibration points, and the potential incomplete phylogenetic sampling for this group, temporal estimates should be taken with caution and not over-interpreted.

Morphology. Results of the morphological analysis are summarized in Table 2. Angolan *Hemidactylus* could be separated into three main morphological groups, which differ from the other non-Angolan congeners by several characters, as analyzed by Ceríaco et al. (2020a). Large sized *Hemidactylus*, a group that includes the *H. mabouia*-complex, differ from the remaining Angolan congeners by the presence of large subcaudal scales. Within the typical Angolan *Hemidactylus*, the *H. longicephalus*-group can be differentiated from the other main congeners by its large size and reduced number of precloacal-femoral pores; a second group with medium to small-sized *Hemidactylus,* which includes the *H. bayonii*-group and closely-related species, that could be well-differentiated by morphological traits by its smaller size and lower number of precloacal pores; and a variable-sized *Hemidactylus*, corresponding to the *H. benguellensis*-group characterized by the presence of large number of precloacal-femoral pores and absence of large subcaudal scales. More details about morphological characteristics of each group are addressed in the following section.

Habitat assessment (Fig. 1A). *Hemidactylus* specimens were recorded in this study from eight of the 13 newly defined biogeographic units for Angola, even though

Table 2. Comparison between the different Angolan *Hemidactylus* (excluding *H. mabouia* and including *H. gramineus* from DRC). Measurements are represented in mm (average and standard deviation), based on newly collected material for this work with exception of *H. nzingae, H.gramineus* and *H. paivae*, where morphological measurements were compiled from information available in Ceríaco et al. (2020a, 2021) and information collected for this work. For abbreviations see Material and Methods section.

Species	***H. faustus*** sp. nov.	***H. pfindaensis*** sp. nov.	***H. carivoensis*** sp. nov.	***H. benguellensis***	***H. cinganji*** sp. nov.	***H. longicephalus*** LINEAGE 1	***H. longicephalus*** LINEAGE 2	***H. paivae***	***H. bayonii***	***H. vernayi***	***H. gramineus***	***H. nzingae***
Specimens	**n=10**	**n=4**	**n=9**	**n=12**	**n=2**	**n=6**	**n=9**	**n=18**	**n=6**	**n=25**	**n=2**	**n=12**
SVL	39.38 ± 3.35	45.54 ± 3.12	38,18 ± 5,16	49.66 ± 8.12	48.72 ± 5.19	46.21 ± 8.76	47.30 ± 3.09	57.31 ± 2.19	36.29 ± 3.46	32.52 ± 4.07	36.65±4.03	44.28 ± 3.88
TL	–	32.93	36,8 ± 7,64	40.23 ± 8.65	42.77 ± 0	44.20 ± 6.94	48.52 ± 1.94	63.05 ± 7.14	30.06 ± 11.11	25.92 ± 4.19	34.40±0.99	40.33 ± 3.48
TRL	16.83 ± 2.51	17.85 ± 3.76	15,82 ± 1,92	21.94 ± 5.93	21.33 ± 4.13	19.25 ± 4.29	18.98 ± 0.09	21.45 ± 2.89	15.02 ± 2.62	13.95 ± 1.88	15.85±2.33	19.41 ± 2.58
BW	7.44 ± 0.93	7.43 ± 0.41	6,99 ± 1,92	10.056 ± 1.83	10.14 ± 0.50	8.28 ± 3.26	8.5 ± 0.81	9.81 ± 0.47	6.69 ± 0.78	6.12 ± 1.26	5±0.14	7.27 ± 1.29
FL	9.10 ± 1.36	6.99 ± 1.35	5,79 ± 0,98	7.32 ± 1.81	7.86 ± 1.30	6.24 ± 1.53	8.57 ± 0.12	7.12 ± 1.14	5.57 ± 0.81	5.89 ± 1.23	4.70±0.28	6.06 ± 0.77
CL	6.32 ± 0.54	8.03 ± 1.73	6,75 ± 1,18	7.74 ± 1.47	8.39 ± 1.98	7.11 ± 0.76	5.47 ± 0.92	7.21 ± 1.47	6.30 ± 0.63	4.90 ± 1.18	5.55±0.21	7.03 ± 0.68
HL	11.62 ± 1.09	13.19 ± 1.40	11,10 ± 0,69	14.25 ± 2.86	12.99 ± 2.62	13.12 ± 2.09	14.02 ± 0.66	14.55 ± 0.59	10.13 ± 1.49	9.59± 0.79	10.5±0.71	12.18 ± 0.27
HW	8.22 ± 0.79	8.65 ± 0.85	6,81 ± 1,10	9.72 ± 1.73	9.57 ± 0.84	8.60 ± 1.55	9.38 ± 0.52	10.02 ± 0.62	6.75 ± 0.56	6.01 ± 0.98	6.35±0.49	8.11 ± 0.57
HH	4.95 ± 0.71	5.26 ± 0.28	4,21 ± 0,69	5.52 ± 0.97	6.32 ± 0.58	4.93 ± 0.99	5.65 ± 0.27	6.12 ± 0.28	4.37 ± 0.49	4.04 ± 0.52	4.25±0.49	5.08 ± 0.55
OD	2.87 ± 0.29	2.81 ± 0.18	2,68 ± 0,36	2.97 ± 0.39	3.14 ± 0.13	2.97 ± 0.48	3.02 ± 0.11	3.21 ± 0.18	2.42 ± 0.14	2.25 ± 0.29	2.10±0.42	2.81 ± 0.34
NE	3.39 ± 0.49	3.81 ± 0.47	3,38 ± 0,51	4.52 ± 0.78	4.18 ± 0.20	4.13 ± 0.64	4.45 ± 0.36	4.54 ± 0.57	2.88 ± 0.67	2.68 ± 0.35	2.95±0.35	4.26 ± 0.68
SE	4.6325 ± 0.31	5.32 ± 0.21	4,46 ± 0,70	6.03 ± 1.13	5.38 ± 0.61	5.29 ± 0.79	6.09 ± 0.85	5.80 ± 0.51	4.02 ± 0.71	3.58 ± 0.45	4.25±0.07	5.21 ± 0.34
EE	3.29 ± 0.36	3.53 ± 0.21	2,91 ± 0,39	3.89 ± 0.68	3.85 ± 0.48	3.21 ± 0.63	3.66 ± 0.46	3.83 ± 0.27	2.9 ± 0.46	2.75 ± 0.39	2.75±0.21	3.56 ± 0.23
EH	0.99 ± 0.15	0.84 ± 0.25	1,73 ± 2,67	1.25 ± 0.55	1.17 ± 0.42	0.92 ± 0.25	0.98 ± 0.09	0.95 ± 0.37	0.69 ± 0.19	0.57 ± 0.12	0.7±0.0	1.07 ± 0.17
IN	1.56 ± 0.24	1.36 ± 0.05	1,21 ± 0,20	3.75 ± 6.35	1.42 ± 0.12	1.41 ± 0.21	1.59 ± 0.15	1.63 ± 0.18	1.27 ± 0.12	1.22 ± 0.18	–	–
OI	3.97 ± 0.40	3.9 ± 1.41	3,51 ± 0,61	4.20 ± 0.66	4.81 ± 0.04	3.47 ± 0.72	4.68 ± 0.17	4.85 ± 0.04	3.3 ± 0.35	2.98 ± 0.49	–	–
Precloacal–Femoral Pores	17–19	8	15–22	23–33	26–28	5–11	6	6–8	4–9	4–6	8	7–8
Post–cloacal (tail) spurs	1/1	1/1	1/1	1–4/1–4	1–2/1–2	0–1/0–1	1–1/1–1	–	1/1	1–2/1–2	–	–
Scales across belly	29–32	28–30	32–38	33–41	30–32	28–37	28–36	28–34	25–32	32–39	23–25	22–27
Dorsal tubercles row	15–17	11–12	12–18	13–18	15	13–17	13–16	13–16	15–16	11–16	12–14	16–21
Supralabials (right/left)	9/9	10/10	11/10–11	10–11/10–11	9/9	10–12	10–12	10–12/10–12	8–9/9–10	9–10/9–10	10/9–0	10–11/10–11
Infralabials (right/left)	8/8	8–10/9–10	9/9–10	9–10/8–10	7–9/8	9–10	9–10	9–10/8–10	7–9/7–8	7–8/7–8	8–9/8–9	8–9/8–9
Subcaudals size	Small (< 1⁄4 tail width)	Small (< 1⁄4 tail width)	Small (< 1⁄4 tail width)	Small (< 1⁄4 tail width)	Small (< 1⁄4 tail width)	Small (< 1⁄4 tail width)	Small (< 1⁄4 tail width)	Small–Medium	Small (< 1⁄4 tail width)	Small (< 1⁄4 tail width)	Small (< 1⁄4 tail width)	Small (< 1⁄4 tail width)
# Granular scales between tubercles	2–3	4–5	2–3	2–5	2–3	3–6	3–4	3–9	2–4	2–4	2–3	2–3
Lamellae 1st finger	5–6	6–5	5	6	5–6	5–6	6	5–8	5–6	5–6	5	5–7
Lamellae 4th finger	7	7	6–7	6–8	7	7–8	7–8	8–9	7	7	7	6–8
Lamellae 1st toe	5–6	5–6	5	5–7	6	5–7	5–6	6–7	6	5–6	5	5–7
Lamellae 4th toe	9–8	7–8	9	8–9	8	8–10	8–19	9–11	8–10	7–8	7	9

material was recovered mostly in the western half of the country, as eastern regions were comparatively poorly surveyed. In addition, all Angolan taxa were confirmed to be present in at least one of the following five recognized AMBU's: Northwestern Forest-Savanna Mosaic, Scarp and Transitional Zone, Angolan Miombo Woodlands, Angolan Highlands, and Semi-arid Savannas. Our findings suggest a certain degree of specialization, with several taxa strongly linked to established biogeographic units and some species confined to specific habitats. A clear exception is *H. mabouia*, which is widely distributed throughout and spanning across most AMBU's, but this species is known to be highly adaptable and sometimes considered as invasive (Rödder et al. 2008; Baldo et al. 2008; Jairman et al. 2016). We found only one very distinct and previously undescribed form, present in the Northwestern Forest-Savanna Mosaic from northern Angola and Cabinda, which display arboreal behavior in closed-canopy gallery forests, although results for this region were hampered by limited sampling. Also, a single form was identified widely distributed and strictly associated to the Angolan Miombo Woodland, corresponding to the recently described, *H. nzingae*. One typical arboreal form was also identified, commonly found and well-distributed in semi-deciduous escarpment forests along the central Angolan escarpment in the Scarp and Transitional Zone, here ascribed to *H. longicephalus*. Its sister species, *H. paivae*, was found marginally present in the Scarp and Transitional Zone but mostly occurs across the northwestern Angolan Miombo Woodland, and sometimes in sympatry with other taxa. Nevertheless, *H. paivae* apparently displays a behavior more adapted to rupestrian niches, which may explain the segregation with sympatric and closely related species and less dependence on vegetation types. Two sister-species were found to occur on coastal regions, and across a gradient ranging from the fringes of the Kaokoveld in the southwest to dry forests and thickets in northwestern Angola. One of these corresponds to *H. bayonii*, which seems to be associated with the drier habitats within the Scarp and Transitional Zone, particularly within the lower Cuanza River drainage, and adapted to a ground-dwelling life among leaf-litter. The second coastal species is the newly described *H. vernayi*, which appears to be a more arid-adapted species, present across the Semi-Arid Savannas, near the coast, and adapted to forage in branches of small bushes, such as *Commiphora benguellensis*. A third new taxon within the *H. benguellensis*-group was also recorded from the Semi-Arid Savannas but proved to be more closely related to southern highland taxa. This species displayed arboreal habits, being often observed foraging at the base of main trunks of acacia trees and sheltering among dead wood.

In the southern block of the Angolan Highlands, we found one population, recently ascribed to *H. benguellensis*, but which appears to be highly adaptable and variable in morphology. Furthermore, some populations ascribed to this taxon have also been found on the coastal plain, scarp and plateau and spanning five additional different ecoregions. However, one different form was only found on the original topotypic locality of *H. benguellensis*, a mountainous region on the interface between the Scarp and Transitional Zone and the northern block of the Angolan Highlands and is apparently specialized to rupicolous habitats. Finally, a further unique and undescribed form was found in the inselbergs of Pungo Andongo. This locality is a well-known and singular geomorphologic feature, and although within the broader Angolan Miombo Woodlands, this potentially new taxon exhibited a high degree of specialization to its unique environment being ground-dwelling and rupestrine.

Systematics

Hemidactylus nzingae-group

Hemidactylus nzingae was described by Ceríaco et al. (2020a), based on a large series of specimens from Cangandala National Park (-9.87266°, 16.70088°, 1092 m a.s.l.), in Malanje Province, Angola. This species is associated with Miombo Woodlands and widely distributed on the Angolan plateau. Subsequently, Ceríaco et al. (2020b) described *Hemidactylus hannahsabinnae* based on morphological variability found in four specimens collected over 90 years ago and previously assigned to *H. nzingae*, from "Pavalange, Luando Natural Reserve, Bié Province; -10.96976°, 17.61243°" (here corrected to Palavanze, Luando Nature Integral Reserve, Malanje Province; -11.36625°, 17.60668°) and "Dande, Malanje Province; -11.1666°, 17.1666°" (here corrected to Dando, Bié Province; -11.24651°, 17.41472°). The historical series from both localities mentioned included sympatric specimens that remained ascribed to *H. nzingae*, thus lacking in biogeographic support. In addition, the morphological assessment of this newly described species does not present convincing morphological differences, and was based on the description of the following meristic information: "*subquadrangulal, smoothly keeled, striated tubercles at midbody* (*vs. subtrihedral, strongly keeled tubercles at midbody in H. nzingae*)*; by having the enlarged tubercles of the same size and with similar keel across the dorsum* (*vs. enlarged tubercles more strongly keeled and slightly larger on flanks and close to the tail than on the dorsum in H. nzingae*)*; by having barely distinct dorsolateral bands, one longitudinal middorsal light stripe evident, eight to nine rows of incomplete transverse dark bands, on a homogeneous light brown background* (*vs. the two well-marked longitudinal cream dorsolateral stripes and the prominent dark W-shaped markings and brown dorsal coloration in H. nzingae*)". However, the phylogenetic analysis presented here does not support the morphological difference used to describe *H. hannahsabinnae,* due to a large variability in dorsal coloration and dorsal scalation revealed within *H. nzingae*. Consequently, in this work, genetically confirmed *H. nzingae* specimens may present dorsal tuberculation subquadrangulal or subtrihedral and differently keeled (Fig. 4). Furthermore, the specimen FKH0060, from a locality very close

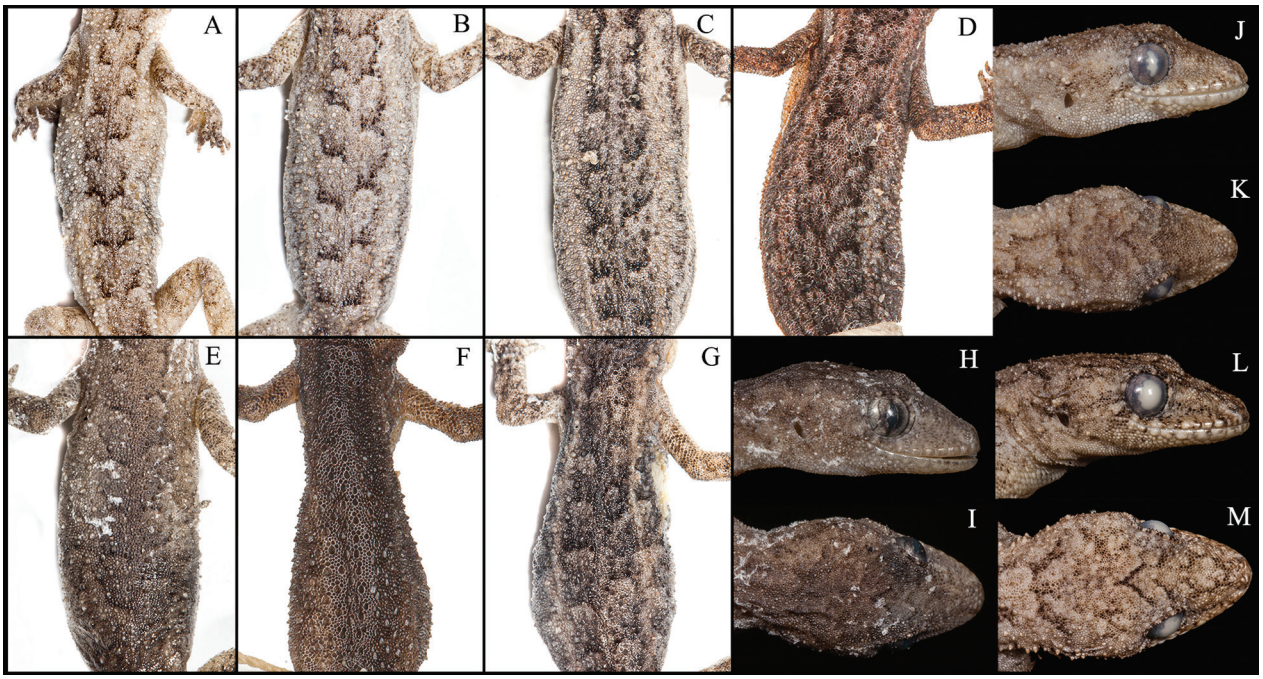

Figure 4. Morphological variability found within *Hemidactylus nzingae*. **A**–**G**: body, in dorsal view, showing variability pattern present in specimens of *H. nzingae* (Tissue codes FKH0282, FKH0289, FKH0299, PEM R19895, KH0060, PEM R23991 and KH0061, respectively). **H**–**M**: lateral and dorsal view of the head in *H. nzingae* (Tissue codes: FKH0060 (**H**–**I**), FKH0282 and FKH0289 (**L**–**M**) (see Table S2 for detailed voucher information). Photographs by Pedro Vaz Pinto (A–C, E, G, H–M) and Werner Conradie (D, F).

to where the type of *H. hannahsabinnae* was obtained, also in Luando Reserve (Table S2), and specimen PEM R24218 from Cuito, Bié Province, were both morphologically preliminarily identified as *H. hannahsabinnae* (Fig. 4E, F), but were subsequently and unequivocally ascribed to *H. nzingae* in the phylogenetic analyses. In addition, the dorsal coloration analysis of *H. nzingae* demonstrates that dorsolateral bands and crossbands can be variable, from clearly marked in some individuals, to barely present or even absent in others (Fig. 4). Based on the biogeographic segregation exhibited within the Angolan *Hemidactylus* group, sympatry between two closely related species should be deemed as highly unlikely. Therefore, due to the large sampling effort provided in this work, the absence of genetic evidence, and the large morphological variability found within *H. nzingae*, we consider *H. hannahsabinnae* a junior synonym of *H. nzingae* and exclude it for comparison in the diagnosis of the following species descriptions.

Finally, the a sister species to *H. nzingae* was subsequently described from the Democratic Republic of the Congo as *H. gramineus* (Ceríaco et al. 2021) with ND2 uncorrelated p-distance of 10.5%. The species was described based on the different number of dorsal tubercle rows (12–14 *vs.* 16–21 in *H. nzingae*) and differences in dorsal color pattern. However, the molecular analysis performed in the current work has lowered the ND2 uncorrelated p-distance from ~10% to 8.42% (Table 1), placing it within intra specific variation. Furthermore, the large variability of dorsal pattern here reported within *H. nzingae* (Fig. 4), reveals an overlap between *H. gramineus* and *H. nzingae*. Therefore, we suggest that the taxonomic status of this species needs future validation by the inclusion of nuclear markers.

Hemidactylus bayonii-group

Hemidactylus bayonii was described by Bocage (1893), based on a single specimen from "Dondo, sur les bords du Quanza" [=Dondo, on the banks of the Cuanza River], Cuanza-Norte Province, Angola. The original type was lost due to a fire in the Lisbon Museum in 1978. Therefore, a neotype was assigned by Ceríaco et al. (2020a) from "Kawa [= Cáua] Camp, Kissama [= Quiçama] National Park" (-9.18303°, 13.37063°, 136 m a.s.l), Luanda Province, Angola. *Hemidactylus bayonii* appears associated with coastal dry forests and mixed woodlands and thickets, within the Scarp and Transitional Zone. Another species, *H. vernayi*, has previously been assigned to this group, and occurs in arid environs on the coastal region of Namibe and Benguela provinces. The group is characterized by their smaller size (less than 42.5 mm maximum SVL) and reduced number of precloacal-femoral pores (usually 6).

Hemidactylus vernayi was described by Ceríaco et al. (2020b), based on four specimens previously ascribed to *H. bayonii*, from Benguela Province, designating a holotype from Lobito (-12.33333°, 13.58333°, < 5 m a.s.l), and three paratypes from Lobito and Hanha do Norte, respectively, exhibiting morphological variability. However, no phylogenetic analysis or biogeographic relationships were included in the study. The characters used to differentiate this newly described species from *H. bay-*

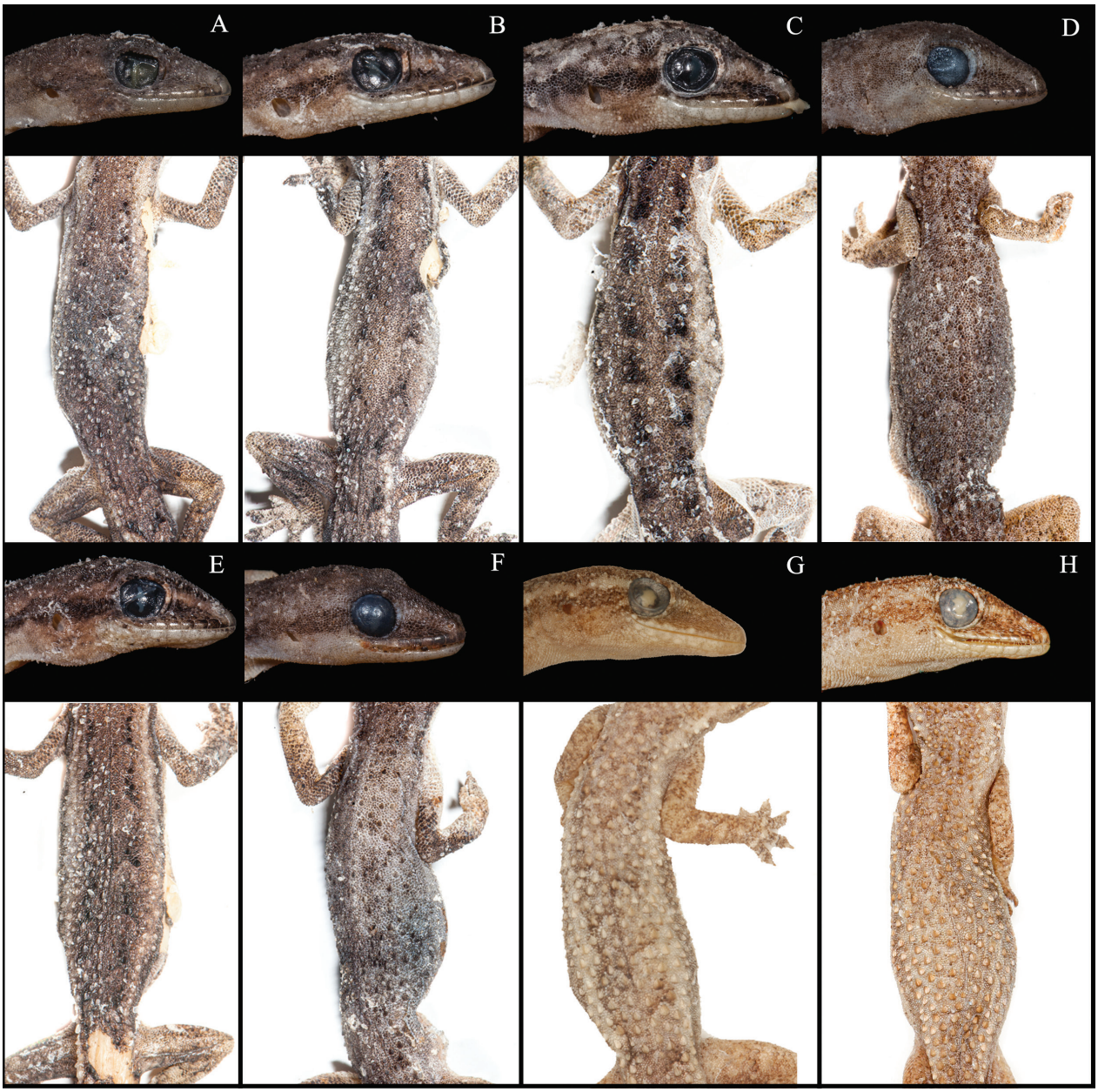

Figure 5. Morphological variability of head and body found within *Hemidactylus bayonii*. **A**–**H**: lateral view of head and dorsal view of the body showing robustness and pattern variability in genetically identified specimens of *H. bayonii* (Catalog Codes: FKH0052, FKH0053, FKH0054, FKH0220, FKH0055, FKH0221, PEM R25190 and PEM R26514, in order) (see Table S2 for detailed voucher information). Photographs by Pedro Vaz Pinto (A–F) and Werner Conradie (G–H).

onii, the most morphologically similar species, were the lower number of precloacal pores (4–5 *vs.* 6–9), the lack of a series of dark parallel dorsolateral markings and having a more robust body and head. However, some incongruences were found on the species description proposed by Ceríaco et al. (2020b). Firstly, the species description of *H. vernayi* referred to a lower number of precloacal-femoral pores (4–5), even though in the table with type measurements presented in that study, half of the specimens displayed 6 precloacal-femoral pores (see Ceríaco et al. 2020b). Moreover, the morphological analysis of *H. bayonii* conducted in the current study, reveals a large variability for this character within *H. bayonii*, whereas for example the specimen FKH0221, clearly related to all *H. bayonii* individuals in our molecular analysis (Fig. 2), and collected in Kikuxi, Luanda Province, has 4 precloacal-femoral pores (Table S3). Additionally, the lack of dorsal pattern in specimens preserved for almost 100 years, were found represented in various recently collected specimens, genetically identified as *H. bayonii* in this study (Fig. 5).

Interestingly, specimens collected from Hanha (paratype locality of *H. vernayi*, see Fig. 6C), were unequivocally identified as an independent taxonomic unit, which validates *H. vernayi* as the sister species to *H. bayonii* (Fig. 2). However, a larger series of *H. vernayi* collected from two sites in northern Namibe Province, reveal large morphological and meristic variability within this newly described species (Table S4) and reinforce the lack of an accurate description and diagnosis of the species, since

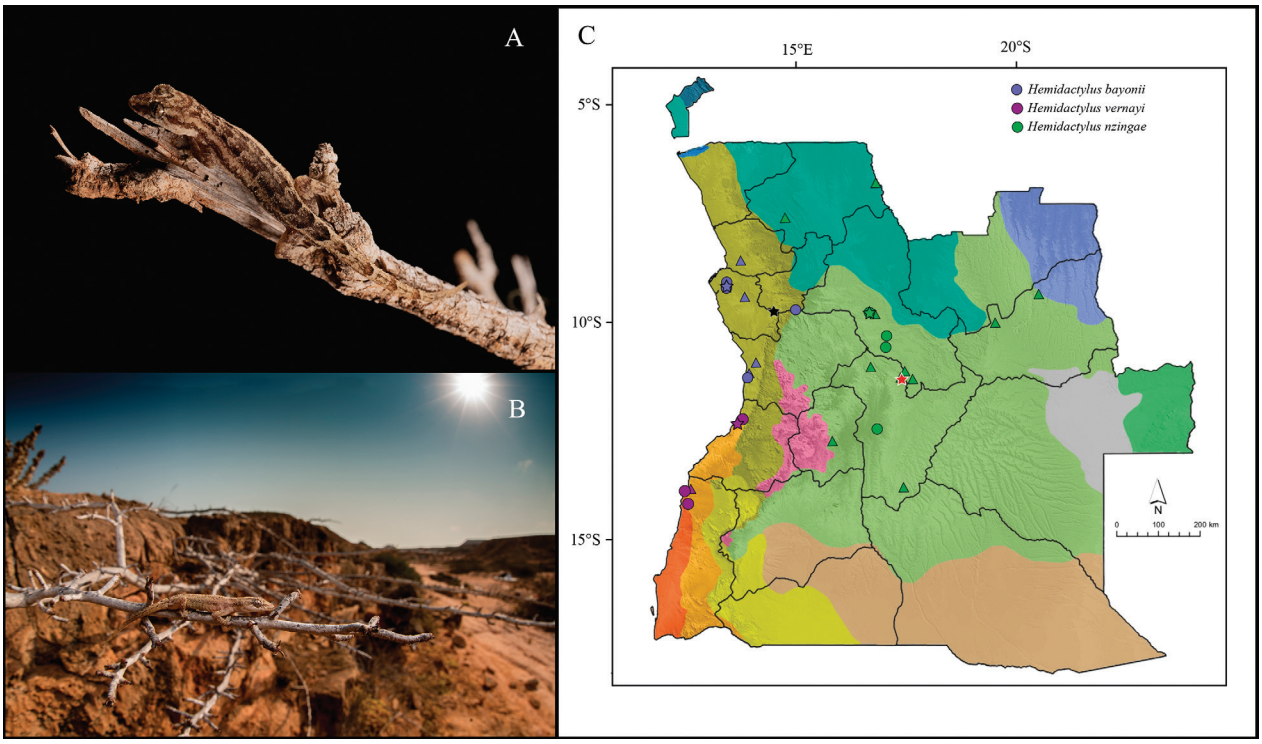

Figure 6. A – dorsal view in life of *Hemidactylus vernayi* (MNCN 50541), **B** – habitat of *H. vernayi*, **C** – updated records of the *H. bayonii*–group and *H. nzingae*–group (blue color represents *H. bayonii*, purple *H. vernayi*, and green *H. nzingae*; circles represent genetically confirmed records, while triangles represent historical or non-genetically assigned records based on Ceríaco et al. (2020a, c); color stars depict the different type localities, black star depicts the original type locality of *H. bayonii* assigned by Bocage (1893), red star depicts type locality of *H. hannahsabinae* by Ceríaco et al. 2020. Photos by Javier Lobón–Rovira (A–B).

the characters identified as diagnostic for *H. vernayi* by Ceríaco et al. (2020b) are not well supported. Additionally, the large variability found within these closely related taxa is reflected in a significant range of overlap between them. Therefore, here we provide an updated description for *H. vernayi.*

Hemidactylus vernayi Ceríaco, Agarwal, Marques and Bauer 2020

Figs 6–7

Based on both phylogenetic hypothesis (BI and ML), *H. vernayi* is sister species to *H. bayonii*, presumably a relic in arid coastal ecosystems (Fig. 2, Fig. 6C), and forming a monophyletic group with *H. bayonii, H. nzingae*, and another species from northern Angola and Cabinda described below. The uncorrected p-distance found within *H. vernayi* for ND2 was 1.52%. The p-distances for ND2 between *H. vernayi* and their closely related species were: 14.15% with *H. bayonii*, 15.55% with *H. nzingae*, and 14.73% with the northern species described below (see Table 1). Small size and other morphological similarities have previously led to a misidentification of this taxon, or to its assignment to *H. bayonii*, by different authors.

Material examined. ANGOLA • 2 ♀; Namibe Prov., Santa Marta, Lucira; -13.87861°, 12.42444°; 48 m a.s.l.; 24 May 2019; Pedro Vaz Pinto; FKH0226–7 and MNCN 50538 • 3 ♂; same collecting data as previous material; FKH0228, MNCN 50539, FKH0232 • 4 ♀, 1 ♂ same collecting data as previous material; 6 Jul. 2019; Pedro Vaz Pinto and Javier Lobón-Rovira; FKH0263–6, MNCN50533 • 1 ♀ juv.; same collecting information as previous material; FKH0268 • 2 ♀; Bentiaba; -14.17596°, 12.44689°; 150 m a.s.l.; 15 Feb. 2020; Pedro Vaz Pinto and Javier Lobón-Rovira; MNCN 50541 and ZMB 90448 • 2 ♂; same collecting information as previous material; FKH0417 and ZMB 90449 • 3 ♂; Lucira; September 1956; Charles Koch; TM 24447, 24450–1 • 1 ♂ and 1 ♀; Benguela Prov., Hanha; -12.24245°, 13.71399°; 39 m a.s.l.; 16 Nov. 2019; Pedro Vaz Pinto; ZMB 90450–1.

Updated comparative diagnosis. *Hemidactylus vernayi* is readily distinguished from non-Angolan congeners by sharing the same distinctive characters as *H. bayonii* (see Ceríaco et al. 2020a). In respect to the Angolan congeners, *H. vernayi* differs from *H. longicephalus*-group in its much smaller maximum size (maximum SVL 42.5 mm [mean=32.67] *vs.* 60.1 mm [mean=46.57] in *H. longicephalus* and 64.8 mm [mean=58.96] in *H. paivae*); from *H. benguellensis* by its lower number of precloacal pores (5–7 *vs.* 23–33); and from *H. mabouia* by having small subcaudal scales and a lower number of precloacal pores (5–7 *vs.* 28–39). *Hemidactylus vernayi* can further be distinguished from *H. nzingae* by fewer [11–16] rows of weakly keeled dorsal and caudal tubercles (*vs.* 16–21 rows of strongly keeled dorsal and caudal tubercles in *H. nzingae*). Interestingly, morphological analysis based on topotypic material of *H. vernayi* show extensive overlap with *H. bayonii*, and no clear diagnostic characters. Nevertheless, when we include the southern specimens

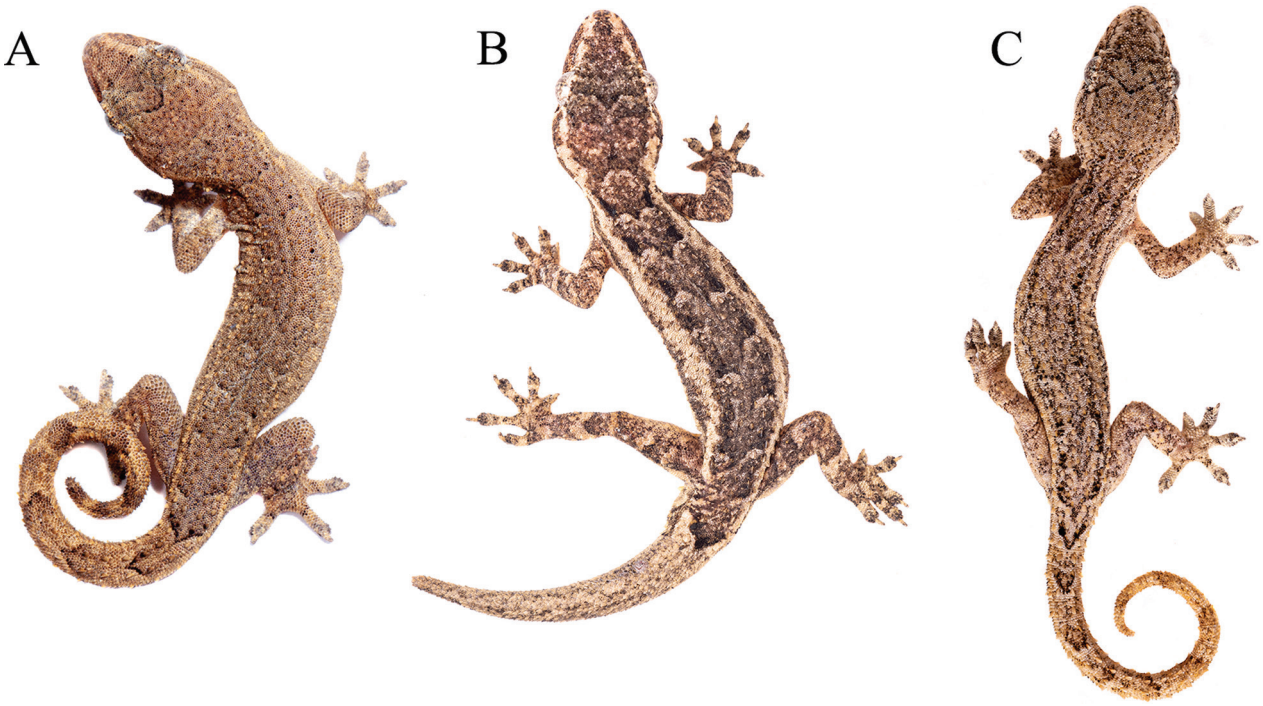

Figure 7. Dorsal photographs showing morphological variability found in *Hemidactylus vernayi* from (**A**) Hanha (ZMB 90450), (**B**) Bentiaba (MNCN 50541) and (**C**) Santa Marta (MNCN50533). Photos by Pedro Vaz Pinto (A) and Javier Lobón–Rovira (B, C).

of *H. vernayi*, these reveal a larger number of ventral scales across the belly (33–39 *vs.* 25–32 in *H. bayonii*, see Tables S3–4). See other new species descriptions for comparisons with this taxon.

Coloration. *In life* (specimen FKH0417; Fig. 6A): dorsum dark brown with two lighter dorsolateral bands from the nares to the anterior part of the tail; the dorsal region presents a darker crossband from occipital to the medium the region of the tail where it fades before disappearing; the crossband in the dorsal region presents a W-shaped marking common in *H. bayonii*-group, which becomes V-shaped as it approach the posterior region; the head displays a linear crossband from the eye region to the occipital; all the crossbands along the body are separated by a light beige section; the ventral region has uniform beige coloration; supralabials have dark coloration while infralabials show the same light beige of the ventral region; limbs with irregular dark and light brownish patches; iris golden with a black narrow pupil and dark brown reticulation. *Variation* (Fig. 7): this species presents high variability in coloration from light whitish cream to brownish. Dorsal pattern can be present or absent. Furthermore, it was observed that in some individuals during the day the darker regions become lighter, making it often difficult to differentiate the dorsal pattern, due to a uniform light beige color across the whole body.

Distribution and conservation (Fig. 6C). This species is considered the sister species of *H. bayonii*, so far only known to occur along the arid coast from Bentiaba in northern Namibe Province, northwards to Hanha in coastal Benguela Province (Fig. 6). Despite being still poorly known, the species is probably widely distributed, and its habitat does not appear at present to be threatened; however, due to limited number of records we cannot calculate the extent of occurrence (EOO) and thus we regard the conservation status of the species as Data Deficient. Further studies are suggested to better assess its full distribution and conservation status.

Natural history and habitat (Fig. 6B). *Hemidactylus vernayi* is an arid-adapted species, found foraging among small shrubs in arid coastal rocky semi-desert environments on the northern fringes of the Kaokoveld desert, and present also in vegetated valleys cutting through coastal semi-arid savannas. The species occurs along a coastal strip within the Semi-Arid Savanna AMBU, a region strongly influenced by the Namibe fog-belt (Cernak et al. 2012; Vaz Pinto et al. 2019). In the southernmost populations, most specimens were found associated with a recently described endemic small bush *Commiphora benguellensis* (Swanepoel 2015), while the northern populations were found in thicker and more diverse bush-dominated habitats. This species was always found foraging at night moving with agility between the spiny branches of small to medium-sized bushes, typically close to the ground and dropping quickly to the ground to seek shelter among crevices and cavities, or under small rocks or leaf-litter, when disturbed. Other species of geckos found in sympatry were *Chondrodactylus fitzsimonsi*, *C. pulitzerae* and *Pachydactylus angolensis*. No other *Hemidactylus* species were found occupying the same ecological niche as *H. vernayi*.

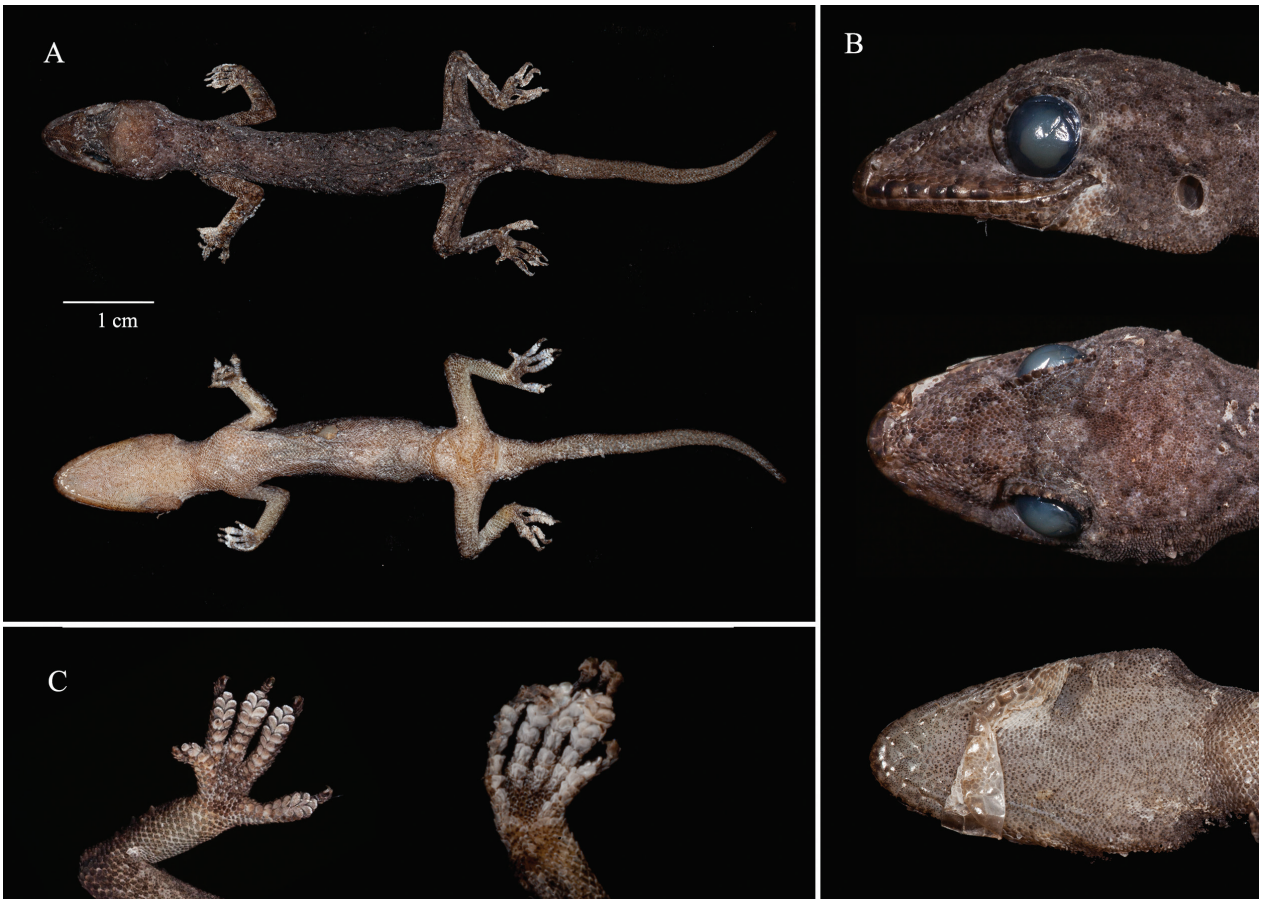

Figure 8. Holotype of *Hemidactylus pfindaensis* **sp. nov.** (FKH0178) from Chiloando, Cabinda Province, Angola. **A** – Dorsal and ventral view of body. **B** – Detail of head in lateral, dorsal and ventral views (from top to bottom). **C** – Detailed of left toes and right fingers (from left to right). Photos by Pedro Vaz Pinto.

Hemidactylus pfindaensis sp. nov.

Figs 8–9

http://zoobank.org/2EBB5713-B3FB-4F65-8EE1-93726E5C-D39E

Hemidactylus paivae: Ernst et al. 2020 [part]

Based on both phylogenetic hypothesis (BI and ML), *Hemidactylus pfindaensis* **sp. nov.** is the sister group of a well-supported clade within the *H. bayonii/nzingae*-group, and represents a northern clade present in the Tropical and Subtropical Moist Forests Biome. Due to the lack of accurate morphological assessments within western African *Hemidactylus* until Ceríaco et al. (2020a), and the lack of detailed and extensive molecular data, this species may have been historically assigned to either *H. longicephalus* or *H. muriceus*, which have been reported from forest regions in northern Angola and Democratic Republic of Congo, respectively. However, morphological and genetic analyses, support *H. pfindaensis* **sp. nov.** as a new species (Table 2). The genetic ND2 p-distance differs 15.17% from *H. bayonii*, 17.21% from *H. longicephalus* and 14.01% from *H. muriceus* topotypic material.

Holotype. ANGOLA • 1 ♀; Cabinda Prov., Chiloando; -5.12083°, 12.36667°; 95 m a.s.l.; 16 Mar. 2019; Pedro Vaz Pinto; FKH0178.
Paratypes. ANGOLA • 1 ♂; same collecting information as the holotype; without tail; MNCN 50537 • 1 ♂; Uíge Prov., Macocola; -7.01802°, 16.07658°; 952 m a.s.l.; 25 Sept. 2018; Pedro Vaz Pinto; without tail; FKH 0044 • 1 ♂; Uíge Prov., Serra do Pingano; -7.68451°, 14.92978°; 957 m a.s.l.; 31 Oct. 2014; Raffael Ernst; MTD 48932.

Diagnosis. A medium sized *Hemidactylus*, with SVL of 45.53 mm (mean) with moderate long snout, 10 supralabials and 8–10 infralabials (Fig. 8). Dorsal pholidosis with 11–12 rows of moderate dorsal keeled tubercle scales and ventral pholidosis with 28–30 smooth scale rows on midbody. The species present a large, triangular mental scale, two large postmentals followed by two enlarged post-postmentals. Base of the tail with four large keeled dorsal tubercle rows and subcaudal scales small, about one fourth of the tail width. Males with 8 continuous precloacal pores. Five divided scansors beneath first digit of both manus and pes, seven beneath fourth digit of manus, seven or eight beneath the fourth digit of pes. Dorsum presents dark coloration with two light brown crossbands from the posterior part of the eye to the sacrum, where the two bands meet each other to form a V-shaped marking.

Comparative diagnosis. *Hemidactylus pfindaensis* **sp. nov.** differs from the other non-Angolan, western and central African congeners, based on the same characteristics of the other Angolan species (Ceríaco et al. 2020a). However, this new species can easily be confused with *H. muriceus*-group, and differs from them by the presence of keeled dorsal tubercle scales *vs.* conical tubercle scales. Additionally, it differs from *H. pseudomuriceus* by lower number of precloacal-femoral pores (8 *vs.* 14–17) and one internasal scale *vs.* 2–3 in *H. pseudomuriceus*; and from *H. echinus* by the presence of considerably larger ventral than dorsal scales *vs.* similar size ventral and dorsal scales, and by reduced number of scansors underneath the 1st and 4th toe (5 and 7–8 *vs.* 10 and 12–13, respectively). Differentiated from *H. steindachneri* by lacking a longitudinal row of ventrolateral keeled tubercles, and from *H. hecqui* in not having the nostrils in contact with the first supralabial. *Hemidactylus pfindaensis* **sp. nov.** can be distinguished from *H. mabouia* by the presence of smaller subcaudal scales (large and elongated in *H. mabouia*) and from *H. benguellensis* by lower number of precloacal-femoral pores (8 *vs.* 23–33), and the dark dorsal color with dorsolateral light stripes and absence of dorsolateral orange tubercle rows (present in *H. benguellensis*). *Hemidactylus pfindaensis* **sp. nov.** differs from *H. longicephalus*-group by having a smaller SVL (maximum length 49.09 mm [mean=45.53] *vs.* 60.08 [mean=46.57] in *H. longicephalus* and 64.8 [mean=58.96] in *H. paivae*), more keeled tubercle scales and a lower number of dorsal tubercle rows (12 *vs.* 13–17 in *H. longicephalus,* and 13–16 in *H. paivae*). It differs from the *H. bayonii*-group by having larger SVL (maximum length 49.09 mm [mean=45.53]), than *H. bayonii* 36.2 mm [mean=34.9] and *H. vernayi* (42.5 mm [mean=32.89]); from *H. bayoni* by having lower number of dorsal tubercle rows (12 *vs.* 14–16 in *H. bayonii*), and head more compressed (HL/HW [mean=1.7] in *H. bayonii vs.* HL/HW [mean=1.5] in *H. pfindaensis* **sp. nov.**); from *H. vernayi* by presence of more precloacal-femoral pores (8 in *H. pfindaensis* **sp. nov.** *vs.* 4–6 in *H. vernayi*), lower number of ventral scales across the belly (28–30) than *H. vernayi* (32–39) and higher number of infralabials (9–10 *vs.* 7–8); and differs from *H. nzingae* and *H. gramineus* by larger number of scales across the belly (28–30 *vs.* 22–27 and 23–25, respectively), lower number of dorsal tubercle rows than *H. nzingae* (12 *vs.* 16–21) and larger number of granular scales between the dorsal tubercle rows than *H. nzingae* and *H. gramineus* (4–5 *vs.* 2–3).

Holotype description. Measurements and meristic characters of the holotype are presented in Table S5. Adult female with a snout-vent-length (SVL) of 49.09 mm, a regenerated tail length (TL) of 32.93 mm. Body slender, nape distinct. Head slightly narrower than the body and largely elongated (HW/HL 0.62). Canthus rostralis not prominent, but well-marked. Eye diameter (2.96 mm), with vertical pupil and crenulated margin. Supraciliar scales small and slightly pointed. Ear height (0.93 mm). Ear to eye distance slightly larger than orbit diameter (3.6 mm). Snout rounded. Frontal scales granular and larger than occipital scales. Occipital scales granular with lateral conical a large tubercle scale. Rostral wider than deep (2.21 *vs*. 1.04 mm, respectively). Rostral semidivided anterodorsally, in contact with 1st supralabial, nostril, prenasal and one internasal scales. 11 supralabials and 11 infralabials. First supralabial in contact with the nostril. Nostril circular rounded by rostral, supranasal, two postnasal and first supralabial. Postnasals larger than supranasal. Nostril in direct contact with the rostral and 1st supralabial. One row of scales between supralabials and the orbit. Mental large and markedly triangular, with two large rectangular postmental scales in broad contact posteriorly to the mental. 5 post-postmental scales, composed by post-postmental slightly smaller than postmental scales in contact with postmentals, 1st and 2nd infralabials, and 3 small post-postmental in contact with postmental scales. Gular scales and granular smaller than ventral scales. Between the gular scales and infralabials, a row of enlarged scales is present, decreasing in size until the 5th infralabial where they become the same size as the gular scales.

Body relatively slender and elongated (TRL/SVL 0.45). Ventral scales about double size than dorsal scales, with 28 scales across the belly. The dorsal pholidosis present heterogenous conical, granular scales interspersed by 12 keeled dorsal tubercle rows at midbody. Dorsal tubercle rows are separated by 4–5 granular scales. Tubercle scales reach the posterior part of head and the nape, where tubercle scales lose the keeling progressively. Base of the tail with four large keeled dorsal tubercle rows dorsally and subcaudal scales small, about one fourth of the tail width. Regenerated tail has no presence of tubercle scales, having largely homogeneous scales along and across the tail. Precloacal scales enlarged and one well-developed postcloacal spurs on each side.

Fore- and hindlimbs relatively short, stout; forearm short (FL/SVL 0.17); tibia short (CL/SVL 0.18). Short digits and clawed. All digits of manus and pes indistinctly webbed. Scansors beneath each toe equally divided, with the exception of 1st and terminal scansor undivided. 4th and 5th toes with 2 and 3 undivided terminal scansors, respectively. Scansors beneath each finger equally divided, with the exception of 1st and two terminal scansor undivided. 1st and 5th fingers with 3 undivided terminal scansors. Number of scansors: 5-7-7-8-7 (right manus), 5-7-8-8-9 (right pes). Relative length of digits: V < IV=III=II > I (right manus); V < IV=III > II > I (right pes).

Variation. Variation in scalation and body measurements of the paratypes of *H. pfindaensis* **sp. nov.** are reported in Table S5. All the material analyzed agrees entirely with the holotype description. However, paratype FKH0179, shows undivided rostral scales and MTD 48932, 3rd and 4th supralabials semi-fused at the base.

Coloration. *In life* (specimen FKH0178; Fig. 9A): this species presents dark coloration over the dorsum with two light brown crossbands from the posterior part of the eye to the sacrum, where the two bands meet each other to form a V-shaped marking; the rest of the dorsal part of

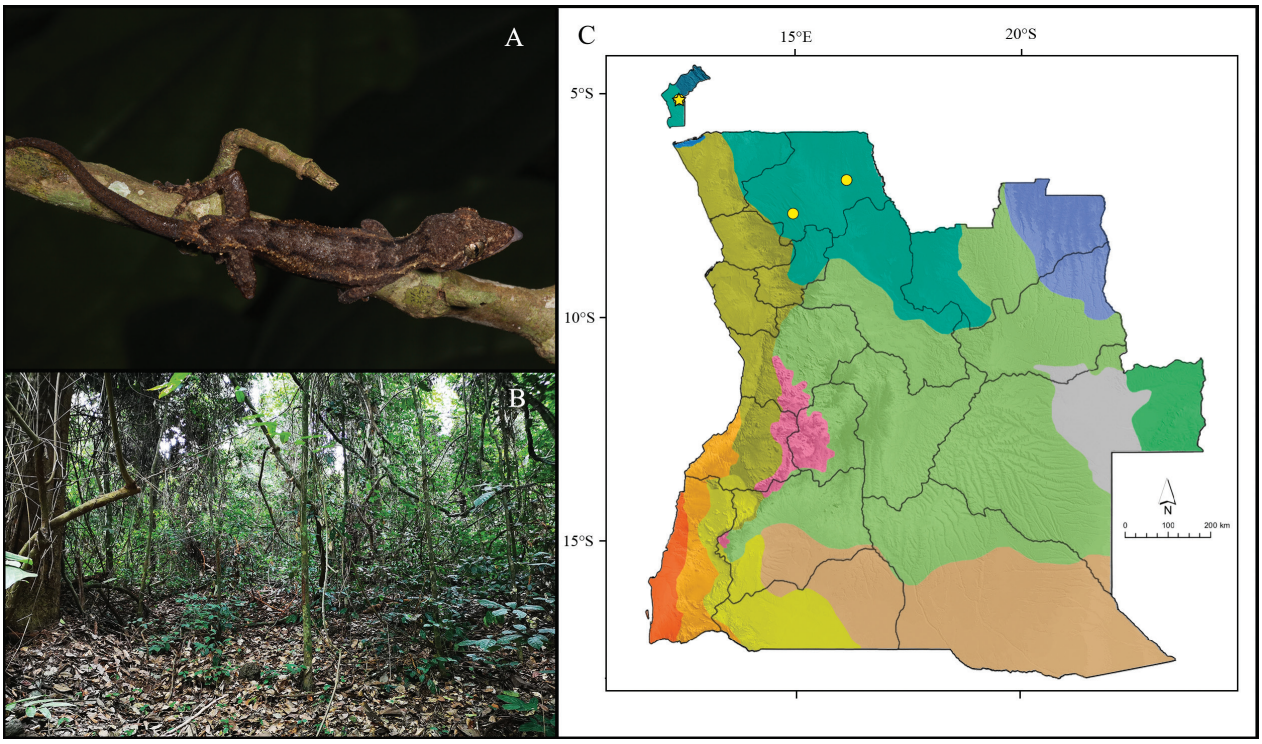

Figure 9. A – Dorsal view of *Hemidactylus pfindaensis* **sp. nov.** (Holotype, FKH 0178). **B** – habitat of *H. pfindaensis* **sp. nov. C** – records of *H. pfindaensis* **sp. nov.** (yellow circles represent records of *H. pfindaensis* **sp. nov.**; star depicts the type locality). Photos by Pedro Vaz Pinto (A) and Luke Verburgt (B).

the body is mostly dark uniformly brownish with some patches of light brown, especially at the nostril area and the hindlimbs. Coloration of the regenerated tail is uniform dark brown. The ventral part of the body is lighter, fully covered with scattered black speckles, from head to tail. Iris golden with a black narrow pupil and brownish-golden reticulation. *In preservative* (Holotype; Fig. 8): dorsum with dark uniform coloration; ventrum is light beige with scattered black speckles. *Variation*: occasionally difficult to differentiate the dorsal pattern, due to a uniform dark coloration across the whole body.

Etymology. The name "*pfindaensis*" derives from the local word "pfinda" which in Kikongo – the main language used in Uíge Province and northwestern Angola – refers to a "gallery forest" or a "continuous block of thick forest", the main habitat type associated with the species.

Distribution and conservation (Fig. 9C). A typical forest gecko, this species has been found in two sites of northern Angola, both in Uíge Province, and on a third site in the enclave of Cabinda. Its known presence north and south of the Congo River, suggests a much larger distribution range, that will likely extend to Democratic Republic of the Congo and Republic of the Congo, and possibly also into Gabon. In Angola, it will also likely be present in the Mayombe Forest and Northeastern Forest-Savanna Mosaic. However, due to limited number of records we cannot calculate the EOO and thus we regard the conservation status of the species as Data Deficient, and further studies are suggested to better assess its full distribution and conservation status. Although central African forests are currently threatened by deforestation and human encroachment, the occurrence of this species across a large geographical and altitudinal range, suggests that it is likely common, yet further studies are necessary to evaluate its conservation status.

Natural history and habitat. *Hemidactylus pfindaensis* **sp. nov.** appears to be a species strongly associated with moist evergreen forests. Specimens were collected at various altitudes, both near sea level and above 900 m a.s.l., but always in moist gallery forest, within the Northwestern Forest-Savanna Mosaic. All specimens were found foraging at night on tree trunks of well-developed trees, approximately 1–2 m above ground. Although never found hiding, it seems likely that it finds shelter under tree bark.

Hemidactylus longicephalus-group

Hemidactylus longicephalus was described in vague terms by Bocage (1873) based on specimens collected in Capangombe, at the base of the Chela Escarpment, in Namibe Province, and Catumbella [= Catumbela], on the coastline of Benguela Province (Bocage 1873). All the Angolan *Hemidactylus* types described by Bocage were lost in the devastating Lisbon fire of 1978. Some confusion derived from the fact that different specific names were applied to this taxon, while subsequently, populations from remote regions in the Democratic Republic of Congo or the islands of São Tomé and Príncipe, were also ascribed to *H. longicephalus* (see Ceríaco et al. 2020a). In an attempt to solve inconsistent identifications of *H. lon-*

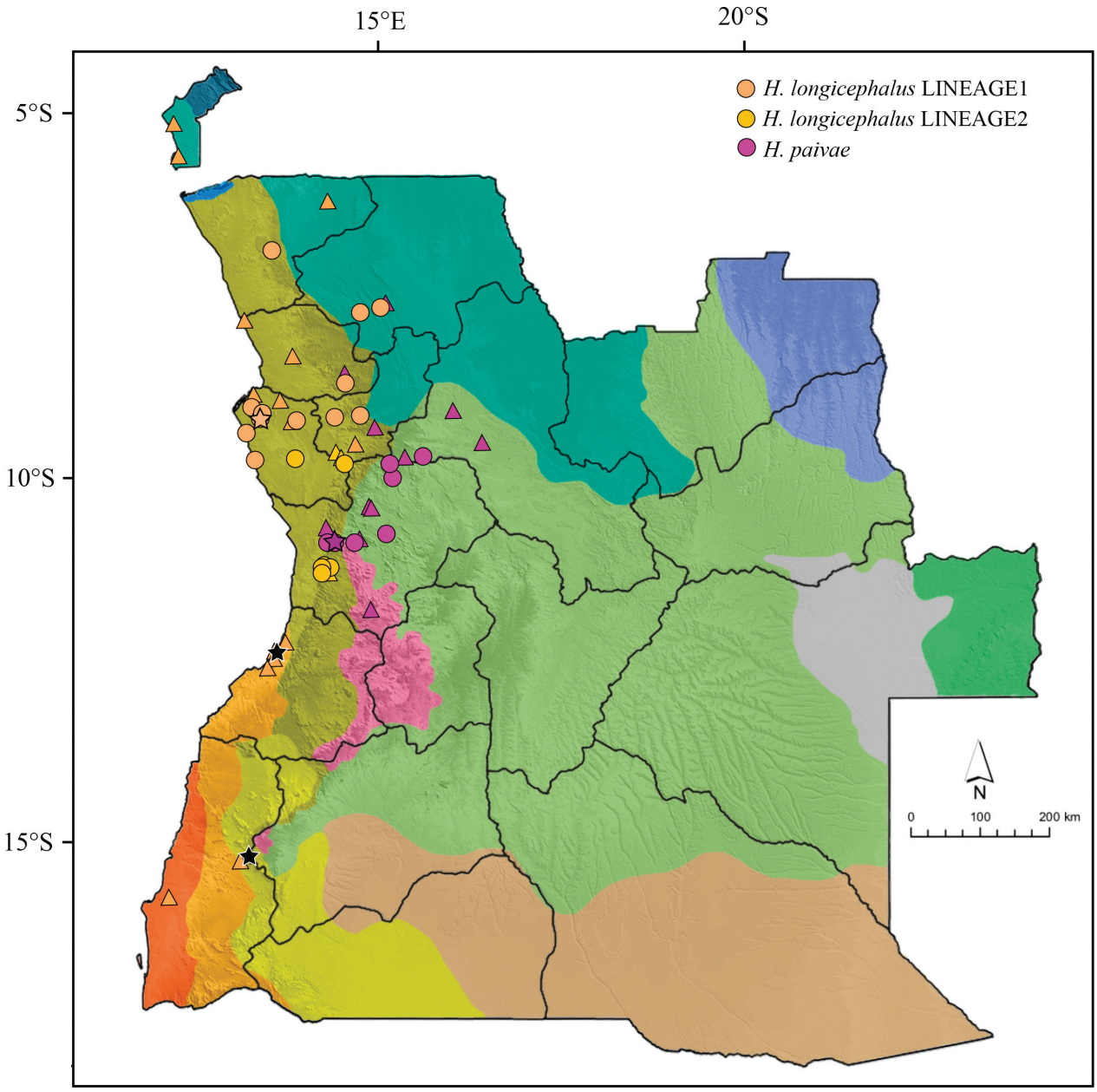

Figure 10. Records of *Hemidactylus longicephalus* species complex. Light orange color represents *H. longicephalus* Lineage 1; dark mustard represents *H. longicephalus* Lineage 2; pink represents *H. paivae*. Circles represent genetically assigned records, while triangles represent historical or morphologically assigned records by Ceríaco et al. (2020a). Stars represent type localities. Black stars represent original type locality of *H. longicephalus* assigned by Bocage (1873).

gicephalus due to the poor original description and inconclusive comparisons with additional material, Ceríaco et al. (2020a) assigned a neotype from Cáua Camp, Quiçama National Park, Luanda Province, Angola, ~370 km and ~650 km north from the original type localities of Catumbela and Capangombe, respectively. Intriguingly, the same authors also provided molecular support to confirm the specimen CAS 218939 collected in São Tomé (yet mistakenly listed in Table S2 of that study as coming from Angola) as true *H. longicephalus* (Ceríaco et al. 2020a). Such unusually disjunct distribution was suggested to derive from either natural colonization or human-induced introduction (Ceríaco et al. 2020a).

Based on the newly assigned *H. longicephalus*, this species represents a large size gecko with maximum SVL of 60.08 mm (mean=46.6), with reduced number of precloacal-femoral glands (6–11 *vs.* 23–33 in *H. benguellensis* group). Ceríaco et al. (2020a) further recognized a second species within this group, widely distributed across the northern Angolan escarpment zone and plateau, *H. paivae* (Fig. 10). The morphological differences used to describe *H. paivae* were the presence of lower number of dorsal tubercle rows on the dorsum (14–16 *vs.* 16–18 in *H. longicephalus*) and a larger maximum size (maximum SVL 68.4 mm *vs.* 54.8 mm) (Ceríaco et al. 2020a).

Our phylogenetic analysis reveals three well-supported lineages within this group. Two closely related western lineages across woodlands, thickets and forests present in the Scarp and Transitional Zone, and including the sample from São Tomé, and a third lineage mostly

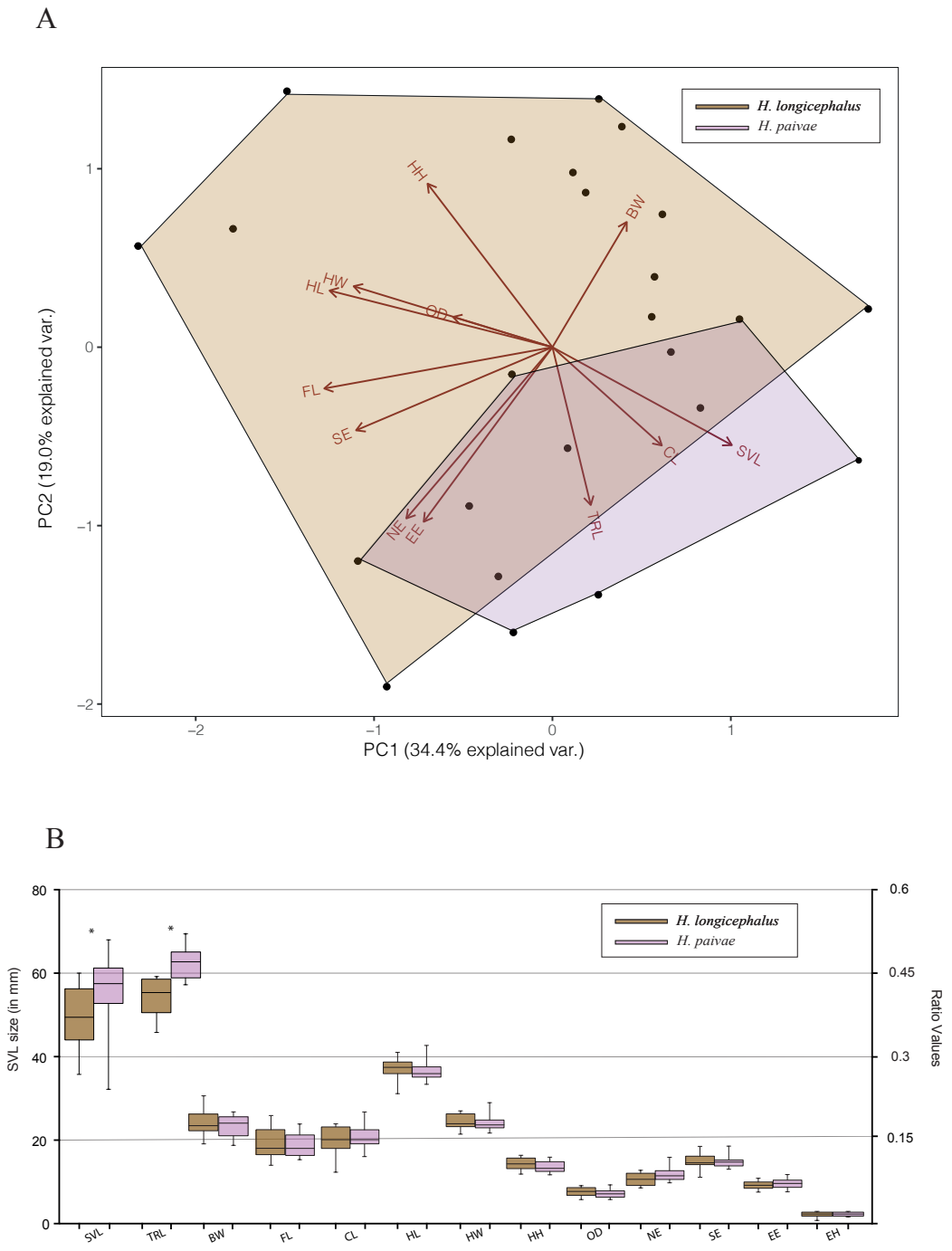

Figure 11. A – PCA plots of the first principal component (PC 1) versus the second (PC 2) of morphometric analysis for *H. longicephalus*–complex. Light brown polygon denote distribution within PCAs of *H. longicephalus* and pink polygon *H. paivae*. **B** – Statistical distribution of morphometric parameters examined by ANOVA. Significant t–values are highlighted by an asterisk (*). For abbreviations see Material and Methods section

found on the plateau in the Angolan Miombo Woodlands represented by *H. paivae*. However, a low p-distance in ND2 was observed within this group (8.99% between both western clades and 8.71% and 10.21% between the plateau clade and the two western clades, respectively). Moreover, the meristic analysis barely support differentiation between these three lineages, with large level of overlap among material examined (see Table 2), where specimens belonging to the *H. longicephalus*-group present dorsal tubercle rows from 11 to 18. Nevertheless, statistical analyses based on 12 morphometric variables show clear morphological difference in the SVL and TRL/SVL-ratio between *H. longicephalus* LINEAGE 1–2 and *H. paivae* (being maximum SVL 57.8 mm [mean=53.04 mm] and 60.08 mm [mean=51.81 mm] in the coastal clades *vs.* 68.4 mm [mean=57.31 mm] for *H. paivae,* while TRL/SVL-ratio < 0.44 mm in *H. longicephalus* and ≥ 0.44 mm in *H. paivae*) (Fig. 11). Some geographic overlap was detected between the three clades, with latitudinal segregation between *H. longicephalus* LINEAGE 1, so far always recorded north of 10ºS, and *H. longicephalus* LINEAGE 2 usually south of that latitude,

but both those clades occurring from the escarpment westwards down to sea level (Fig. 10). Interestingly, the sample from São Tomé nested well within LINEAGE 1. Furthermore, *H. paivae* has been recorded on top of the escarpment near populations of *H. longicephalus* LINEAGE 2, but is more widely distributed inland across the plateau (Fig. 10). Possibly more relevant might be the observed use of different niches. *Hemidactulus longicephalus* LINEAGE 1 and 2 appear to be essentially arboreal, and most specimens from both lineages were collected under similar circumstances, while *H. paivae* was always found foraging or closely associated with large rock boulders or rocky cliffs and therefore is here considered to be a rock-dwelling form. Interestingly, one specimen from Uíge Province, genetically assigned to *H. longicephalus* LINEAGE 1 (MTD 49869) and previously assigned to *H. paivae* (Ernst et al. 2020), was recovered from inside a cave wall and displayed unusual features, such as a much paler coloration that was maintained even after preservation. Additional specimens collected nearby in forest environment (MTD 49868, MTD 49870), assigned to *H. paivae* (Ernst et al. 2020), clustered genetically with the previous *H. longicephalus* LINEAGE 1, but displayed distinc species coloration and behavior (Ernst et al. 2020).

A large series of *H. longicephalus* and *H. paivae* provided in this work, show a large overlap between these closely related species (Table 2), and reinforce the lack of an accurate original species description and diagnosis, as the diagnostic features used to identify *H. paivae* in Ceríaco et al. (2020a) are not well-supported. Therefore, we here provide an updated diagnosis for *H. paivae.*

Updated comparative diagnosis of *Hemidactylus paivae*

A large sized *Hemidactylus*, with SVL of 57.31 mm (mean). *Hemidactylus paivae* differs from the other non-Angolan western and central Africa congeners based on the same characteristics as *H. longicephalus* (Ceríaco et al. 2020a). It differs from *H. mabouia* by the absence of large subcaudal scales and a smaller number of precloacal-femoral pores (6–8 *vs.* 28–39); from *H. benguellensis* by having fewer precloacal-femoral pores (6–8 *vs.* 23–33); from *H. nzingae* by its larger size (max SVL 64.8 [mean=58.96] *vs.* 48.0 [mean=44.28]), lower number of tubercle rows on the dorsum (13–16 *vs.* 18–21); from *H. bayonii* and *H. vernayi* by its larger maximum size (58.96 mm *vs.* 36.2 and 32.52 mm in average), by having strongly keeled and pointed dorsal and caudal tubercles (*vs.* feebly keeled in *H. bayonii* and *H. vernayi*). *Hemidactylus paivae* differs from *H. pfindaensis* **sp. nov.** by having a larger SVL (maximum length 64.8 [mean=58.96] in *H. paivae vs.* 49.09 mm [mean=45.53] in *H. pfindaensis* **sp. nov.**), less keeled tubercle scales and a larger number of dorsal tubercle rows (13–16 *vs.* 12 in *H. pfindaensis* **sp. nov.**). Finally, *H. paivae* can be distinguished from *H. longicephalus* by its larger size (64.8 [mean=58.96] *vs.* 60.08 [mean= 46.57] in *H. longicephalus*) and large TRL/SVL-ratio (>0.44 in *H. paivae vs.* <0.43 in *H. longicephalus*, see Fig. 11). See new species accounts for comparisons with these taxa.

Hemidactylus benguellensis-group

Hemidactylus benguellensis was described by Bocage (1893) based on two specimens (one male and one female) from "Cahata", Benguela Province, Angola, collected in 1891 by J.A. de Anchieta (Bocage 1893). Unfortunately, and as it happened with so many early Angolan material, the type series was lost in the 1978 fire that destroyed the Museum Bocage. In 1937, the species was collected by Monard (1937) at Ebanga, located also on the Benguela highlands and a mere 45 km south of the type locality. The species has often been confused with other taxa or misidentified (e.g. Loveridge 1947; Hellmich 1957; Rösler 2015), and until recently, the referred specimens from Cahata and Ebanga constituted the only material unambiguously ascribed to *H. benguellensis* (e.g., Marques et al. 2018). On a review of Angolan *Hemidactylus*, historical material collected from Hanha during the Vernay Angola Expedition (VAE) in 1925 and from Entre Rios by Hellmich in 1953, and previously ascribed to *H. longicephalus*, was reassigned to *H. benguellensis* (Ceríaco et al. 2020a). Additional series were recently recovered from southern provinces, including the first published records from Huíla Province (Butler et al. 2019), and subsequently a neotype was allocated for *H. benguellensis* from N'Dolondolo [= Ndolondolo], Namibe Province, Angola, ~250 km southwest from the original type locality (Ceríaco et al. 2020a). Nevertheless, no critical material from the original topotypic region nor from anywhere within the Benguela Province, has been collected since at least the early 1950's.

The *Hemidactylus benguellensis*-group represents variable forms mostly in overall size (mean SVL=46.59 mm; standard deviation 8.34; based on adult material only) and widely distributed, spanning from the central Angolan highlands and southern plateau to the coastal arid lowlands in Namibe Province. This group, which until the present work comprised only the species *H. benguellensis*, is characterized by a large number of precloacal-femoral pores (higher than 23), and absence of large subcaudal scales characteristic of *H. mabouia* (Table 2). However, many records of this species have been based on morphological analysis of historical museum material and were not supported by genetic data. Based on our phylogenetic analyses, three major clades are identifiable within this group: one morphologically well-supported new species, which occurs in the south-west, in the coastal region of Benguela Province, a second clade representing the recently reassigned *H. benguellensis,* and a third clade of new material collected from near the original type locality. This last clade recovered from the original topotypic region, differs by 11.53% ND2 p-distance from specimens recently established as *H. benguellensis*, thus suggesting a candidate

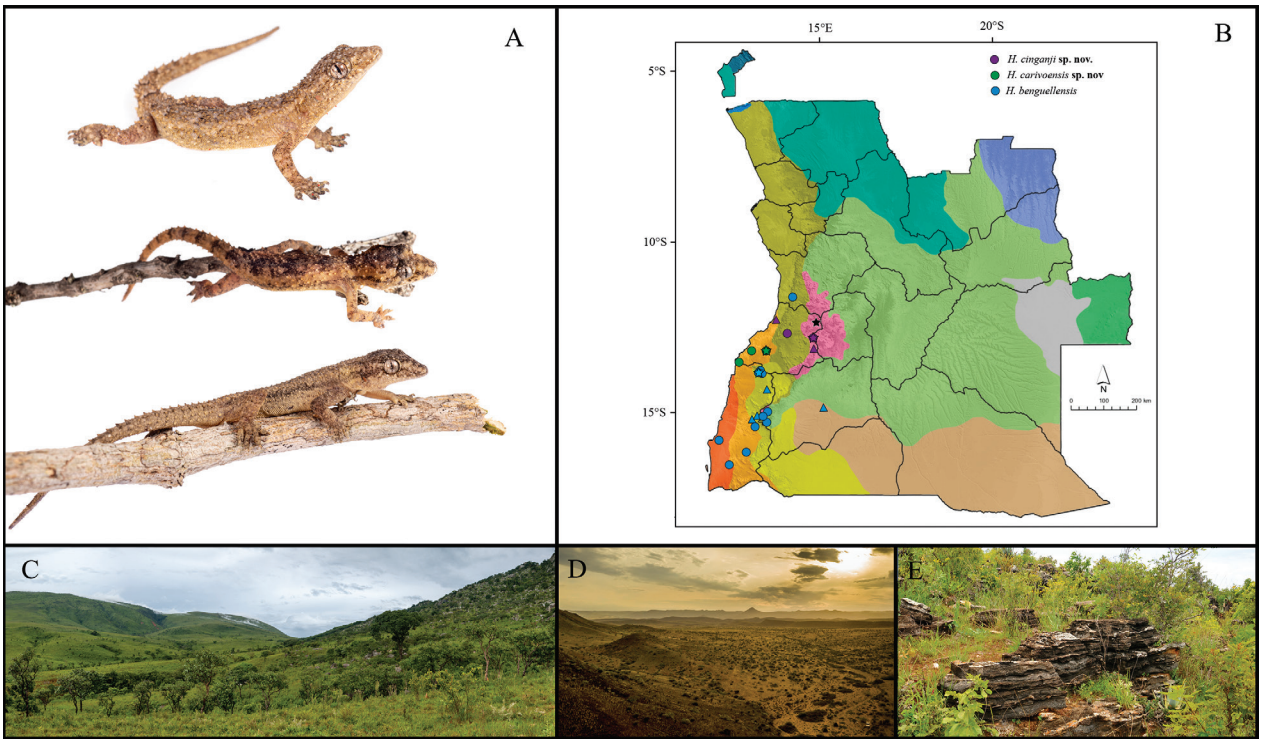

Figure 12. A – From top, dorsolateral view of *Hemidactylus cinganji* **sp. nov.** (FKH0435), *H. benguellensis* (FKH0413) and *H. carivoensis* **sp. nov.** (MNCN 50543); **B** – records of *H. benguellensis*–group (purple color represents records of *H. cinganji* **sp. nov.**; blue *H. benguellensis*; dark green *H. carivoensis* **sp. nov.**; circles represent genetically assigned records, while triangles represent historical or non-genetically assigned records by Ceríaco et al. 2020a; color stars depict type or neotype localities; black star depicts original type locality of *H. benguellensis* assigned by Bocage (1893); **C** – habitat of *H. cinganji* **sp. nov.** at Ebanga; **D** – habitat of *H. carivoensis* **sp. nov** between Dombe–Echimina**. E** – habitat of *H. benguellensis* at Tchivinguiro. Photos Javier Lobón–Rovira (A–D) and William R. Branch (E).

third species to be present in this group. Species within this group are treated below.

Hemidactylus cinganji sp. nov.

Figs 12–13

http://zoobank.org/23D0A398-1B90-44EA-9452-CEA948171671

Hemidactylus benguellensis: Bocage (1893:115; 1895:12); Monard (1937:52)

Hemidactylus benguellensis: Marques et al. 2018; Ceríaco et al. 2020 [part]

The original description of *H. benguellensis* by Bocage make reference to "*... species with 16 to 18 longitudinal series, 9 upper labials and 9 lower and 26 pre-cloacal and femoral pores, 13 on each side in a continuous series*". These characters were later corroborated by Monard (1937), with one male from Ebanga differing only from Bocage material on the number of preclocal-femoral pores (28 *vs.* 26).

In February 2020, a survey was conducted at Ebanga, Benguela Province, about 40 kilometers south of Cahata, the original type locality (Bocage 1893), and from where some of the earliest material ascribed to this species had been collected (Monard 1937). During this expedition an adult male morphologically assigned to *H. benguellensis* was collected on a granite rock boulder. A few days after, a second male was collected on a rock face overhanging a stream, near Passe, Benguela Province, ~80 km west from Ebanga and the type locality (Table S2, Fig. 12).

Interestingly, our phylogenetic analysis revealed a genetically separate lineage well-differentiated from the material assigned to *H. benguellensis* by Ceríaco et al. (2020a) (Fig. 2), with uncorrected p-distance 11.64% (Table 1). However, the available historical material collected between 1925 and 1953, from Ebanga, Hanha and Entre Rios (Ceríaco et al. 2020a), was morphologically included as part of the taxon genetically assigned to *H. benguellensis* by Ceríaco et al. (2020a), without any molecular support. It should be noted that, not only it is unknown to which phylogenetic clade should the material from Hanha and Entre Rios be assigned to, but the problem is further compounded by some geographic inconsistencies. The specimens from Hanha, obtained during the VAE were most likely collected at Hanha Estate (also known as Hanha do Norte) and located on the semi-arid coast north of Lobito (see Branch et al. 2017 for a detailed discussion on misinterpretations surrounding the toponym Hanha), and not on the geographic location given by Ceríaco et al. (2020a), about 130 km to the southeast and on the base of the escarpment at 917 m a.s.l. On the other hand, the locality of Entre Rios (meaning "between rivers") can

also be confusing, as several historical toponyms in Angola bear that name, and various publications have placed Entre Rios in different locations, ranging from 1,200 to 1,500 m a.s.l. in Benguela and Huambo provinces (e.g. Conradie et al. 2013; Marques et al. 2018; Ceríaco et al. 2020a). On his first Angolan expedition, Hellmich established his main base at the farm of Entre Rios, owned by a German citizen named Alfons Burger (Hellmich 1957), which is located further south than previously acknowledged, at –13.30385° 14.70761°, 1076 m a.s.l, Benguela Province. Two specimens were here collected by Hellmich in 1953 and a third specimen was added by Herr Burger in the following year, all initially identified as *H. mabouia*, and only recently reassigned to *H. benguellensis* (Ceríaco et al. 2020a). Nevertheless, the lack of phylogenetic context, the morphological variability recognized for specimens belonging to the neotypic clade, small sample size of the topotypic material, and the fact that Hanha and Entre Rios are intermediately located in relation to specimens genetically ascribed to different clades, recommends caution before assigning those specimens.

Based on field observations, the material assigned to *H. benguellensis* by Ceríaco et al. (2020a) is a very variable species present in different biomes and biogeographic units and occupying different niches, often showing arboreal habits, frequently found on the trunk or branches of trees, but sometimes in rocks, and also around human infrastructures such as man-made walls. In contrast, the new linage revealed here from the topotypic region, was only found associated with large granitic boulders in mountain habitats, even though it is a very limited sample.

Furthermore, the material recently assigned to *H. benguellensis* by Ceríaco et al. (2020a) presents some incongruence with our new topotypic material and the original *H. benguellensis* description. The historical material collected from Cahata and Ebanga (Bocage 1893; Monard 1937), makes reference to large sized specimens (SVL 55 mm and 42 mm, respectively), with 9 supralabials and 26–28 precloacal-femoral pores. Remarkably, this description agrees fully with the new specimens collected in Ebanga and Passe while underscoring differences from the recently reassigned *H. benguellensis*, which consistently presents 10–11 supralabials (Table S6). Moreover, the neotype specimen that was ascribed to *H. benguellensis* by Ceríaco et al. (2020a) is an adult male with 40.8 SVL and 33 precloacal-femoral pores. Therefore, based on a morphological evidence and incongruence with the original description, clear well-differentiated genetic distance and morphological differences between the two clades were detected, adding to the large distance from the original type locality (>250 km). Notably, the new specimens found near the original topotypic agrees perfectly with the original *H. benguellensis* described by Bocage (1893) and later reported by Monrad (1937) from Ebanga. However, due to the recent redescription and new type locality assigned by Ceríaco et al. (2020a), and in order to maintain taxonomic stability and to avoid more confusion within this group, we consider the new material recovered from near the original type locality of *H. benguellensis* as a new species.

Holotype. ANGOLA • 1 ♂; Benguela Prov., Ebanga; -12.77082°, 14.77102°; 1916 m a.s.l; 22 Feb. 2020; Pedro Vaz Pinto and Javier Lobón-Rovira; FKH0439.

Paratype. ANGOLA • 1 ♂; Benguela Prov., Passe; -12.66774°, 14.01607°; 828 m a.s.l; 13 Feb. 2020; Pedro Vaz Pinto and Javier Lobón-Rovira; FKH0413.

Diagnosis. A large sized *Hemidactylus*, with maximum SVL of 55 mm (mean) and maximum width of 10.5 mm (Fig. 13). Nine supralabials and 9–11 infralabials. Dorsal pholidosis with 13–18 rows of moderate strongly keeled tubercle scales and ventral pholidosis with 33–41 smooth and rounded scale rows on midbody. *Hemidactylus cinganji* **sp. nov.** present a moderate, triangular mental scale, two large postmentals followed by two medium post-postmentals. Tail with six strongly keeled dorsal tubercles rows dorsally and subcaudal scales medium sized, interspersed by 11 horizontal whorls of keeled scales on the original portion of the tail. Males with 26–28 continuous precloacal-femoral pores and 1–4 postcloacal tail spurs. Six divided scansors beneath first digit of both manus and pes, seven or eight beneath fourth digit of manus, eight or nine beneath the fourth digit of pes. Dorsum presents dark orange-beige coloration across the body with darker coloration on the dorsal part of the head that continues along the medial part of the dorsum until the sacrum.

Comparative diagnosis. *Hemidactylus cinganji* **sp. nov.** can be distinguished from other non-Angolan western and central Africa congeners based on the same characteristics of *H. benguellensis* (Ceríaco et al. 2020a). *Hemidactylus cinganji* **sp. nov.** can be distinguished from *H. mabouia* by the presence of smaller subcaudal scales (*vs.* large, elongated scales). It differs from the *H. bayonii*-group by its large size, largely keeled dorsal tubercle scales *vs* slightly keeled and larger number of precloacal-femoral pores (26–28 *vs.* 4–9 in *H. bayonii,* 4–6 in *H. vernayi*, 7–8 in *H. nzingae* and 8 in *H. gramineus*). It differs from *H. longicephalus*-group by larger number of precloacal-femoral pores (26–28 *vs.* 6–11 in *H. longicephalus* and 6–8 in *H. paivae*). It differs from *H. benguellensis* by lower number of supralabials (9 *vs.* 10–11 in *H. benguellensis*).

Holotype description (Fig. 13). Measurements and meristic characters of the holotype are presented in Table S6. Adult male with a snout-vent-length (SVL) of 45.05 mm and a tail length (TL) slightly smaller than SVL 42.07 mm. Body slender, nape distinct. Head slightly narrower than the body and moderate head length (HW/HL 0.72). Canthus rostralis not prominent. Eye diameter (3.05 mm), with vertical pupil and crenulated margin. Supraciliar scales small and rounded. Ear height (1.47 mm). Ear to eye distance slightly larger than orbit diameter (4.17 mm). Snout rounded and pointed. Frontal scales granular and larger than occipital scales. Occipital scales granular interspersed with large number of smooth and keeled tubercle scales from eyes to nape. Rostral undivided, in contact with 1st supralabial, nostril, supranasal and one internasal scales. 9 supralabial and 8–9 in-

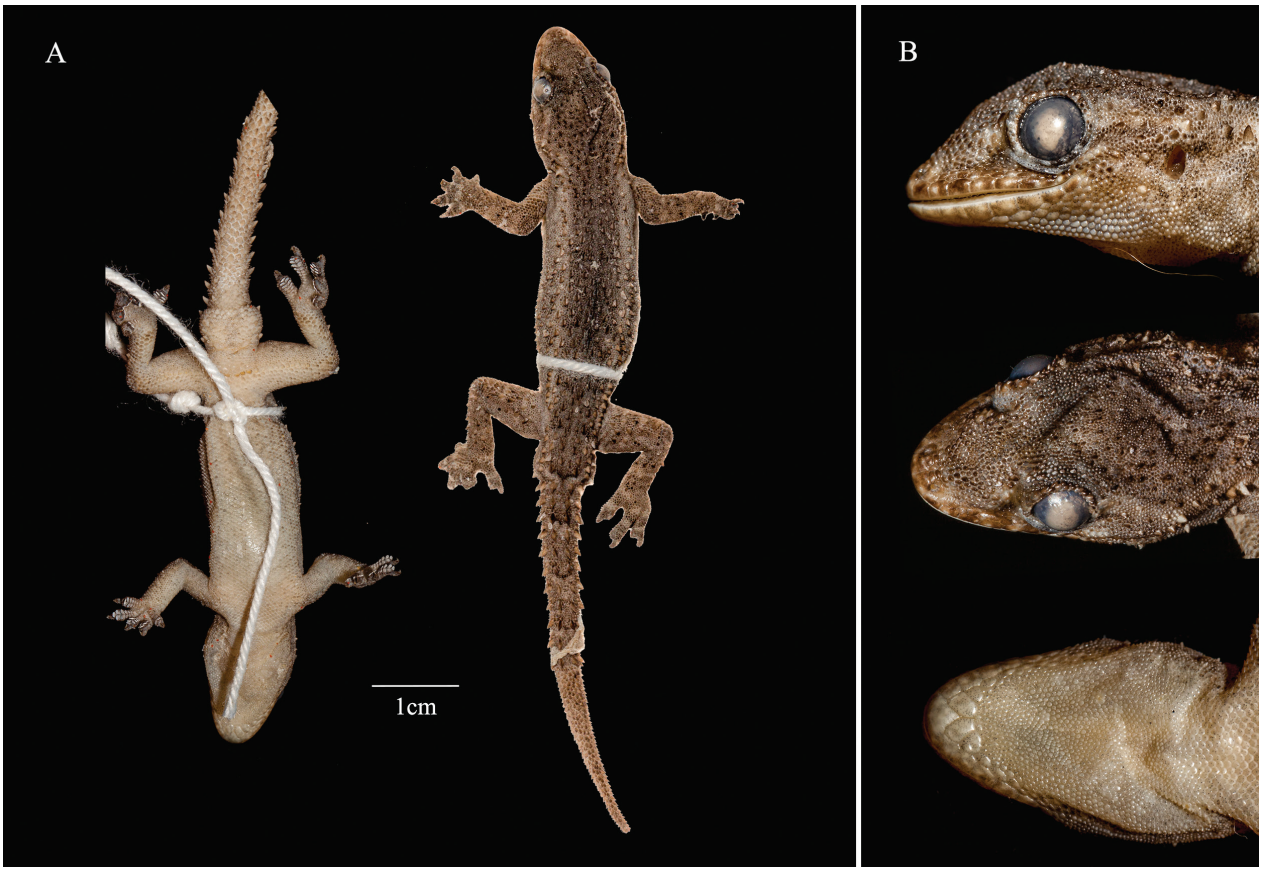

Figure 13. Holotype of *Hemidactylus cinganji* **sp. nov.** (FKH0439) from Ebanga, Benguela Province, Angola. **A** – Ventral and dorsal view of body. **B** – Detailed of head in lateral, dorsal and ventral views (from top to bottom). Photos by Pedro Vaz Pinto (A) and Rogério Ferreira (B).

fralabials. First supralabial and rostral in direct contact with the nostril. Nostril circular rounded by rostral, 1st supralabial, supranasal, and two postnasals. One row of scales between supralabials and the orbit. Mental large, triangular and rounded posteriorly, with two larges rectangular postmental scales in broad contact posteriorly to the mental. 2 post-postmental scales, in contact with post-postmental slightly smaller than postmental scales and 1st and 2nd infralabials. Gular scales slightly smaller than ventral scales and granular.

Body relatively robust and slightly elongated (TRL/SVL 0.40). Ventral scales widely larger than dorsal scales, with 32 scales across the belly. The dorsal pholidosis present heterogenous conical, granular scales interspersed by 15 strongly keeled dorsal tubercle rows of at midbody. Dorsal tubercle rows are separated by 3 granular scales. Tubercle scales reach the posterior part of the eye region where tubercle scales remain keeled. Tail with six strongly keeled dorsal tubercles rows dorsally and subcaudal scales medium sized, interspersed by 11 horizontal whorls of keeled scales on the original portion of the tail. Regenerated portion of the tail presents homogeneous scales all around the surface without tubercle scales. 27 precloacal-femoral pores enlarged and 2 well-developed postcloacal spurs on each side.

Fore- and hindlimbs relatively short, stout; forearm short (FL/SVL 0.15); tibia short (CL/SVL 0.16). Short digits strongly clawed. All digits of manus and pes indistinctly webbed. Scansors beneath each toe composed by 1st and terminal scansor undivided with the exception of 4th and 5th toes with 3 and 2 undivided terminal scansor, respectively. Scansors beneath each finger equally divided, with exception of 1st and last terminal scansor undivided. Number of scansors: 5-5-6-7-6 (right manus), 6-8-8-9-7 (right pes). Relative length of digits: V < IV=III > II > I (right manus); V < IV < III > II > I (right pes).

Variation. Variation in scalation and body measurements of the holotype and paratype of *H. cinganji* **sp. nov.** are reported in Table S6.

Coloration. *In life* (holotype FKH0439; Fig. 12A): this species displays a dark orange-beige coloration across the body with darker coloration on the dorsal part of the head that continues along the medial part of the dorsum until the sacrum; in the dorsal section it presents two lighter cream dorsolateral bands from the nares to the tail; the ventral part of the head shows a cream coloration with dispersed black speckles that increase in the anterior part of the infralabials; ventrum is uniform light beige or cream; supralabials are darker than infralabials; fore- and hindlimbs with irregular dark brownish coloration; tail with similar color and slightly banded; iris silvered with a black narrow pupil and brownish-golden reticulation. *In preservative* (Holotype; Fig. 13): dorsum with dark brownish coloration and two lighter dorso-

lateral bands from the narine till the sacrum; ventrum is light uniform beige. *Variation*: no variation was observed.

Etymology. The name "*cinganji*" is a widespread traditional word used in Angolan local languages that represents an ancestral spiritual entity that reincarnates assuming different physical forms in different places and occasions. This name is suitable as the new species corresponds to a taxon that was first described under a different name, then became lost and now resurfaces after its original name had been hijacked by a surrogate sister-species. The species epithet is used as a neuter singular noun in opposition to the generic name.

Distribution and conservation (Fig. 12B). The full distribution range of the species remains unknown, even though so far it has only been confirmed to occur in the interior of Benguela Province, from Cahata to Passe and Ebanga, above 800 m a.s.l. Due to poor sampling and few material confirmed to belong to this species, we cannot calculate the EOO and thus we regard the conservation status of the species as Data Deficient. Additional data will need to be collected to address its conservation status.

Natural history and habitat (Fig. 12C). *Hemidactylus cinganji* **sp. nov** exhibited a rock-dwelling behavior associated to large granitic boulders in mountainous regions from medium to high altitudes. The confirmed records fall in Benguela's transition region between the Scarp and Transitional Zone and the Angolan Highlands. Both specimens were collected at night while foraging in large vertical granitic walls, one on a mountain cliff and the other on a boulder overhanging a forest stream. However, due to the poor sampling of this species, its natural history and real habitat requirements remain uncertain.

Hemidactylus carivoensis sp. nov.

Figs 12 and 14

http://zoobank.org/472B97D3-9FF3-4676-B40B-B55A4CFDD44F

Hemidactylus carivoensis **sp. nov.** represents a new form genetically divergent from the two related species, with ND2 p-distance of 12.51% from *H. cinganji* **sp. nov.** and 12.48% from *H. benguellensis* (Table 1). Given the hypervariable morphology of the *H. benguellensis*-group, and the lack of molecular and morphological information before Ceríaco et al. (2020a), it is possible that some historical records of *H. benguellensis* may be assignable to this species. However, the morphological characteristics of *H. carivoensis* **sp. nov.** allows it to be unequivocally distinguished from *H. benguellensis* and *H. cinganji* **sp. nov.** (Table 2). Moreover, *H. benguellensis* has not yet been reported within the known distribution range of this newly described species (Marques et al. 2018; Ceríaco et al. 2020a; this study).

Holotype. ANGOLA • 1 ♀; Benguela Prov., Fazenda Carivo; -13.19167°, 13.41806°; 382 m a.s.l.; 15 Jul. 2018; Pedro Vaz Pinto; good condition with a ventral-lateral incision for the removal of liver sample and some torn skin in the ventrum; FKH0033.

Paratypes. ANGOLA • 1 ♀, juv.; Benguela Prov., Santa Maria, Praia do Meva; -13.19167°, 12.99139°; 287 m a.s.l.; 12 Nov. 2016; Pedro Vaz Pinto and William R. Branch; PEM R24218 (field number AG 16.63) • 1 ♂; same collecting locality as holotype; 7 Jan. 2020; MNCN 50542 • ♂; same collecting locality as holotype; Dec. 2020; ZMB 90453 • 1 ♂; Benguela Prov., between Dombe and Equimina; -13.18333°, 12.99139°; 367 m a.s.l.; 14 Feb. 2020; Pedro Vaz Pinto and Javier Lobón-Rovira; MNCN 50543 • 1 ♀; same collecting details as previous material; ZMB 90452.

Additional material. ANGOLA • 2 ♂, subadult; same collecting locality as holotype; Dec. 2020; MNCN 50544 and FKH0499 • 1 ♀; same collecting locality as previous; FKH0500.

Diagnosis. A medium sized *Hemidactylus*, with SVL of 43.2 mm (mean) and maximum width of 8.8 mm (Fig. 14). 9–11 supralabials and 8–10 infralabials. Dorsal pholidosis with 15–22 rows of moderate strongly keeled tubercle scales and ventral pholidosis with 32–38 smooth and rounded scale rows around midbody. *Hemidactylus carivoensis* **sp. nov.** present a moderate, triangular, moderate rounded posteriorly mental scale, two large postmentals followed by two large post-postmentals. Tail with four strongly keeled dorsal tubercles rows dorsally and subcaudal scales small, about one fourth of the tail width, interspersed by large series of horizontal whorls of keeled scales. Males with 15–22 continuous precloacal-femoral pores. Five divided scansors beneath first digit of both manus and pes, seven or eight beneath fourth digit of manus, nine beneath the fourth digit of pes. Dorsum darker coloration on the dorsal part of the head that continues along the medial part of the dorsum until the sacrum.

Comparative diagnosis. *Hemidactylus carivoensis* **sp. nov.** can be distinguished from other non-Angolan western and central African congeners based on the same characteristics of *H. benguellensis* (Ceríaco et al. 2020a). *Hemidactylus carivoensis* **sp. nov.** can be distinguished from *H. mabouia* by the presence of smaller subcaudal scales (vs. large elongated scales). It differs from the *H. bayonii*-group by the presence of largely keeled dorsal tubercle scales *vs.* slightly keeled, larger number of precloacal-femoral pores (17–22 *vs.* 4–9 in *H. bayonii,* 4–6 in *H. vernayi,* 7–8 in *H. nzingae* and 8 in *H. gramineus*), larger number of ventral scales across the belly (34–38) than *H. bayonii* (29–32), *H. nzingae* (22–27), *H. gramineus* (23–25) and *H. faustus* **sp. nov.** (29–32). The new species differs from *H. longicephalus*-group by a larger number of precloacal-femoral pores (17–22 *vs.* 6–11 in *H. longicephalus* and 6–8 in *H. paivae*), smaller SVL (maximum SVL 45.2 mm [mean=43.19] in *H. carivoensis* **sp. nov.** *vs.* 60.07 mm [mean=46.6] in *H. longicephalus* and 68.4 mm [mean=58.96] in *H. paivae*) and lower number

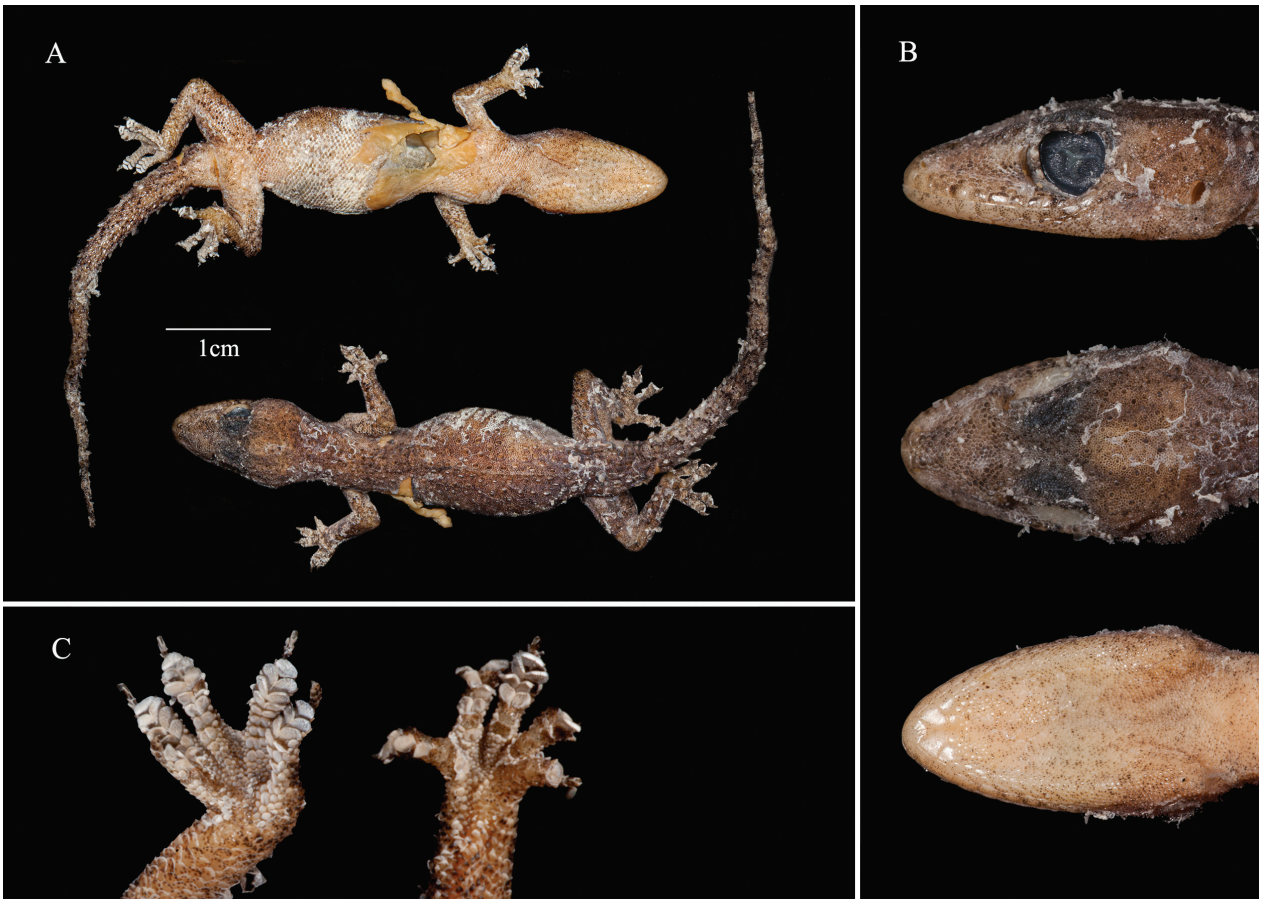

Figure 14. Holotype of *Hemidactylus carivoensis* **sp. nov.** (FKH0033) from Carivo, Benguela Province, Angola. **A** – Ventral and dorsal view of body. **B** – Details of head in lateral, dorsal and ventral views (from top to bottom). **C** – Details of right toes and left fingers (from left to right). Photos by Pedro Vaz Pinto.

of lamellae under 1st toe (5 in *H. carivoensis* **sp. nov.** *vs.* 6–7 in *H. longicephalus*-group). *Hemidactylus carivoensis* **sp. nov.** differs from *H. benguellensis*-group by less keeled and rounded dorsal tubercles, number of precloacal-femoral pores (15–22 *vs.* 23–33 in *H. benguellensis* and 26–28 in *H. cinganji* **sp. nov.**), the presence of consecutive series of keeled subcaudal scales under the tail whorls, larger number of ventral scales across the belly (34–38 in *H. carivoensis* **sp. nov.** *vs.* 30–32 in *H. cinganji* **sp. nov.**) and large number of supralabials (10–11 in *H. carivoensis* **sp. nov.** *vs.* 9 in *H. cinganji* **sp. nov.**) (see Table 2, for comparison with other Angolan congeners).

Holotype description (Fig. 14). Measurements and meristic characters of the holotype are presented in Table S7. Adult female with a snout-vent-length (SVL) of 45.16 mm and a tail length (TL) about the same size than SVL 44.79 mm. Body slender, nape distinct. Head slightly narrower than the body and largely elongated (HW/HL 0.65). Canthus rostralis not prominent. Eye diameter (3.04 mm), with vertical pupil and crenulated margin. Supraciliar scales small and rounded. Ear height (0.83 mm). Ear to eye distance slightly larger than orbit diameter (3.46 mm). Snout rounded and pointed. Frontal scales granular and larger than occipital scales. Occipital scales granular interspersed with large number of smooth and conical tubercle scales from eyes to nape. Rostral wider than deep (2.31 *vs.* 0.93 mm, respectively). Rostral semi-divided posterodorsally, in contact with 1st supralabial, nostril, two postnasals and one internasal scales. Eleven supralabials and 9 infralabials. First supralabial in contact with the nostril. Nostril circular rounded by rostral, supranasal and two postnasals. Postnasals larger than supranasal. One or two rows of scales between supralabials and the orbit. Mental large, triangular and rounded posteriorly, with two large rectangular postmental scales in broad contact posteriorly to the mental. 4 post-postmental scales, composed by post-postmental slightly smaller than postmental scales in contact with postmentals and 1st and 2nd infralabials, and 2 post-postmental half size than lateral post-postmental in contact with postmental scales. Gular scales slightly smaller than ventral scales and granular. Between the gular scales and infralabials a row of enlarged scales is present, decreasing in size until the 5th infralabial where they become the same size as the gular scales.

Body relatively robust and slightly elongated (TRL/SVL 0.39). Ventral scales widely larger than dorsal scales, with 36 scales across the belly. The dorsal pholidosis present heterogenous conical, granular scales interspersed by 17 strongly keeled dorsal tubercle rows of at midbody. Dorsal tubercle rows are separated by 3 granular scales. Tubercle scales reach the posterior part of the eye region where tubercle scales lose the keeling

progressively. Tail with four strongly keeled dorsal tubercles rows dorsally and subcaudal scales small, about one fourth of the tail width, interspersed by 22 horizontal whorls of keeled scales. Precloacal scales enlarged and one well-developed postcloacal spur on each side.

Fore- and hindlimbs relatively short, stout; forearm short (FL/SVL 0.16); tibia short (CL/SVL 0.18). Short digits and clawed. All digits of manus and pes indistinctly webbed. Scansors beneath each toe composed by 1st and two terminal scansor undivided. 4th toes with 3 undivided terminal scansors. Scansors beneath each finger equally divided, with the exception of 1st and last terminal scansors undivided. Number of scansors: 6-6-7-7-7 (right manus), 7-8-9-10-7 (right pes). Relative length of digits: V < IV=III > II > I (right manus); V < IV < III > II > I (right pes).

Variation. Variation in scalation and body measurements of the paratypes of *H. carivoensis* **sp. nov.** are reported in Table S7. All the material analyzed is in agreement entirely with the holotype.

Coloration. *In life* (specimen MNCN 50543; Fig. 12A): this species displays an orange-beige coloration across the body with darker coloration on the dorsal part of the head that continues along the medial part of the dorsum until the sacrum; in the dorsal section presents two lighter dorsolateral bands from the nares to the tail; the ventral part of the head shows a cream coloration with dispersed black speckles that increase towards the anterior part of the infralabials; ventrum is uniform light beige or cream; supralabials are darker than infralabials; fore- and hindlimbs present an irregular dark brownish coloration; tail with similar color and slightly banded; iris silvered with a black narrow pupil and brownish-golden reticulation. *In preservative* (Holotype; Fig. 14): dorsum with dark greyish coloration and two lighter dorsolateral bands from the narine till the sacrum; ventrum is light uniform beige. *Variation*: ventrum can be uniform beige or present scattered black speckles; crossband of the tail can be present or absent.

Etymology. The species epithet "*carivoensis*" refers to the Farm Carivo, an old estate situated along the banks of the mid-lower Coporolo River on the coastal plain of Benguela Province, and where most of the type series was collected. The species proved to be common in the area, and by recognizing the farm, we also acknowledge the ongoing support from the owners to researchers, similar to the Chapmans nearly a century ago.

Distribution and conservation (Fig. 12C). The full distribution range of the species remains unknown, even though so far it has only been confirmed to occur across the coastal plain of western Benguela Province. Due to the variable morphology of the taxon known as *H. benguellensis* and which formerly included material now assigned to *H. cinganji* **sp. nov.**, it is possible that some historical material was wrongly identified and should instead belong to this newly described species. Spiny savannas are well distributed in western Angola, suggesting that the new species might be common across a wider range than what is currently known, but available data is still poor. However, due to limited material confirmed to belong to this species, we can't calculate the EOO and we regard the conservation status of this species as Data Deficient. Therefore, it is important for future studies to establish the real distribution of *H. benguellensis*, *H. cinganji* **sp. nov**. and *H. carivoensis* **sp. nov.** to better determine the conservation status of the species.

Natural history and habitat (Fig. 12B). *Hemidactylus carivoensis* **sp. nov.** represents an arboreal species occurring on coastal savanna habitats dominated by small acacia (*Senegalia* spp.) trees and bushes, and often with abundant accumulation of dead wood. Their preferred habitat is well contained within the Semi-arid Savannas. The species was found during night surveys and in sympatry with *Afrogecko ansorgi*, albeit in different niches. While individuals of *A. ansorgi* were found foraging in small twigs and branches at medium height of bushes (Vaz Pinto et al. 2019), *H. carivoensis* **sp. nov.** were always collected at the base of bushes and tree trunks, or in fallen branches or dead wood on the ground.

Species not assignable to specific species groups

Hemidactylus faustus sp. nov.

Fig. 15–16

http://zoobank.org/0EE8A34E-473A-496D-80A6-8259896BC4B5

The phylogenetic analysis revealed that *Hemidactylus faustus* **sp. nov.** clusters within a large clade, which includes the *H. nzingae*-group, *H. bayonii*-group, *H. benguellensis*-group, and *H. pfindaensis*, although its phylogenetic position is not well-stablished (Fig. 2). However, according to the morphological and genetic analysis performed, this species represents a well-differentiated clade from *H. bayonii*-group and *H. benguellensis*-group, with 17.85% and 16.72% uncorrected p-distance, respectively (Table 1). This species represents a micro-endemic form only known from a unique geological formation, possibly a relic species confined to the massive conglomerate inselbergs of Pungo Andongo and surrounds, in Malanje Province. Due to their exclusive morphological characteristics and the elusive behavior of the species, we consider that no other specimens have been reported before and mistaken with any of its congeners.

Holotype. ANGOLA • 1 ♀; Malanje Prov., Pungo Andongo; -9.67333°, 15.59222°; 1217 m a.s.l.; 11 Jul. 2019; Pedro Vaz Pinto and Javier Lobón-Rovira; good condition with partially regenerated tail; FKH0281.
Paratypes. ANGOLA • 1 ♂; same collecting details as holotype; MNCN50534 • 2 ♀; same collecting details as holotype; MNCN50535

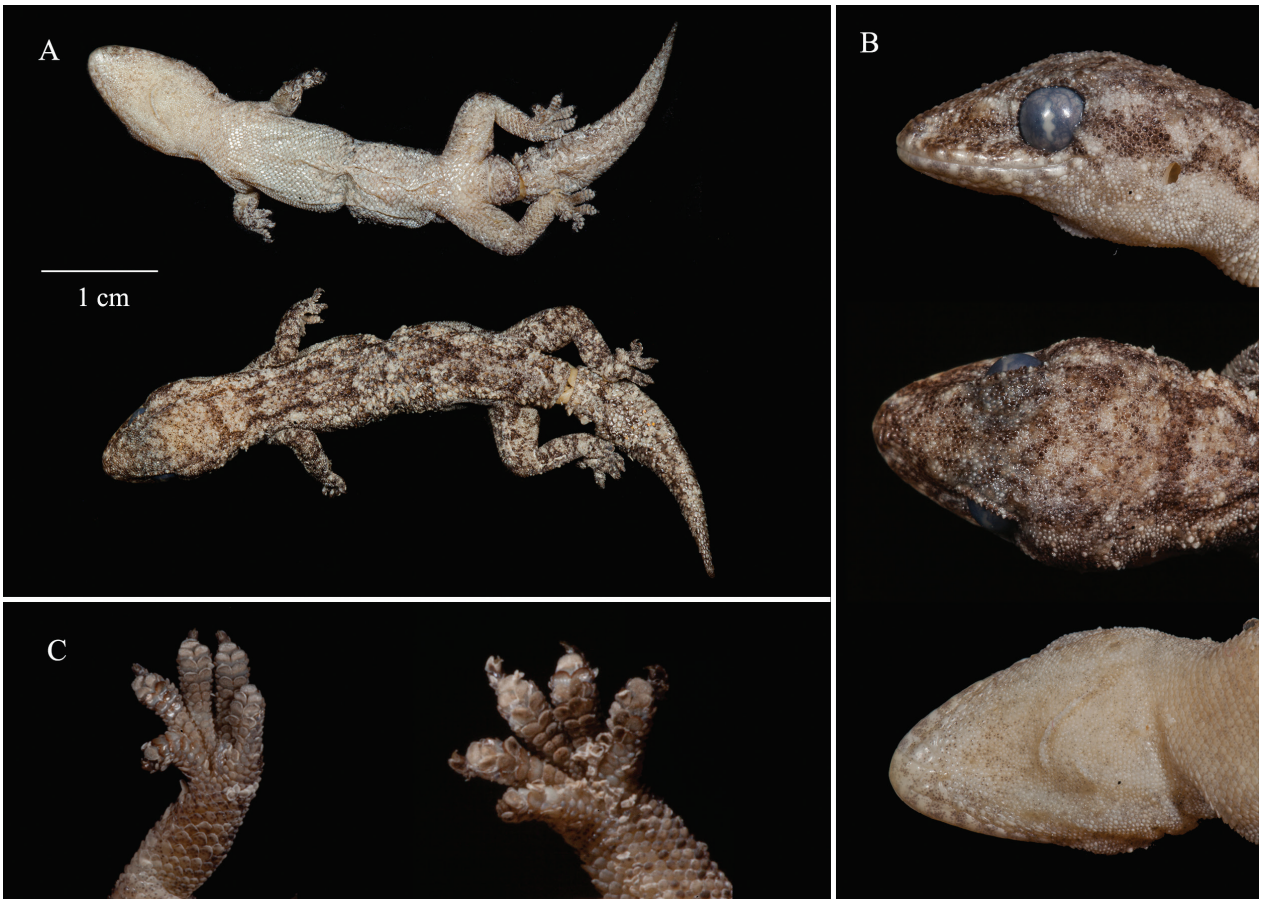

Figure 15. Holotype of *Hemidactylus faustus* **sp. nov.** (FKH0281) from Pungo Andongo, Malanje Province, Angola. **A** – Ventral and dorsal view of body. **B** – Details of head in lateral, dorsal and ventral views (from top to bottom). **C** – Details of left toes and right fingers (from left to right). Photos by Pedro Vaz Pinto.

and ZMB 90447 • 1 ♀; same collecting locality as holotype; 11 Aug. 2018; Beatriz Vaz Pinto; FKH0023.

Additional material examined. ANGOLA • 1 ♀; same locality as type material; 11 Aug. 2018; Pedro and Afonso Vaz Pinto; ZMB 90446 • 1 ♂, juv.; same collecting details as previous material; ZMB 90445 • ♀; same locality as type material; 15 Oct. 2020; Pedro Vaz Pinto; MNCN 50536.

Diagnosis. A robust medium sized *Hemidactylus*, with SVL of 39.4 mm (mean) and maximum width of 7.4 mm (Fig. 15). 8–9 supralabials and 7–8 infralabials. Dorsal pholidosis with 15–17 rows of moderate keeled tubercle scales and ventral pholidosis with 29–32 smooth and rounded scale rows around midbody. *Hemidactylus faustus* **sp. nov.** present a moderate, triangular mental scale, two large postmentals followed by two large post-postmentals. Tail with thickness at the base tail with conical tubercle rows laterally. Regenerated tail with regular larger scales. Males with 17–19 continuous precloacal-femoral pores. Five or six divided scansors beneath the first digit of both manus and pes, seven beneath the fourth digit of manus, eight or nine beneath the fourth digit of pes. Dorsum coloration with two darker dorsolateral bands from the occiput to the tail, which includes 5 W-shaped darker crossbands in contact with both lateral bands; each dark crossbar is separated by lighter blotches.

Comparative diagnosis. Head slightly more quadrangular than the other members of the Angolan *Hemidactylus* (HL/HW ≤1.4 *vs.* >1.5 Angolan congeners) and regenerated thickened tail found in all specimens collected (n=8), a feature never recorded among Angolan congeners. It can be distinguished from the other non-Angolan western and central Africa congeners based on the same characteristics of the other Angolan species (Ceríaco et al. 2020a). *Hemidactylus faustus* **sp. nov.** can be distinguished from Angolan congeners by the thickness at the base tail. Additionally, it could be distinguished from *H. mabouia* by the presence of smaller subcaudal scales, and from *H. benguellensis*-group by lower number of precloacal-femoral pores (17–19 *vs.* 23–33 in *H. benguellensis*, and 26-28 *H. cinganji* **sp. nov.**), less keeled tubercle rows, smaller maximum length (45.3 mm [mean=39.8] *vs.* 54.5 [mean=47.5]), the dark dorsal uniform color with dorsolateral light stripes and absence of dorsolateral orange tubercle rows (present in *H. benguellensis*-group). It differs from *H. carivoensis* **sp. nov.** by the absence of keeled subcaudal scales, less keeled dorsal tubercle rows, and dark dorsal uniform color with dorsolateral light stripes and absence of dorsolateral orange tubercle rows. *Hemidactylus faustus* **sp. nov.** differs from the *H. longicephalus*-group by having smaller SVL (maximum length 45.3 mm [mean=39.8] *vs.* 60.08 [mean=46.57] in *H. longicephalus* and 64.8 [mean=58.96] in *H. pai-*

vae), larger number of precloacal-femoral pores (17–19 *vs.* 6–11 in *H. longicephalus* and 6–8 in *H. paivae*) and lower number of granular scales between the dorsal tubercles (2–3 *vs.* 3–6 in *H. longicephalus* and 4–9 in *H. paivae*). It differs from the *H. bayonii*-group by having a larger SVL (maximum SVL 45.3 mm [mean=39.8]), than *H. bayonii* 36.2 mm [mean=34.9] and *H. vernayi* (42.5 mm [mean=32.7]), and lower than *H. nzingae* (51.5 mm [mean=44.3]) and larger number of precloacal-femoral pores (17–19 *vs.* 4–9 in *H. bayonii,* 4–6 in *H. vernayi*, 7–8 in *H. nzingae* and 8 in *H. gramineus*).

Holotype description (Fig. 15). Measurements and meristic characters of the holotype are presented in Table S8. Adult female with a snout-vent-length (SVL) of 39.39 mm and regenerated tail length (TL) of 22.84 mm. Robust body, nape slightly distinct. Head slightly wider than the body and shorten (HW/HL 0.67). Canthus rostralis not prominent, but slightly marked. Eye diameter (3.05 mm), with vertical pupil and crenulated margin. Supraciliar scales small and pointed. Ear height (0.98 mm). Ear to eye distance slightly larger than orbit diameter (3.17 mm). Snout rounded. Frontal scales granular and of similar size as occipital scales. Occipital scales granular interspersed with large number of smooth and conical tubercle scales from eyes to nape. Rostral wider than deep (1.66 *vs.* 0.91 mm, respectively). Rostral semi divided posterodorsally, in contact with 1st supralabial, nostril, two postnasal and one internasal scales. 9 supralabial and 7 infralabials. First supralabial in contact with the nostril. Nostril circular rounded by rostral, supranasal, prenasal and 2 postnasals. Prenasal, postnasal and supranasal same size. One row of scales between supralabials and the orbit. Mental large, triangular, with two larges rectangular postmental scales in short contact posteriorly to the mental. 7 post-postmental scales, composed by 2 post-postmental half size of postmental scales in contact with postmentals and 1st and 2nd infralabials, and 5 small post-postmentals in contact with postmental scales. Gular scales half size than ventral scales and granular. Between the gular scales and infralabials a row of enlarged scales is present, decreasing in size towards the 5th infralabial where they become the same size as the gular scales.

Body robust and slightly short (TRL/SVL 0.41). Ventral scales widely larger than dorsal scales, with 31 scales across the belly. The dorsal pholidosis presents heterogenous conical, granular scales interspersed by 16 conical dorsal tubercle rows at midbody. Dorsal tubercle rows are separated by 3 granular scales. Tubercle scales reach the posterior part of the eye region where they lose the keeling progressively. Tubercle in the base of tail is well developed. Tail with lateral conical tubercle rows. Regenerated tail with regular larger scales (after precloacal) enlarged and 2 well-developed postcloacal spurs on each side.

Fore- and hindlimbs relatively short, stout; forearm medium sized (FL/SVL 0.23); tibia short (CL/SVL 0.18). Digits short and clawed. All digits of manus and pes indistinctly webbed. Scansors beneath toes and fingers are equally divided and composed by 1st scansor undivided and variable number of undivided terminal scansors. Number of scansors: 6-8-7-7-7 (right manus), 7-10-11-10-9 (right pes). Relative length of digits: V < IV < III > II > I (right manus); V < IV < III > II > I (right pes).

Variation. Variation in scalation and body measurements of the paratypes and additional material of *H. faustus* **sp. nov.** are reported in Table S8. All the material examined is in concordance with the description of the holotype.

Coloration. *In life* (specimen MNCN 50534; Fig. 16A): this species displays a nocturnal greyish or brownish coloration above with two darker dorsolateral bands from the occiput to the tail, which includes 5 W-shaped darker crossbands in contact with both lateral bands; each dark crossbar is separated by lighter blotches; head with an irregular dark and light brownish patch and a dark brownish band from the narine to anterior portion of the forelimb; light beige ventrally and laterally, with scattered black speckles in the venter; upper and lower labials beige; limbs with irregular dark-and-light brownish patches; tail with similar color and slightly banded; iris silvered with a black narrow pupil and brownish-golden reticulation. During the day, this species presents a uniform pattern along the body. *In preservative* (Holotype; Fig. 15): dorsum with dark coloration and five spaced darker W-shaped crossbars from the occiput to the tail that could be difficult to distinguish, with lighter dorsolateral bands; ventrum light beige with scattered black speckles. *Variation*: from light brownish to totally dark dorsal coloration; cross-bands can be difficult to distinguish; ventrum can be uniform beige or have scattered black speckles.

Etymology. The name "*faustus*" applies to a Latin word that designate 'good luck', evoking the serendipitous discovery of this species. The species epithet is used as a masculine adjective singular. The first specimen was found by Beatriz Vaz Pinto, daughter of PVP, under a small stone which was removed while preparing a campsite. This unexpected find led to further collecting of this new and previously unrecorded form, albeit from a locality that had been regularly surveyed since the mid-19th century.

Distribution and conservation (Fig. 16C). This species is likely a micro-endemic form, strictly associated with the conglomerate inselbergs of Pungo Andongo also known as Pedras Negras (Black Rocks), just north of the mid-Cuanza River in western Malanje Province, Angola (Fig. 16C). At the moment the only know population occurs on this site, which covers approximately 4,000 ha of huge rocky conglomerate boulders. A similar and nearby inselberg system – Pedras Jingas, albeit smaller, shares identical geological features as Pungo Andongo, being situated some 20kms to the northeast. It is quite possible that the species is present at Pedras Jingas and also in a few smaller isolated inselbergs nearby, but these areas have not been surveyed yet. All considered, it is likely that *H. faustus* **sp. nov.** is contained within about 6,000 ha of suitable habitat in the region. However, due to the

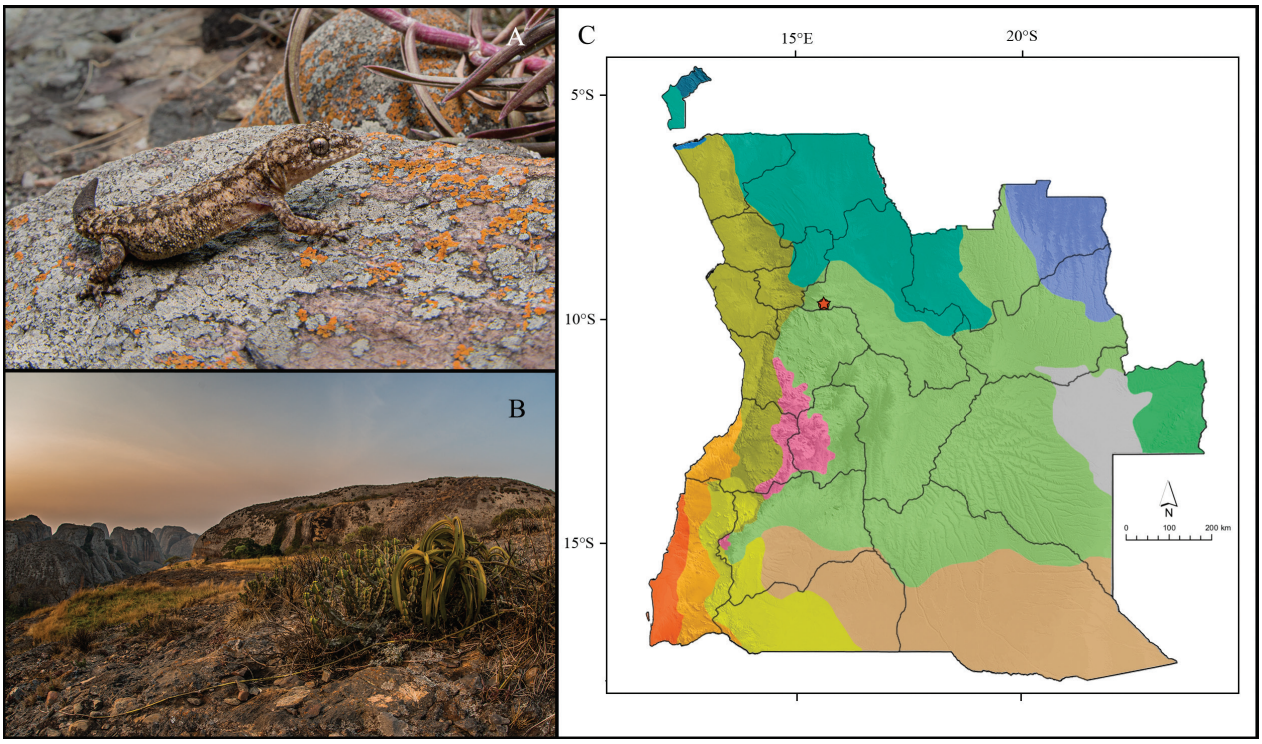

Figure 16. A – Dorsolateral view of *Hemidactylus faustus* **sp. nov.** (MNCN 50534). **B** – Pungo Andongo, habitat of *H. faustus* **sp. nov. C** – records of *H. faustus* **sp. nov.** (star depicting type locality and only known locality). Photos by Javier Lobón–Rovira.

limited material confirmed to belong to this species, we cannot calculate the EOO and we regard the conservation status of this species as Data Deficient. This species needs further studies about the real extent of its range and current population trends to better address its conservation status. Due to its small distribution range and highly specialized niche this species may provisionally warrant a threat status.

Natural history and habitat (Fig. 16B). *Hemidactylus faustus* **sp. nov.** represents a ground-dwelling rupicolous species apparently associated with the unique geological formation of conglomerate massifs in northern Angola. It was found sheltering under small rocks or between the cavities created by plant roots growing on the flattened top of massive inselbergs, at around 1250 m a.s.l. Most specimens were collected at night foraging on the ground or at times climbing the sparse and stunted vegetation present, possibly hunting small spiders and other invertebrates. The specimens displayed an elusive behavior, jumping and disappearing quickly between the cavities and among vegetation roots when disturbed. The species occurs in sympatry with *H. paivae* (see Table S2 for *H. paivae* recorded localities), which occupies a different ecological niche, the latter living on the vertical and inaccessible walls of the conglomerate boulders. Both species could also be found in the rocky conglomerate base that makes the transition between various inselbergs. The site where the species was discovered lies within the Angolan Miombo Woodlands, even though the local ecological conditions can be considered atypical.

Hemidactylus mabouia

Hemidactylus mabouia is the most genetically distant species from all the Angolan congeners (minimum ND2 uncorrected p-distance >26%, see Table 1). Furthermore, *H. mabouia* can be easily differentiated from all its Angolan congeners by the presence of enlarged medial subcaudals, being absent in all Angolan *Hemidactylus* (Ceríaco et al. 2020a). Therefore, all records genetically or morphologically assigned to *H. mabouia* have been considered as unequivocal records, in absence of more accurate and recently studies within *H. mabouia*-group.

Consequently, this work provides 25 new records (Table S2, Fig. 17) for *H. mabouia* within Angolan territory. It is remarkable that this work provides the first records of *H. mabouia* in Bié Province, collected by Werner Conradie, Luke Verburgt and Alexander Rebelo between 2016 and 2018, and the eastern-most record within Angola territory from Lucapa, Lunda Norte Province, collected by William R. Branch and Werner Conradie in 2011 (Fig. 17). Moreover, this work demonstrates the large adaptability of *H. mabouia*, being present in at least 8 of the 13 AMBUs defined in this work (Fig. 17).

Key of morphological identification of species of *Hemidactylus* occurring in Angola (adapted from Ceríaco et al. 2020a):

1a) Median subcaudals broadened transversely (> ½ tail width)..... ***H. mabouia***
1b) Median subcaudals small, not forming broad transverse plates (< ½ tail width) **2**
2a) Regenerate and original tail widened at the base..... ***H. faustus* sp. nov.**
2b) Regenerate and original tail not widened at the base..... **3**
3a) Precloacal-femoral pores > 15 ..... **4 (*H. benguellensis*-group)**
3b) Precloacal-femoral pores < 11 ..... **6**
4a) Series of keeled subcaudal scales under the tail whorls and precloacal-femoral pores < 22 ..... ***H. carivoensis* sp. nov.**
4b) Lack of keeled subcaudal scales and precloacal-femoral pores > 23 ..... **5**
5a) 9 Supralabials..... ***H. cinganji* sp. nov.**
5b) ≥ 10 Supralabials..... ***H. benguellensis***
6a) Feebly keeled dorsal and caudal tubercles..... **7**
6b) Strongly keeled dorsal and caudal tubercles..... **10**
7a) SVL of adult individuals < 43 mm ..... **8 (*H. bayoni*-group)**
7b) SVL of adult individuals > 44 mm ..... **9 (*H. longicephalus*-group)**

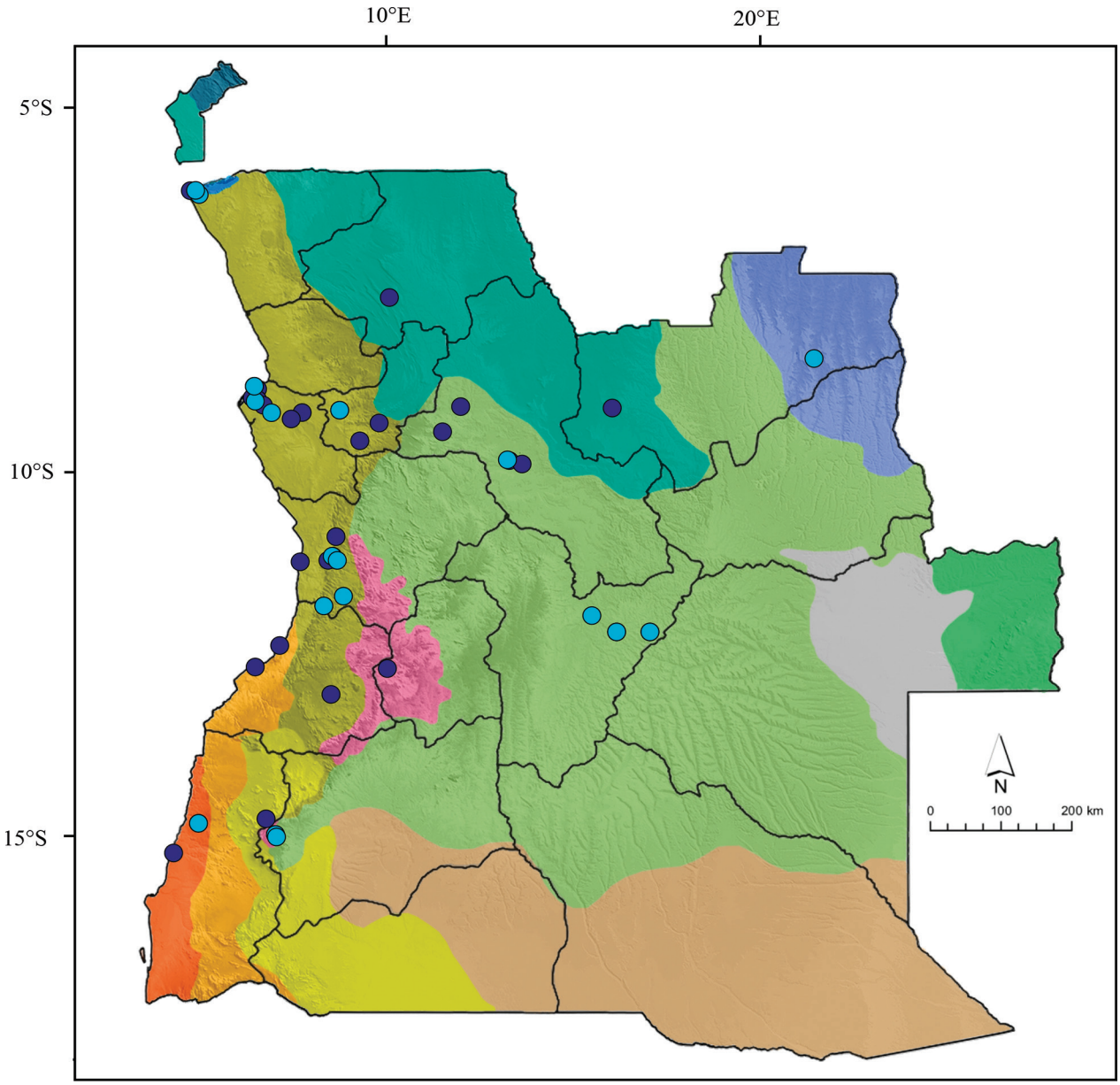

Figure 17. Records of *Hemidactylus mabouia* in Angola. Dark blue circles represent records provided by Ceríaco et al. 2020a; light blue circles depict new records provided by this work.

8a) Scales across the belly usually more than 32 ..... ***H. vernayi***
8b) Scales across the belly usually less than 32 ..... ***H. bayonii***
9a) TRL/SVL ratio ≥ 0.44 ..... ***H. paivae***
9b) TRL/SVL ratio < 0.44 ..... ***H. longicephalus***
10a) Scales across the belly < 27 and dorsal tubercle rows more than 15 ..... ***H. nzingae***
10b) Scales across the belly ≥ 28 and dorsal tubercle rows less than 13 ..... ***H. pfindaensis* sp. nov.**

Discussion

Knowledge on Angolan herpetofauna has notably increased in recent years, with several new reptile species being described in recent years (Conradie et al. 2020; Marques et al. 2020; Branch et al. 2021; Ceríaco et al. 2020a, b, c; Hallerman et al. 2020). Yet, we are still far from having a clear picture on the real levels of diversity within the country, despite recent efforts. Thorough studies combining molecular, morphological, and ecological data are much needed to accomplish this goal.

This work provides the first integrative taxonomic assessment for Angolan *Hemidactylus*, in which large biogeographic, phylogenetic and morphological datasets were analyzed to address variability and cryptic diversification in the genus. The study highlights that integrative taxonomy provides a more robust tool to resolve traditional taxonomical hypotheses thereby avoiding misidentifications (Schlick-Steiner et al. 2010). Based on genetic, morphological, and biogeographic data we described four new species (*H. pfindae* **sp. nov.**, *H. cinganji* **sp. nov.**, *H. carivoensis* **sp. nov.** and *H. faustus* **sp. nov.**), enhanced the diagnosis and taxonomic position of two recently described species (*H. vernayi* and *H. paivae*) and synonymized one recently described species (*H. hannahsabinae*). Consequently, the number of Angolan *Hemidactylus* now increased from eight to 11 species.

Time-tree analysis shows that most Angolan *Hemidactylus* lineages have diversified during the Miocene, coinciding with a progressively cooling climate and increased climatic seasonality in southern Africa, leading to the expansion of moist savannas and increased ecological heterogeneity (Herbert et al. 2016), which has been associated with speciation across different taxonomical groups, including reptiles (Gamble et al. 2008; Agarwal and Karanth 2015; Zimkus et al. 2017; Werneck et al. 2018; Xu et al. 2020). The currently recognized Angolan *Hemidactylus* (with the exception of *H. mabouia* which is a widespread species across Africa and the Americas) could be traced to seven recognized lineages at the end of the Miocene. These include one lineage represented today by the inland species *H. nzingae*, possibly splitting from the clades currently represented by the coastal cluster *bayonii-vernayi*, and from the lineage leading to *H. pfindaensis* **sp. nov.**, a rainforest specialist. Even though no clear morphological differences were found, the molecular substructure found within *H. pfindaensis* **sp. nov.** in both mitochondrial and nuclear markers, when comparing material from Cabinda and Uíge Provinces, suggest that it may include specific differentiation. However, such scenario could not be explored further due to the very small sample size available.

A fourth lineage of uncertain phylogenetic relationships is represented by the highly specialized and micro-endemic form *H. faustus* **sp. nov.**, whose ancestors may have persisted in the inselberg regions of Pungo Andongo as climatic instability could have increased selection pressure over *Hemidactylus* populations, possibly leading to local extinctions and higher specialization. Two other closely related Miocene lineages may have primarily evolved in the highly heterogeneous and mountainous regions of southern central Angola, possibly splitting into a coastal form represented today by *H. carivoensis* **sp. nov.**, and a highland lineage that includes the cluster *H. benguellensis-cinganji*. The seventh and most divergent of all Angolan *Hemidactylus* lineages includes the *H. longicephalus*-group, which may have evolved in moister habitats along the Angolan escarpment forests. Our findings suggest that three of these seven lineages may have split further in response to habitat shifts resulting in niche specialization, likely during the Pliocene. We now recognize several of these younger lineages as species. The coastal lineage may have split into an arid-adapted arboreal form, represented by *H. vernayi*, and a more woodland/thickets ground-dwelling form, represented by *H. bayonii*. The highland lineage is represented by one form *H. cinganji* **sp. nov.**, which to date has only been found in Benguela's escarpment and its lower highlands where it may have evolved, and a second, highly variable taxon in southern Angola, now recognized as *H. benguellensis*. The latter species is atypical among Angolan *Hemidactylus*, because of its morphological variability and adaptability to different niches and ecological conditions. Furthermore, it is present across different biomes and a high range of altitudes, from montane environments to the Namib Desert. Interestingly, a similar speciation pattern was found in another Angolan gekkonid of the genus *Afroedura*, in which the species present in the southern highlands is also widespread across the coastal plain while showing a much deeper divergence with remaining highland species (Branch et al. 2021). Being often found in highly impacted environments, it is possible for *H. benguellensis* to take advantage of habitat transformation and human intervention, which could have led to some recent opportunistic expansion. On the other hand, the morphological variability across its range suggests some degree of adaptive plasticity.

Finally, the more divergent *H. longicephalus*-complex, may also have diversified during the Pliocene, forming three clades, two within *H. longicephalus*, and the other represented by *H. paivae*. The two H. *longicephalus* clades showed only moderate genetic differentiation and could not be separated morphologically or ecologically. Therefore, we speculate that both arboreal forms are likely going through an incipient process of speciation, with two lineages that may have evolved segregated by the Cuanza River. Angolan Scarp forests are known to promote speciation, which has been well documented in the case of birds, for which there are endemic representatives on the scarp forest blocks north and south of the Cuanza River (Dean et al. 2019). Nevertheless, the fact that *H. longicephalus* does not appear to be a strictly forest-bound species but is rather also distributed across the intermediate coastal woodlands and thickets may explain some of the current geographic overlap between these two lineages. On the other hand, human-mediated dispersal could be involved and explain the species occurrence in São Tomé. The fact that a relatively recent speciation process along the Angolan escarpment is not discernible in a conspecific population present in a remote volcanic island, makes it extremely unlikely for the colonization of São Tomé by *H. longicephalus* to have been a natural process. The most parsimonious explanation is that specimens from the northern lineages, may have been accidentally introduced to the island following maritime commerce routes, active for centuries and linking the former Portuguese colonies of Angola and São Tomé. Similar faunal introductions have previously been documented for São Tomé, as for example the introduction of a bird species, *Euplectes aureus*, otherwise endemic to western Angola (Christy and Clarke 1998). Finally, the third closely related clade, *H. paivae*, may represent a lineage, which adapted to a rupicolous niche and expanded eastwards in response to climatic changes such as droughts followed by local extinction and fragmentation in escarpment populations.

Nevertheless, the relatively poor molecular support, absence of clear morphological differentiation and possible distributional and molecular overlap with sister-clades, suggests that the validity of *H. paivae* and *H. gramineus* (from the Congo basin) may be questionable and should be reassessed in the future appending availability of larger series with better geographical coverage and additional molecular data.

We applied a preliminary biogeographic overview framework extracted from a rendition of Angola's Main Biogeographic Units (AMBU), which is currently being elaborated (Veríssimo et al. *in prep.*). This categorization is used to tentatively provide interpretations of scenarios for the distributions and ecological requirements of regional populations of *Hemidactylus*. Notably all strictly Angolan taxa, with the exception of the highly adaptable *H. benguellensis*, which has been confirmed to be present in at least seven different AMBU's, are associated with a single AMBU, or in some cases are only marginally represent in transition zones between two AMBUs. Nevertheless, some *Hemidactylus* species are known to exhibit remarkable adaptability, being successful colonizers, such as *H. mabouia* (Vences et al. 2004) or *H. turcicus* (Meshaka et al. 2006; Locey and Stone 2006). In any case, given the crypticity, morphological overlap and geographical proximity between some sister species, such as *H. longicephalus*/*H. paivae, H. bayonii*/*H.vernayi*, or *H. benguellensis*/*H. cinganji* **sp. nov.**, we recommend future efforts in potential contact zones to provide more information about diagnostic features and the spatial segregation between sister species.

The phylogenetic hypothesis provided in this work highlights Angola as an important source of diversification within *Hemidactylus* in west-central Africa. The discovery of several micro-endemic species of *Hemidactylus* (*H. faustus* **sp. nov.** and *H. carivoensis* **sp. nov.**) as well as of other reptiles (Branch et al. 2021; Bates et al. unpub. data), along with the fact that large areas in Angola remain herpetologically unexplored, strongly suggests that the diversity of Angolan *Hemidactylus* still remains underestimated.

Acknowledgments

Special thanks to the late William R. Branch, to whom we dedicate this work. He was part of this project since the very beginning and his collection, knowledge and contributions were highly needed to achieve this work. We thank Beatriz Vaz Pinto, who found the first specimen ever of the newly described species, *H. faustus* **sp. nov.**, and Afonso Vaz Pinto for his enthusiastic and incredible support on the field, collecting and processing crucial material for this work. We thank to Raquel Godinho for her help in the molecular analysis. We thank to CTM-CIBIO workers for their support on genetic and lab efforts, specially to Susana and Rocio. We thank the Angolan Ministry of Environment Institute of Biodiversity (MINAMB) issuing export permits (31/GGPCC/2016) for biodiversity surveys that resulted in the discovery of the new species, and in particular the Director of Instituto Nacional da Biodiversidade e Áreas da Conservação (INBAC), Dr. Albertina Nzuzi. RE's fieldwork was made possible through the help of the University of Kimpa Vita in Uíge and partially funded through a travel grant from the German Academic Exchange Service (DAAD) and the "strategic partnership" program of the TU Dresden (C. Neinhuis and T. Lautenschläger). Additional surveys were supported by the Ministério do Ambiente - Instituto Nacional da Biodiversidade e Áreas de Conservação (INBAC) within the project agenda "Expansão e Fortalecimento do Sistema de Áreas Protegidas em Angola" through a grant provided by GEF under the auspices of UNEP. RE thanks M. F. Branquima, J. Lau and M. Hölting for support in the field. Permission to conduct biodiversity research in Angola and to export specimens was granted by the Instituto Nacional da Biodiversidade e Áreas de Conservação (INBAC), Ministério do Ambiente, República de Angola and the Gabinete Provincial da Agricultura, Pecuária e Pescas do Uíge under permission numbers 122/INBAC. MINAMB/2013, no. 17/014, no. 02/018; no. 05/2019. The lab work was supported by a grant from the Paul-Ungerer-Stiftung. We also recognize the unconditional, and crucial support and advice received by Vladimir Russo, and the kind hospitality of Álvaro Eugénio hosting the team at Fazenda Carivo. We thank Luke Verburgt and Rogério Ferreira for providing some photographs used in this study. Funding for fieldwork was provided by the National Research Foundation of South Africa (to William R. Branch), the South African National Biodiversity Institute (2009 expedition), and the National Geographic Okavango Wilderness

Project (2016 to 2019 expeditions). NLB and JLR are currently supported by Fundação para a Ciência e Tecnologia (FCT) contract SFRH/PD/BD/140810/2018 and PD/BD/140808/2018, respectively.

References

Ampai N, Wood Jr PL, Stuart BL, Aowphol A (2020) Integrative taxonomy of the rock-dwelling gecko *Cnemaspis siamensis* complex (Squamata, Gekkonidae) reveals a new species from Nakhon Si Thammarat Province, southern Thailand. ZooKeys 932: 129. https://doi.org/10.3897/zookeys.932.50602

Agarwal I, Karanth KP (2015) A phylogeny of the only ground-dwelling radiation of *Cyrtodactylus* (Squamata, Gekkonidae): diversification of *Geckoella* across peninsular India and Sri Lanka. Molecular Phylogenetics and Evolution 82:193–199. https://doi.org/10.1016/j.ympev.2014.09.016

Bandelt HJ, Forster P, Röhl A (1999) Median-joining networks for inferring intraspecific phylogenies. Molecular Biology and Evolution 16:37–48. https://doi.org/10.1093/oxfordjournals.molbev.a026036

Baldo D, García J, Borteiro C, Brusquetti F, Prigioni C (2008) Reptilia, Gekkonidae, *Hemidactylus mabouia*, *Tarentola mauritanica*: Distribution extension and anthropogenic dispersal. Check List 4: 434.

Baptista NL, António T, Branch WR (2019) The herpetofauna of Bicuar National Park and surroundings, southwestern Angola: a preliminary checklist. Amphibian and Reptile Conservation 13(2): 96–130.

Baptista NL, Tolley KA, Bluhm M, Finckh M, Branc WR (2020) Rediscovery, range extension, habitat and phylogenetic relation of the endemic Scaled Sandveld Lizard *Nucras scalaris* Laurent, 1964 (Sauria: Lacertidae) in the central Angolan plateau. African Journal of Herpetology 69(1):12–28. https://doi.org/10.1080/21564574.2020.1778108

Bauer AM, Jackman TR, Greenbaum E, Giri VB, de Silva A (2010) South Asia supports a major endemic radiation of *Hemidactylus* geckos. Molecular Phylogenetics and Evolution 57 (1): 343–352. https://doi.org/10.1016/j.ympev.2010.06.014

Bocage JVB (1873) Mélanges erpétologiques. II. Sur quelques reptiles et batraciens nouveaux, rares ou peu connus d'Afrique occidentale. Jornal de Sciencias Mathematicas, Physicas e Naturaes 4: 209–227.

Bocage JVB (1893) Diagnoses de quelques nouvelles espèces de reptiles et batraciens d'Angola. Jornal de Sciencias Mathematicas, Physicas e Naturaes, Segunda Série 3: 115–121.

Branch WR (2018) Snakes of Angola: An annotated checklist. Amphibian and Reptile Conservation 12(2): 41–82 (e159).

Branch WR, Baptista N, Keates C, Edwards S (2019a) Rediscovery, taxonomic status, and phylogenetic relationships of two rare and endemic snakes (Serpentes: Psammophiinae) from the southwestern Angolan plateau. Zootaxa 4590(3): 342–366. https://doi.org/10.11646/zootaxa.4590.3.2

Branch WR, Conradie W, Vaz Pinto P, Tolley K (2019b) Another Angolan Namib endemic species: a new *Nucras* Gray, 1838 (Squamata: Lacertidae) from south-western Angola. Amphibian and Reptile Conservation 12(2): 85–95.

Branch WR, Conradie W (2013) *Naja annulata annulata* (Bucholtz & Peters, 1876). African Herp News 59: 50–53.

Branch WR, Vaz Pinto P, Baptista N, Conradie W (2019c) The Reptiles of Angola: History, Diversity, Endemism and Hotspots. In: Huntley B, Russo V, Lages F, Ferrand, N (Eds) Biodiversity of Angola, Science & Conservation: A Modern Synthesis. Springer, Cham, pp. 283–334. https://doi.org/10.1007/978-3-030-03083-4_13

Branch, WR, Schmitz A, Lobón-Rovira J, Baptista NL, António T, Conradie W (2021) Rock island melody: A revision of the *Afroedura bogerti* Loveridge, 1944 group, with descriptions of four new endemic species from Angola. Zoosystematics and Evolution 97: 55. https://doi.org/10.3897/zse.97.57202

Bouckaert RR, Drummond AJ (2017) bModelTest: Bayesian phylogenetic site model averaging and model comparison. BMC evolutionary biology 17(1):42. https://doi.org/10.1186/s12862-017-0890-6

Burgess N, D'Amico Hales J, Underwood E, Dinerstein E, Olson D, Itoua I, Schipper J, Ricketts T, Newman K (2004) Terrestrial ecoregions of Africa and Madagascar: a conservation assessment. Island Press, Washington D.C 524 pp. (xxiii + 501)

Carranza S, Arnold, EN (2006) Systematics, biogeography, and evolution of *Hemidactylus* geckos (Reptilia: Gekkonidae) elucidated using mitochondrial DNA sequences. Molecular Phylogenetics and Evolution 38: 531–545. https://doi.org/10.1016/j.ympev.2005.07.012

Carranza S, Arnold, EN (2012) A review of the geckos of the genus *Hemidactylus* (Squamata: Gekkonidae) from Oman based on morphology, mitochondrial and nuclear data, with descriptions of eight new species. Zootaxa 3378(1): 1–95 https://doi.org/10.11646/zootaxa.3378.1.1

Ceríaco LM, Bauer AM, Blackburn DC, Lavres ACF (2014) The herpetofauna of the Capanda Dam Region, Malanje, Angola. Herpetological Review 45(4): 667–674.

Ceríaco LM, de Sá SC, Bandeira S, Valério H, Stanley E, Kuhn AL, Marques M, Vindum JV, Blackburn DC, Bauer AM (2016) Herpetological survey of Iona National Park and Namibe Regional Natural Park, with a Synoptic list of the Amphibians and Reptiles of Namibe Province, Southwestern Angola. Proceedings of the California Academy of Sciences 63(2): 15–61.

Ceríaco LM, Agarwal I, Marques MP, Bauer AM (2020a) A review of the genus *Hemidactylus* Goldfuss, 1820 (Squamata: Gekkonidae) from Angola, with the description of two new species. Zootaxa 4746(1): 1–71. https://doi.org/10.11646/zootaxa.4746.1.1

Ceríaco LM, Agarwal I, Marques MP, Bauer AM (2020b) A correction to a recent review of the genus *Hemidactylus* Goldfuss, 1820 (Squamata: Gekkonidae) from Angola, with the description of two additional species. Zootaxa 4861(1): 92–106. https://doi.org/10.11646/zootaxa.4861.1.6

Ceríaco LM, Heinicke MP, Parker K, Marques MP, Bauer AM (2020c) A review of the African snake-eyed skinks (Scincidae: *Panaspis*) from Angola, with the description of a new species. Zootaxa 4747: 77–112. https://doi.org/10.11646/zootaxa.4747.1.3

Ceríaco, L. M., Bauer AM, Kusamba, C., Agarwal, I., Greenbaum, E. (2021). A New Species of Ground-Dwelling *Hemidactylus* (Squamata: Gekkonidae) from Southwestern Democratic Republic of the Congo. Journal of Herpetology, 55(2), 105–111. https://doi.org/10.1670/20-094

Cermak J (2012) Low clouds and fog along the South- Western African coast. Satellite-based retrieval and spatial patterns. Atmospheric Research 116: 15–21. https://doi.org/10.1016/j.atmosres.2011.02.012

Chaitanya R, Agarwal I, Lajmi A, Khandekar A (2019) A novel member of the *Hemidactylus brookii* complex (Squamata: Gekkonidae) from the Western Ghats of Maharashtra, India. Zootaxa 4646(2): 236–250. https://doi.org/10.11646/zootaxa.4646.2.2

Christy P, Clarke WV (1998) Guide des Oiseaux de São Tomé et Príncipe. ECOFAC, São Tomé, 144pp.

Conradie W, Bourquin S (2013) Geographical Distributions: *Acontias kgalagadi kgalagadi* (Lamb, Biswas and Bauer, 2010). African Hep News 60: 29–30.

Conradie W, Measey GJ, Branch WR, Tolley KA (2012) Revised phylogeny of African sand lizards (*Pedioplanis*), with the description of two new species from south-western Angola. African Journal of Herpetology, 61(2): 91–112. https://doi.org/10.1080/21564574.2012.676079

Conradie W, Deepak V, Keates C, Gower, DJ (2020) Kissing cousins: a review of the African genus *Limnophis* Günther, 1865 (Colubridae: Natricinae), with the description of a new species from north-eastern Angola. African Journal of Herpetology 69(1): 79–107. https://doi.org/10.1080/21564574.2020.1782483

Conroy CJ, Papenfuss T, Parker J, Hahn NE (2009) Use of Tricaine Methanesulfonate (MS222) for Euthanasia of Reptiles. Journal of the American Association for Laboratory Animal Science 48(1): 28–32.

Dean WRJ, Melo M, Mills MSL (2019) The avifauna of Angola: richness, endemism and rarity. In: Huntley BJ, Russo V, Lages F. Ferrand N (Eds). Biodiversity of Angola. Science and Conservation: A Modern Synthesis. Springer Nature, Cham, 335–356.

Drummond AJ, Suchard MA, Xie D, Rambaut A (2012) Bayesian phylogenetics with BEAUti and the BEAST 1.7. Molecular Biology and Evolution 29: 1969–1973. https://doi.org/10.1093/molbev/mss075

Ernst R, Kehlmaier C, Baptista NL, Pinto PV, Branquima MF, Dewynter M, Fouquet A, Ohler A, Schmitz A (2021) Filling the gaps: The mitogenomes of Afrotropical Egg-guarding Frogs based on historical type material and a re-assessment of the nomenclatural status of Alexteroon Perret, 1988 (Hyperoliidae). Zoologischer Anzeiger 293: 125–224. https://doi.org/10.1016/j.jcz.2021.06.002

Ernst R, Lautenschläger T, Branquima MF, Hölting M (2020) At the edge of extinction: a first herpetological assessment of the proposed Serra do Pingano Rainforest National Park in Uíge Province, northern Angola. Zoosystematics and Evolution 96: 237. https://doi.org/10.3897/zse.96.51997

Ernst R, Nienguesso ABT, Lautenschläger T, Barej MF, Schmitz A, Hölting M (2014) Relicts of a forested past: Southernmost distribution of the hairy frog genus *Trichobatrachus* Boulenger, 1900 (Anura: Arthroleptidae) in the Serra do Pingano region of Angola with comments on its taxonomic status. Zootaxa 3779: 297–300. https://doi.org/10.11646/zootaxa.3779.2.10

Ernst R, Schmitz A, Wagner P, Branquima MF, Hölting M (2015) A window to Central African forest history: distribution of the *Xenopus fraseri* subgroup south of the Congo Basin, including arst country record of *Xenopus andrei* from Angola. Salamandra 51:147–155.

Gamble T, Greenbaum E, Jackman TR, Russell AP, Bauer AM (2012) Repeated origin and loss of adhesive toepads in geckos. PLoS ONE 7: e39429. https://doi.org/10.1371/journal.pone.0039429

Gamble T, Simons AM, Colli GR, Vitt LJ (2008) Tertiary climate change and the diversification of the Amazonian gecko genus *Gonatodes* (Sphaerodactylidae, Squamata). Molecular Phylogenetics and Evolution 46(1): 269–277. https://doi.org/10.1016/j.ympev.2007.08.013

Haacke WD (2008). A new leaf-toed gecko (Reptilia: Gekkonidae) from south-western Angola. African Journal of Herpetology 57(2): 85–92.

Hall TA (1999) BioEdit: a user-friendly biological sequence alignment editor and analysis program for Windows 95/98/NT. Nucleic Acids Symposium 41: 95–98.

Hallerman J, Ceríaco LM, Schmitz A, Ernst R, Conradie W, Verburgt L, Marques MP, Bauer AM (2020) A review of the Angolan House snakes, genus *Boaedon* Duméril, Bibron and Duméril (1854) (Serpentes: Lamprophiidae), with description of three new species in the *Boaedon fuliginosus* (Boie, 1827) species complex. African Journal of Herpetology 69(1): 29–78. https://doi.org/10.1080/21564574.2020.1777470

Heinicke MP, Daza JD, Greenbaum E, Jackman TR, Bauer AM (2014) Phylogeny, taxonomy and biogeography of a circum-Indian Ocean clade of leaf-toed geckos (Reptilia: Gekkota), with a description of two new genera. Systematics and Biodiversity 12(1): 23–42. https://doi.org/10.1080/14772000.2013.877999

Hellmich W (1957) Herpetologische Ergebnisse einer Forschungsreise in Angola. Veröffentlichungen der Zoologischen Staatssammlung München 5: 1–92.

Herbert TD, Lawrence KT, Tzanova A, Peterson LC, Caballero-Gill R, Kelly CS (2016) Late Miocene global cooling and the rise of modern ecosystems. Nature Geoscience 9(11): 843–847. https://doi.org/10.1038/ngeo2813

Huelsenbeck JP, Hillis DM (1993) Success of phylogenetic methods in the four-taxon case. Systematic Biology 42(3): 247–264. https://doi.org/10.1093/sysbio/42.3.247

Huntley BJ, Russo V, Lages F, Ferrand N (2019) Biodiversity of Angola. Science and Conservation: A Modern Synthesis. Springer Nature, Champ, 549 pp.

Huntley BJ, Ferrand N (2019) Angolan Biodiversity: Towards a modern Synthesis. In: Huntley, B.J., Russo, V., Lages, F., Ferrand, N. (eds). Biodiversity of Angola. Science and Conservation: A Modern Synthesis. Springer Nature, Cham, 3–14.

Jairam R, d'Orgeix CA, d'Orgeix CH, Harris A (2016) Range extension and distribution of the invasive Moreau's Tropical House Gecko, *Hemidactylus mabouia* (Moreau de Jonnès, 1818) (Squamata: Gekkonidae), in Suriname. Check List 12(5): 1978.

Kalyaanamoorthy S, Minh BQ, Wong TK, von Haeseler A, Jermiin LS (2017) ModelFinder: fast model selection for accurate phylogenetic estimates. Nature Methods 14(6): 587–589. https://doi.org/10.1038/nmeth.4285

Lanfear R, Frandsen PB, Wright AM, Senfeld T, Calcott, B (2016) PartitionFinder 2: new methods for selecting partitioned models of evolution formolecular and morphological phylogenetic analyses. Molecular Biology and Evolution 34 (3): 772–773. https://doi.org/10.1093/molbev/msw260

Larsson A (2014) AliView: a fast and lightweight alignment viewer and editor for large datasets. Bioinformatics 30(22): 3276–3278. https://doi.org/10.1093/bioinformatics/btu531

Locey KJ, Stone PA (2006) Factors affecting range expansion in the introduced Mediterranean gecko, *Hemidactylus turcicus*. Journal of Herpetology 40(4): 526–530. https://doi.org/10.1670/0022-1511-(2006)40[526:FAREIT]2.0.CO;2

Loveridge A (1947) Revision of the African lizards of the family Gekkonidae. Bulletin of the Museum of Comparative Zoölogy 98:1–469 (pls.1–7).

Macey JR, Larson A, Ananjeva NB, Fang Z, Papenfuss TJ (1997) Two novel gene orders and the role of light- strand replication in rearrangement of the vertebrate mitochondrial genome. Molecular Biology and Evolution 14: 91–104. https://doi.org/10.1093/oxfordjournals.molbev.a025706

Maddison WP, Maddison DR (2019) Mesquite: a modular system for evolutionary analysis. Version 3.61 http://www.mesquiteproject.org

Marques MP, Ceríaco LMP, Buehler MD, Bandeira S, Janota JM, Bauer AM (2020) A revision of the Dwarf Geckos, genus *Lygodactylus* (Squamata: Gekkonidae), from Angola, with the description of three

new species. Zootaxa 4583(3): 301–352. https://doi.org/10.11646/zootaxa.4853.3.1

Marques MP, Ceríaco LMP, Bandeira S, Pauwels OSG, Bauer AM (2019a) Description of a new long-tailed skink (Scincidae: *Trachylepis*) from Angola and the Democratic Republic of Congo. Zootaxa 4568(1): 51–68. https://doi.org/10.11646/zootaxa.4568.1.3

Marques MP, Ceríaco LMP, Stanley EL, Bandeira S, Agarwal I, Bauer AM (2019b) A new species of girdled lizard (Squamata: Cordylidae) from Serra da Neve inselberg, Namibe province, southwestern Angola. Zootaxa 4668(4): 503–524. https://doi.org/10.11646/zootaxa.4668.4.4

Marques MP, Ceríaco LMP, Blackburn DC, Bauer AM (2018) Diversity and distribution of the amphibians and terrestrial reptiles of Angola – Atlas of historical and bibliographic records (1840–2017). Proceedings of the California Academy of Sciences, Series 4, 65(2): 1–501.

Meshaka Jr WE, Marshall SD, Boundy J, Williams AA (2006) Status and geographic expansion of the Mediterranean gecko, *Hemidactylus turcicus*, in Louisiana: implications for the southeastern United States. Herpetological Conservation and Biology 1(1): 45–50.

Miller MA, Pfeiffer W, Schwartz T (2010) Creating the CIPRES Science Gateway for inference of large phylogenetic trees. In: Proceedings of the Gateway Computing Environments Workshop (GCE), November 2010, New Orleans, LA 1–8. https://doi.org/10.1109/GCE.2010.5676129

Mirza ZA, Gowande GG, Patil R, Ambekar M, Patel H (2018) First appearance deceives many: disentangling the *Hemidactylus triedrus* species complex using an integrated approach. PeerJ 6: e5341. https://doi.org/10.7717/peerj.5341

Monard A (1937) Contribution à l'herpétologie d'Angola. Arquivos do Museu Bocage 8: 19–154.

Padial JM, Miralles A, De la Riva I, Vences M (2010) The integrative future of taxonomy. Frontiers in Zoology 7(1): 1–14.

Portik DM, Bauer AM, Jackman TR (2010) The phylogenetic affinities of *Trachylepis sulcata nigra* and the intraspecific evolution of coastal melanism in the western rock skink. African Zoology 45: 147–159. https://doi.org/10.3377/004.045.0217

Rödder D, Solé M, Böhme W (2008) Predicting the potential distributions of two alien invasive House geckos (Gekkonidae: *Hemidactylus frenatus*, *Hemidactylus mabouia*). North-Western Journal of Zoology 4(2): 236–246.

Ronquist F, Teslenko M, Van der Mark P, Ayres DL, Darling A, Höhna S, Larget B, Liu L, Suchard MA, Huelsenbeck JP (2012) MrBayes 3.2: efficient Bayesian phylogenetic inference and model choice across a large model space. Systematic Biolology 61: 539–542. https://doi.org/10.1093/sysbio/sys029

Rösler H (2015) Bemerkungen über einige Geckos der Zoologischen Staatsammlung München. 1. Teil: Afrika und Amerika, mit einer übersicht zur morphologischen variation arabischer und afrikanischer Hemidactylus-Arten. Chimaira, Frankfurt, 54 pp.

Rozas J, Ferrer-Mata A, Sánchez-del Barrio JC, Guirao-Rico S, Librado P, Ramos-Onsins SE, Sánchez-Gracia A (2017) DnaSP 6: DNA sequence polymorphism analysis of large data sets. Molecular Biology and Evolution 34(12): 3299–3302. https://doi.org/10.1093/molbev/msx248

Schlick-Steiner BC, Steiner FM, Seifert B, Stauffer C, Christian E, Crozier RH (2010) Integrative taxonomy: a multisource approach to exploring biodiversity. Annual Review of Entomology 55: 421–438.

Šmíd J, Mazuch T, Nováková L, Modrý D, Malonza PK, Elmi HSA, Carranza S, Moravec J (2019) Phylogeny and systematic revision of the gecko genus *Hemidactylus* from the Horn of Africa (Squamata: Gekkonidae). Herpetological Monographs 33(1): 26–47.

Stanley EL, Ceríaco LM, Bandeira S, Valerio H, Bates MF, Branch WR (2016) A review of *Cordylus machadoi* (Squamata: Cordylidae) in southwestern Angola, with the description of a new species from the Pro-Namib desert. Zootaxa 4061(3): 201–226. https://doi.org/10.11646/zootaxa.4061.3.1

Trifinopoulos J, Nguyen LT, von Haeseler A, Minh BQ (2016) W-IQ-TREE: a fast online phylogenetic tool for maximum likelihood analysis. Nucleic Acids Research 44(1):232–235. https://doi.org/10.1093/nar/gkw256

Vasconcelos R, Perera A, Geniez P, Harris DJ, Carranza S (2012) An integrative taxonomic revision of the *Tarentola* geckos (Squamata, Phyllodactylidae) of the Cape Verde Islands. Zoological Journal of the Linnean Society 164(2): 328–360. https://doi.org/10.1111/j.1096-3642.2011.00768.x

Vaz Pinto P, Luis Veríssimo L, Branch WR (2019) Hiding in the bushes for 110 years: rediscovery of an iconic Angolan gecko (*Afrogecko ansorgii* Boulenger, 1907, Sauria: Gekkonidae). Amphibian and Reptile Conservation 13(2): 29–41.

Vences M, Wanke S, Vieites DR, Branch WR, Glaw F, Meyer A (2004) Natural colonization or introduction? Phylogeographical relationships and morphological differentiation of house geckos (*Hemidactylus*) from Madagascar. Biological Journal of the Linnean Society 83(1): 115–130. https://doi.org/10.1111/j.1095-8312.2004.00370.x

Vieites DR, Wollenberg KC, Andreone F, Köhler J, Glaw F, Vences M (2009) Vast underestimation of Madagascar's biodiversity evidenced by an integrative amphibian inventory. Proceedings of the National Academy of Sciences 106(20): 8267–8272.

Werneck FP, Gamble T, Colli GR, Rodrigues MT, Sites Jr JW (2012) Deep diversification and long-term persistence in the South American 'dry diagonal': Integrating continent-wide phylogeography and distribution modeling of geckos. Evolution: International Journal of Organic Evolution 66(10): 3014–3034. https://doi.org/10.1111/j.1558-5646.2012.01682.x

Xu W, Dong WJ, Fu TT, Gao W, Lu CQ, Yan F, Wu YH, Jiang K, Jin JQ, Chen HM, Zhang YP, Hillis DM, Che J (2020) Herpetological phylogeographic analyses support a Miocene focal point of Himalayan uplift and biological diversification. National Science Review 2020: nwaa263. https://doi.org/10.1093/nsr/nwaa263

Zimkus BM, Lawson LP, Barej MF, Barratt CD, Channing A, Dash KM, Dehling JM, Preez LD, Gehring P, Greenbaum E, Gviždik V, Harvey J, Kielgast J, Kusamba C, Nagy ZT, Pabijan M, Penner J, Rödel MO, Vences M, Lötters S (2017). Leapfrogging into new territory: How Mascarene ridged frogs diversified across Africa and Madagascar to maintain their ecological niche. Molecular Phylogenetics and Evolution 106: 254–269. https://doi.org/10.1016/j.ympev.2016.09.018

Supplementary material 1

File 1

Authors: Lobón-Rovira J, Conradie W, Buckley Iglesias D, Ernst R, Veríssimo L, Baptista N, Pinto PV (2021)
Data type: .xlsx
Explanation note: Table S1. Different Angolan Main Biogeographic Units (AMBUs) defined on this work with ID Codes, names and descriptions.

Link: https://doi.org/10.3897/vz.71.e64781.suppl1

Supplementary material 2

File 2

Authors: Lobón-Rovira J, Conradie W, Buckley Iglesias D, Ernst R, Veríssimo L, Baptista N, Pinto PV (2021)
Data type: .xlsx
Explanation note: Table S2. List of material used for the genetic and morphological analyses with information on coordinates, localities, source, type of record (G – genetics; V – voucher; L – Lost Material), Catalog numbers, Field numbers and GenBank accession numbers. Asterisks (*) denoted historical *Hemidactylus* material which species ID requires reevaluation based on new species description.

Link: https://doi.org/10.3897/vz.71.e64781.suppl2

Supplementary material 3

File 3

Authors: Lobón-Rovira J, Conradie W, Buckley Iglesias D, Ernst R, Veríssimo L, Baptista N, Pinto PV (2021)
Data type: .xlsx
Explanation note: Table S3. Measurements (in mm) and scale counts for newly collected material of *Hemidactylus bayonii*. For abbreviations see Material and Methods section.

Link: https://doi.org/10.3897/vz.71.e64781.suppl3

Supplementary material 4

File 4

Authors: Lobón-Rovira J, Conradie W, Buckley Iglesias D, Ernst R, Veríssimo L, Baptista N, Pinto PV (2021)
Data type: .xlsx
Explanation note: Table S4. Measurements (in mm) and scale counts for newly collected material of *Hemidactylus vernayi*. For abbreviations see Material and Methods section.

Link: https://doi.org/10.3897/vz.71.e64781.suppl4

Supplementary material 5

File 5

Authors: Lobón-Rovira J, Conradie W, Buckley Iglesias D, Ernst R, Veríssimo L, Baptista N, Pinto PV (2021)
Data type: .xlsx
Explanation note: Table S5. Measurements (in mm) and scale counts of the holotype and paratypes of *Hemidactylus pfindaensis* **sp. nov.** For abbreviations see Material and Methods section.

Link: https://doi.org/10.3897/vz.71.e64781.suppl5

Supplementary material 6

File 6

Authors: Lobón-Rovira J, Conradie W, Buckley Iglesias D, Ernst R, Veríssimo L, Baptista N, Pinto PV (2021)
Data type: .xlsx
Explanation note: Table S6. Measurements (in mm) and scale counts of the holotype and paratypes of *Hemidactylus cinganji* **sp. nov.** For abbreviations see Material and Methods section.

Link: https://doi.org/10.3897/vz.71.e64781.suppl6

Supplementary material 7

File 7

Authors: Lobón-Rovira J, Conradie W, Buckley Iglesias D, Ernst R, Veríssimo L, Baptista N, Pinto PV (2021)
Data type: .xlsx
Explanation note: Table S7. Measurements (in mm) and scale counts of the holotype and paratypes of *Hemidactylus carivoensis* **sp. nov.** For abbreviations see Material and Methods section.

Link: https://doi.org/10.3897/vz.71.e64781.suppl7

Supplementary material 8

File 8

Authors: Lobón-Rovira J, Conradie W, Buckley Iglesias D, Ernst R, Veríssimo L, Baptista N, Pinto PV (2021)
Data type: .xlsx
Explanation note: Table S8. Measurements (in mm) and scale counts of the holotype and paratypes of *Hemidactylus faustus* **sp. nov.** For abbreviations see Material and Methods section.

Link: https://doi.org/10.3897/vz.71.e64781.suppl8